Climate Risk and its Impact on Insurance

Jose Garrido, Xavier Milhaud, Anani Olympio, Max Popp

CNP assurances

Insuring a more open world

DIALog

Digital insurance and long term risk

Chaire d'Excellence

Green Book

Climate Risk and its Impact on Insurance

June 2024

FORWARD

We all measure it on a daily basis: climate change is accelerating, threatening human lives, property and the entire economy.

Recent reports from the World Health Organisation (WHO) are unequivocal. 3.6 billion people already live in areas highly sensitive to climate change - that's half of humanity. Between 2030 and 2050, climate change is expected to cause around 250,000 additional deaths each year.

Climate risk challenges the models used by actuaries, who are experts in quantifying risks, and CNP Assurances' mission to protect as many people as possible. It also calls into question our role as an investor and encourages us to direct our financing towards a low-carbon economy.

We have decided to turn this major challenge into an opportunity. That is why we are mobilising experts and researchers to help the insurance industry move towards new technical solutions. This green book is the first step in this direction.

The DIALog[1] Chair of Excellence team draws on the multi-disciplinary expertise of pioneering climate experts to quantify the impact of climate risk on insurance, particularly in the health and life sectors, CNP Assurances' traditional business.

I have confidence in the expertise and creativity of the CNP Assurances teams, and in the mobilisation of market players to make use of these ideas, which are driving forward the science of climate change.

Marie-Aude Thépaut, CNP Assurances General Manager

[1] Digital insurance and long term risk

Digital insurance and long term risk
Chaire d'Excellence

Climate Risk and its Impact on Insurance




Auteurs: **José Garrido**
Chaire DIALog

Xavier Milhaud
Chaire DIALog

Anani Olympio
CNP Assurances

Max Popp
EcoAct

This green book was produced by the Digital Insurance And Long term risk - DIALog chair and CNP Assurances' Strategic Research and Foresight Department, under the co-direction of José Garrido, Xavier Milhaud and Anani Olympio. It involved a number of experts, researchers and collaborators whom we would like to thank for their contribution and their time.

Our thanks to J.-L. Gouthon, M. Hyvernaud, E. Mauboussin and M. Valla for their contribution to the editorial work.

We also thank the general management of CNP Assurances; the members of the executive committee; the stakeholder dialogue, communication and sponsorship department; the teams of the research and strategic foresight department; the members of the steering committee of the DIALog chair and our partner, the Risk Foundation of the Louis Bachelier Institute.

Date of publication: July 12, 2024

Contents

Introduction

This book presents an introduction for beginners to climate science from an insurance perspective. The focus is on the measurement of climate change and of its impact on policyholders and their insurers.

Climate change presents several challenges for society, endangering food supply and water security, affecting human health, and threatening transportation systems (Dundon et al., 2016) as well as property (Warren-Myers et al., 2018; Miljkovic et al., 2018). It also affects the economy (Pryor, 2017). The consequences of this environmental change are expected to be deep and far-reaching, particularly in insurance sectors such as agriculture, property-casualty, health and life.

As a result, climate change can threaten the sustainability of insurance programs, in different ways. First, because the increase in total losses may require hikes in premiums and solvency capital. A precise quantitative assessment of this increase is not yet determined, but it is clear that both recent and future costs are a serious threat; according to Munich Re (2024), losses caused by natural disasters in 2023 reached US$ 250 bn, with US$ 95 bn of which being insured. Although no disasters of the magnitude of Hurricane Ian occurred in 2023, a fair share of the losses were associated with several severe storms occurred in the US and Europe. These related events are considered as evidence of the global warming trend, with a potential impact particularly on property and casualty insurance (Gupta and Venkataraman, 2024; Golnaraghi, 2021). In this particular insurance sector, Swiss Re (2021) forecasts increased frequency and severity of events due to climate change that will cost 30%-63% more in insured catastrophe losses by 2040. This cost increase could even reach 90%-120% in specific markets, such as China, the UK, France and Germany.

Secondly, climate change puts into question some fundamental principles of insurance, such as risk insurability, pooling, diversification, and risk transfer. The literature discusses the possible outcomes and implications for the insurance industry (Charpentier, 2008; Thistlethwaite and Wood, 2018; Courbage and Golnaraghi, 2022). Other, more optimistic perspectives suggest that far from being the victim of climate change the insurance business could find in it an opportunity, through the development of new technical solutions (Rao and Li, 2023; Savitz and Dan Gavriletea, 2019; Wagner, 2022). For now, climate change already has forced the strategic withdrawal of insurers in certain markets in the USA (California, 2023).

The general objective of this book is to present an actuarial perspective on the study of cli-

mate change and its impact on the insurance industry. Actuaries are experts at measuring and managing risks. The DIALog Research Chair team regroups several members, both from industry and academia, with ample actuarial expertise. Hence it was natural for the DIALog team to tackle this project and explore the impact of climate change on the insurance industry, more particularly in health and life insurance.

This study starts by exploring the need for a standardized method to measure climate change. This is crucial in order to compare different regions and periods in a standardised analysis. In recent years the actuarial community has developed actuarial climate indices to measure climate change in an factual, objective and consistent way. First, Chapter 1 reviews the recent scientific literature on the few actuarial climate indices that have been defined so far and extends the existing methodology to calculate an actuarial index for climate data in France.

Then Chapter 2 describes how climate science can be used to link a physical climate risk to insurance costs. In particular it focuses on the impact of heat waves on excess mortality. A deterministic and a stochastic model are proposed to link the Heat Index to excess mortality. The chapter includes a frank discussion of the advantages and difficulties with the approach.

Finally Chapter 3 further explores the link between extreme temperatures and excess mortality in France. A more technical exposure is used, in order to propose a new mortality forecasting model that includes explanatory terms capturing the correlation between temperature and mortality, as well as the effect of high temperature anomalies.

1

Climate risk and actuarial science

1.1. Climate risk

Climate change refers to long-term variations in temperature, precipitation patterns, sea levels, and other aspects of Earth's climatic system. Mitigating the effects of climate change is one of the most complicated and pressing challenges that society faces, with heavy implications in particular for the insurance sector, affected by an increased loss frequency and severity in different lines of business. Apart from more frequent and intense extreme weather events, climate change is associated with rising sea levels that threaten coastal areas, with water scarcity and droughts in other regions, disruption of ecosystems and the loss of biodiversity, adverse impact on agriculture and food security, public health risks, significant economic consequences, and displacement and migration of populations.

According to the Intergovernmental Panel on Climate Change (IPCC), the observed global surface temperature from 2011 to 2020 was 1,1°C higher than the average in the last half of the 19-th century, with land surface temperature increasing by 1,59°C; see IPCC (2023). For insurance companies, any increase in extreme weather events such as hurricanes, floods, wildfires, and droughts, that can cause significant damages would result in higher insurance claims. Moreover, if historical data are no longer representative due to changing weather patterns, insurers need to reassess the risk models they use and incorporate climate change projections and long-term climate risk assessments into their pricing to determine premiums accurately.

In order to help insurance companies predict and manage climate risks, North-American actuaries have defined the Actuaries Climate Index™ (ACI), that combines information from several important weather variables from the historical record of United States and Canada. The next section provides an introduction to the different actuarial indices that have been defined so far.

1.2. Actuarial climate indices

Just as the Consumer Price Index (CPI) tracks changes in the cost of a standard basket of goods and services over time, the Actuaries Climate Index™ (ACI) measures climate risks through a basket of extreme climate events and changes in the sea level.

Actuaries measure and manage different types of risk. The ACI provides a simple tool to help actuaries extend their expertise to climate risk. It serves as a proxy for the complex climate change phenomenon, to use as an actuarial model input. An index increase points to more frequent extreme climate events.

For insurance companies, any increase in extreme weather events such as heat waves, wind storms, floods, wild-fires, and droughts, that can cause deaths and significant damages, would result in higher insurance claims. Moreover, if historical data are no longer representative due to changing weather patterns, insurers need to reassess their risk models and incorporate climate change projections and long-term climate risk assessments into their pricing, to accurately determine premiums.

1.2.1. Review of the literature

At the turn of the 20^{th} century, the World Climate Research Program proposed several indices that could provide useful information on climate change (see Peterson et al., 2001). In 2012, the Climate Index Working Group (CIWG) of the CAS Climate Change Committee summarised the scientific knowledge on climate change, and proposed in a report to develop a composite index, termed the Actuaries Climate Change Index (ACCI), to include information from several climate variables, (see Solterra Solutions, 2012).

The development of the Actuaries Climate Index™ (ACI), which studies climate change in the United States and Canada, was proposed by this CIWG working group in 2014 and was launched in November 2016.

The Actuaries Climate Index™ was jointly developed by the Canadian Institute of Actuaries (CIA), the Society of Actuaries (SOA), the Casualty Actuarial Society (CAS), and the American Academy of Actuaries (AAA), from climate data in North America ; (see ACI, 2018). It is intended to provide actuaries, public policymakers, and the general public with a neutral, factual and helpful climate change monitoring tool, to learn about climate change and its associated risks.

The focus is on extreme weather events rather than averages; extremes have a greater impact on policyholders and their insured goods, as well as on society and the economy. The index consists of six components, each forming a monthly time series starting in 1961, from records of the National Oceanic and Atmospheric Administration (NOAA, Menne et al., 2012), GHCNDEX1 (CLIMDEX, Donat et al., 2013), and from the Permanent Service for Mean Sea Level (PSMSL, 2023).

The ACI is calibrated to average to 0 over the 1961-1990 reference period. From Figure 1.1 we see that since then, the seasonal values of the index (vertical bars) are almost exclusively above average and the systematic increase of the index 5-year moving average since 1990.

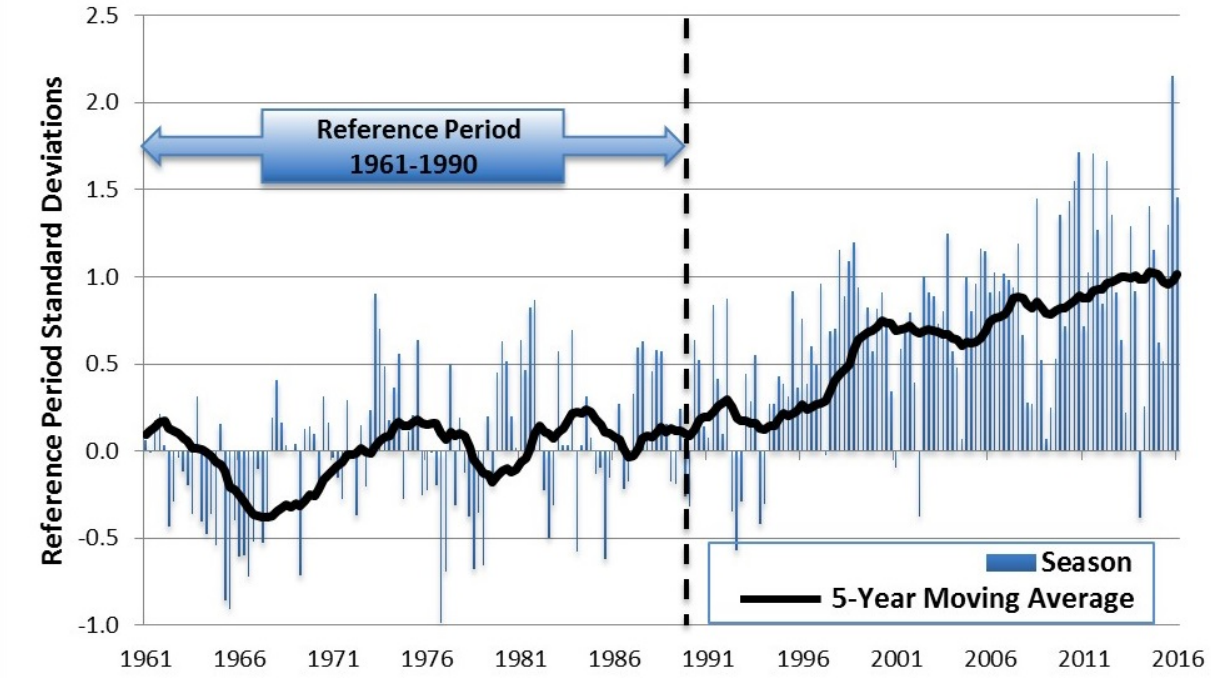

Figure 1.1. ACI values; 1961-1990 reference period to 2021.

Source: https://actuariesclimateindex.org/explore/.

Compare it to Figure 1.2, which shows the progression of insured losses over a similar period, we can see a strong correlation.

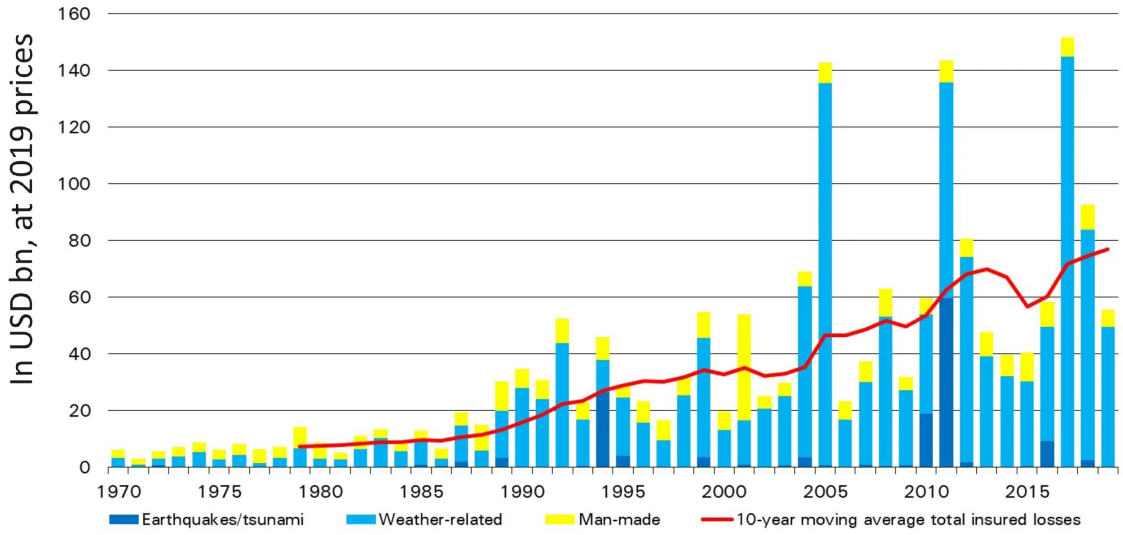

Figure 1.2. Catastrophe-related global insured losses.

Source: www.swissre.com/media/press-release/nr-20191219-global-catastrophes-estimate.html.

Curry (2015) investigates the extension of the ACI formula to the UK and Europe. He reviews the ACI definition and methodology and finds them applicable to this region without modification, although some climate data is missing for the geographical area studied, for extreme precipitation for instance.

In 2018, the Institute of Actuaries of Australia developed the Australian Actuaries Climate Index (AACI), using the ACI methodology, to monitor climate change in Australia; AACI (2018). The AACI is calibrated also to a 0-average, but over a different reference period, 1981-2010. From Figure 1.3 we see that, like for the ACI, the seasonal values of the AACI are almost exclusively above average and that the index 5-year moving average has systematically increased since about 2001.

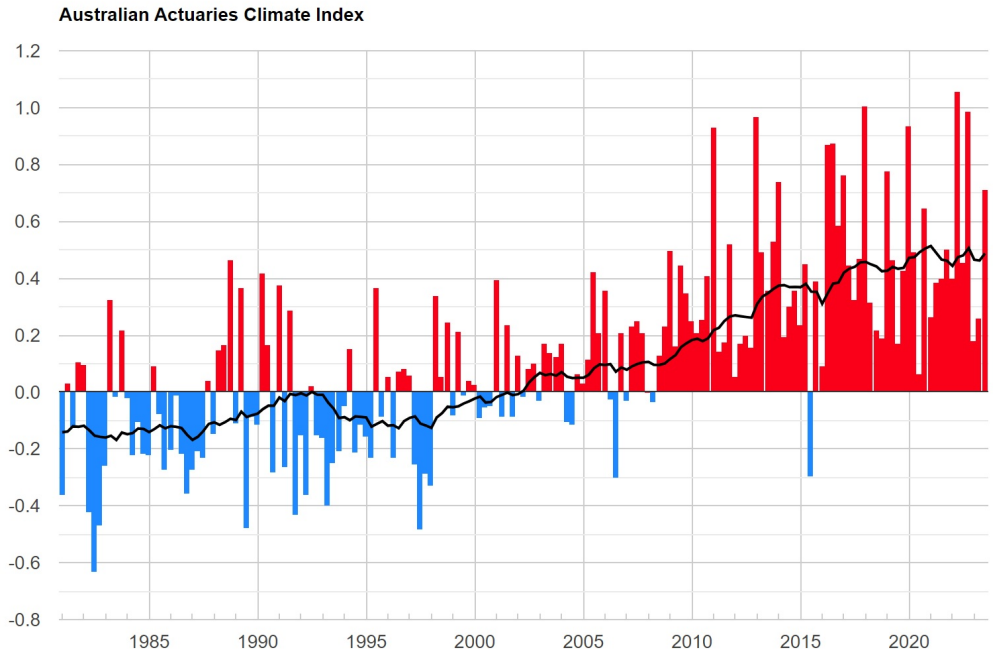

Figure 1.3. AACI values; 1981-2010 reference period to 2023.

Source: https://actuaries.asn.au/microsites/climate-index/explore/component-graphs.

In addition, Nevruz et al. (2022) propose to apply the ACI in Turkey, adapting it to the conditions in Ankara, to develop an index suitable for this region. They suggest that choosing the best grid data-set for their ACI[1] is more important than changing how the index is calculated.

Bridging the gap between the physical risk and insurance, Pan et al. (2022) investigate the effectiveness of the ACI in predicting crop yields for (re)insurance rate-making. They find that the ACI has significant predictive power for crop yields and yield losses, and argue that a high-resolution index could benefit the insurance industry.

More recently, in an oral presentation at an event of the Spanish Institute of Actuaries (IAE), a first draft defines a Spanish version of the ACI, over a shorter, more recent reference period than the ACI (1975-1995 in general and 1993-2000 for sea levels). Their temperature variables also differ, using average highs and average lows, in their composite index formula. This index is not yet published, but some details can be found at IAE (2023).

[1] A grid cell corresponds to a portion of the territory (measured in longitude and latitude).

Zhou et al. (2023) published the first actuarial climate index for European countries, using the same methodology and reference period as the North-American ACI; this allows for direct comparisons between the indices on 3 continents. The climate data used is from the Iberian peninsula (continental Spain and Portugal) and is extracted from the ERA-5 Copernicus database (voir Copernicus Climate Change Service (C3S), Climate Data Store (CDS), 2022).This Iberian ACI is denoted IACI. It uses the same methodology as the North-American ACI; it is calibrated to a 0-average also over the 1961-90 reference period.

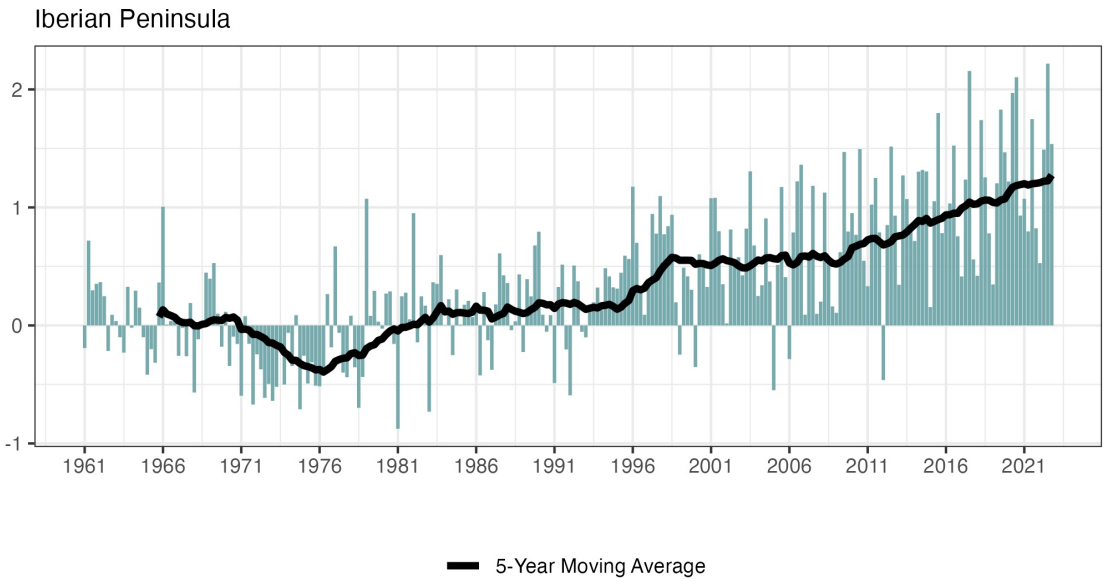

Figure 1.4. IACI values; 1961-1990 reference period to 2022.
Source: Zhou et al. (2023).

From Figure 1.4 we observe that, as for the ACI and AACI, the seasonal IACI values are mostly above average and the systematic increase of the 5-year moving index average since 1990.

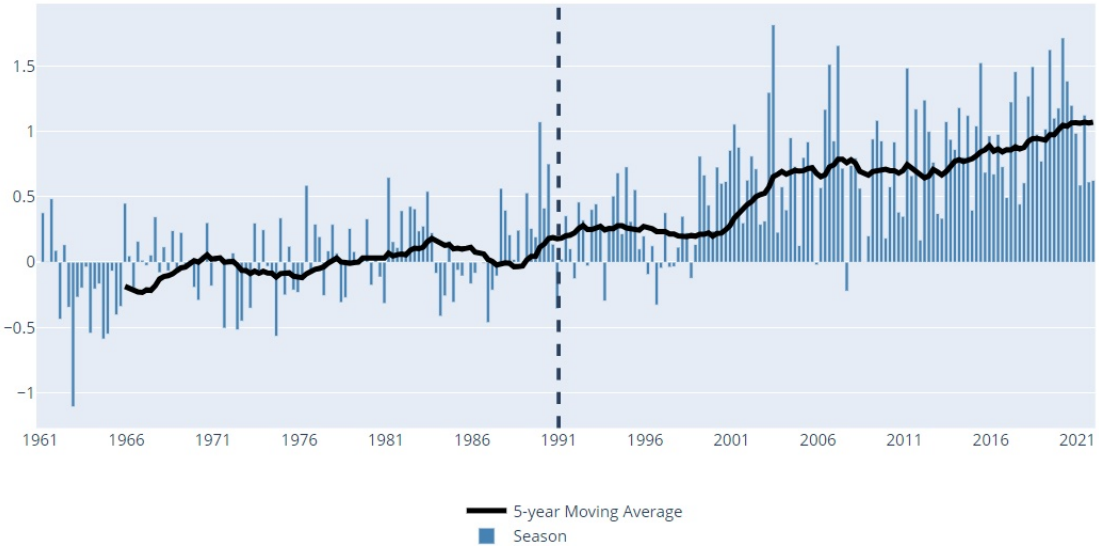

Figure 1.5. FACI values; 1961-1990 reference period to 2022.
Source: Garrido et al. (2023).

Similarly, Garrido et al. (2023) calculates an actuarial climate index for France, also using climate data from ERA-5 and the conclusions are quite similar (see Figure 1.5). We review here the first results for this French index and how it compares to the few indices listed above.

The next section first recalls the main features of the North-American ACI methodology, as most other actuarial climate indices defined so far are based on it.

1.2.2. The North-American ACI methodology

Version 1.1[2] of the Actuaries Climate Index™ (ACI) combines six components, listed in Table 1.1, each being a monthly time series beginning in 1961.

The data from the 1961-1990 reference period produce the means and the standard deviations used to standardise anomalies for each component. Each monthly value is standardised with the mean and standard deviation of the monthly values of the corresponding month over the reference period (like a Z-score). For example, for an observation for the month of January, the standardisation is with the mean and standard deviation of the 30 months of January in the reference period.

Component	**Notation**	**Definition**
Temperature highs	*T90*	Frequency of temperatures $> 90^{th}$ percentile
Temperature lows	*T10*	Frequency of temperatures $< 10^{th}$ percentile
Precipitation	*P*	Max. rainfall/month in 5 consecutive days
Droughts	*D*	Annual maximum consecutive dry days
Wind speed	*W*	Frequency of wind speed $> 90^{th}$ percentile
Sea level	*S*	Change in sea level

Table 1.1. Definition of the ACI components.

Then, the standardised anomalies of all 6 components are averaged to form the composite index:

$$ACI = \frac{1}{6}(T90_{std} - T10_{std} + P_{std} + D_{std} + W_{std} + S_{std}),$$

where the temperature lows $T10_{std}$ is subtracted instead of added; as the climate warms, the occurrence of extreme low temperatures decreases and the temperature distribution curve shifts to the right. A linear formula with equal component weights might seem overly simple; what matters here is the evolution of the ACI relative values over time more than its absolute values.

The ACI is calculated monthly, as well as on a seasonal basis (meteorological seasons). The latter is determined by taking seasonal averages, for example, the winter average is based on the calendar months of December, January, and February. Then the seasonal standardisation is just as for the monthly index..

[2] Version 2.0 of the ACI is currently under design.

Figure 1.6 plots the 5-year moving averages of all 6 components seasonal values, and of the composite ACI, from 1961 to 2022, inclusive. For more details on the methodology and some sample calculations of the 6 components and the composite index, see ACI (2018, 2019).

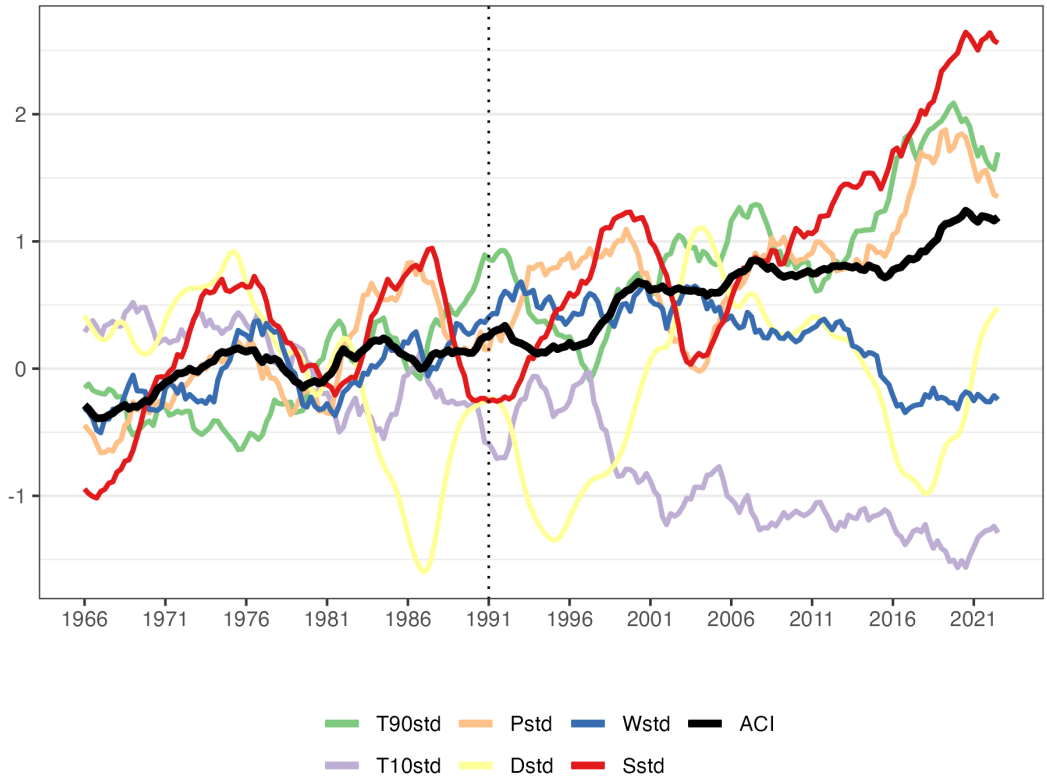

Figure 1.6. 5-year moving averages; ACI and its 6 components.
Source: Zhou et al. (2023).

1.2.3. The French actuarial climate index

Garrido et al. (2023) defines the French actuarial climate index (FACI), using data from the ERA5-Land reanalysis data-set (Copernicus Climate Change Service (C3S), Climate Data Store (CDS), 2022) and tide gauge data from the PSMSL (2023). All calculations are performed at each individual grid cell level, and then aggregated at the regional level, for all of France and Corsica, component by component, simply by taking averages.

The ERA5–Land reanalysis data has a high–resolution, set at 0.1° x 0.1° degrees of latitude and longitude, about 122 km^2, resulting in more than 10.000 grid cells to cover France and Corsica. Reanalysis combines model data with observations from various sources (e.g. satellites, weather stations, and ocean buoys) to create a globally comprehensive and consistent data–set using the laws of physics; see Muñoz-Sabater et al. (2021). Unlike observational data, that can exhibit non-homogeneity and some instrumental biases, reanalysis provides a more accurate representation of past climate conditions. Table 1.2 lists the few variables from ERA5 used in the analysis of Garrido et al. (2023).

Figure 1.7 plots the 5-year moving averages of all 6 components seasonal values, and of the composite French actuarial climate index, from 1961 to 2021, inclusive, obtained in Garrido et al. (2023). The next section compares it to the other indices listed above.

Name	Units	Description
2m temperature	k	Air temperature at 2m above the surface of land, sea, or in-land waters. Convert temperatures in Kelvin to degrees Celsius () by subtracting 273.15.
Total precipitation	m	Accumulated liquid and frozen water, that includes rain and snow fallen on Earth's surface. Does not include fog, dew, or the precipitation that evaporates before landing on Earth's surface. Precipitation units are depth in metres.
10m u-component of wind	m/s	Eastward component of the 10m wind. It is the horizontal speed of air moving eastwards, at a height of ten metres above Earth's surface, in metres per second.
10m v-component of wind	m/s	Northward component of the 10m wind (same description as 10m u-component above).

Table 1.2. Selected ERA5-Land dataset variables.

1.2.4. Index comparisons

The IACI indices defined for the Iberian Peninsula (the SACI for Spain and PACI for Portugal) are based on exactly on the same methodology of the North American ACI (for the US and Canada). So they can be compared directly with the French FACI. We do not include the Australian AACI index in this comparison. Although it was initially based also on the North American ACI methodology, it was revised keeping only 3 out the 6 climate variables, making it less comparable to the other indices. Also, the AACI is calibrated to a 0-average, but over a different reference period, 1981-2010. Nevertheless, we see in Figure 1.3 that, like for the ACI, the seasonal AACI values are almost exclusively above average and that the index 5-year moving average has systematically increased since about 2001.

Figure 1.7 combines the graphs of the 5-year moving averages of the seasonal ACI and its 6 components for the US, to the same graph for Canada, as well as to the separate IACI for Portugal and for Spain (see Zhou et al., 2023) and the FACI for France.

The first observation is that the sea level change is dominant in all graphs (red curve), except that of Canada. The other 4 countries show similar increasing trends and onset times, around the mid-90's. Portugal and Spain experienced the highest increases, with an S_{std} anomaly now at more than 4.5 standard deviations over its 0-mean. Then in the US it is currently at a level of about 3.5, and France at around 2.5. The S_{std} in Canada experienced a large cyclical decrease at the end of the 1990's and has never caught up with the US since. Note that

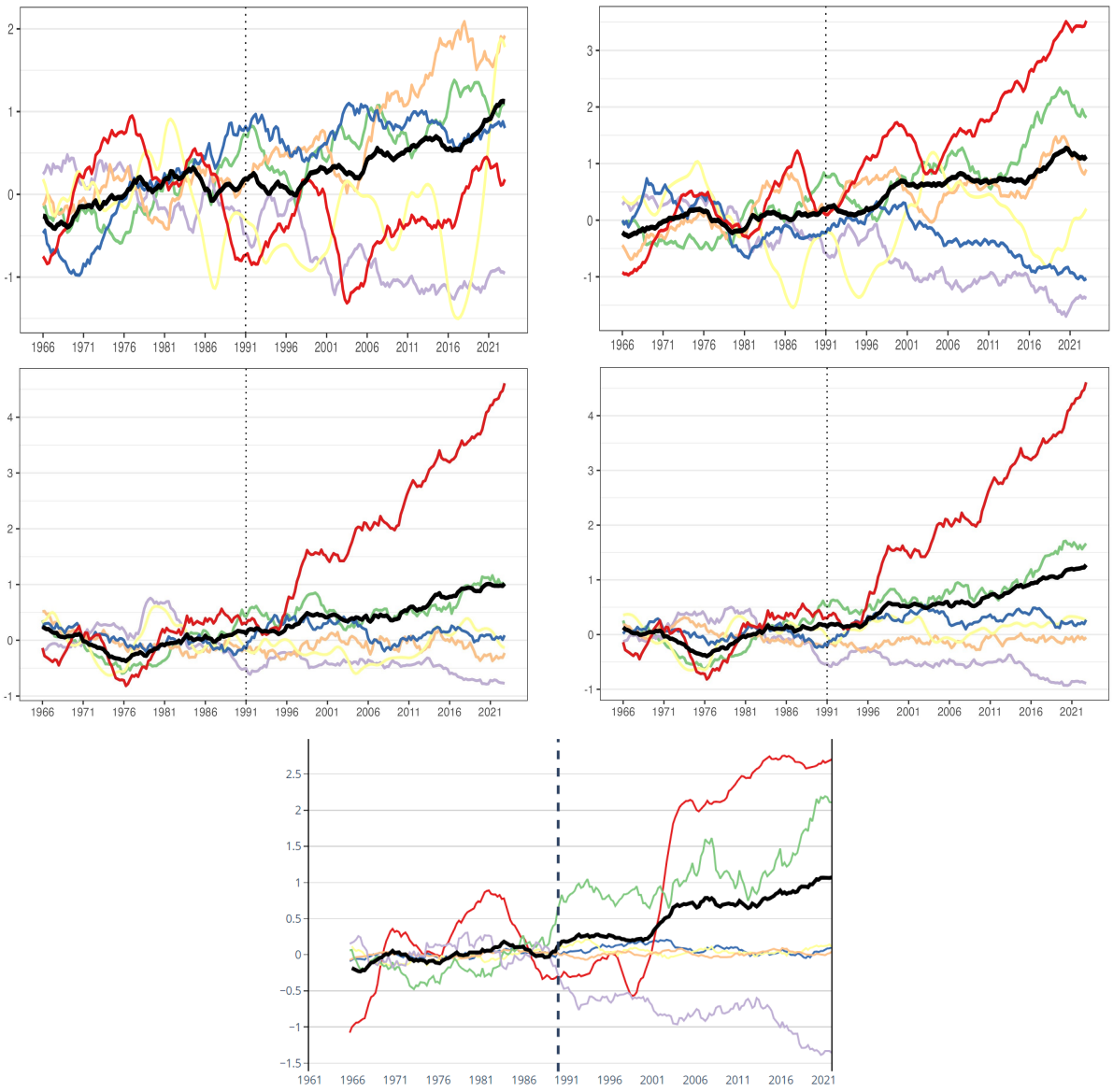

Figure 1.7. Seasonal 5–year moving averages of components used in the ACI (green: $T90_{std}$, purple: $T10_{std}$, orange: P_{std}, yellow: D_{std}, blue: W_{std}, red: S_{std}, black: ACI). From top left to bottom right: Canada, USA, Portugal, Spain and France.

ocean and sea level changes depend on the region, within these countries. For instance, in Alaska the S_{std} 5-year moving averages have been constantly decreasing since 1961; see https://actuariesclimateindex.org/maps/. The literature also points out to longer term cycles in sea level variations that are not picked-up by 30-year reference periods like that of the ACI (see Pineau-Guillou et al., 2021, and the references therein). Plus, it is not clear how changes in ocean and sea levels affect inland regions climate. For all these reasons, it is difficult to draw general trend conclusions, other than the significance of the change in the S_{std} variable, after the reference period, and the fact that the colder coastal waters of Canada seem to experience a lesser impact than in the other 4 countries.

The next dominant change, for all 5 graphs, is for the temperature highs (green curve). The $T90_{std}$ anomalies are currently highest in France, at around 2.5, and similar in the other countries, at values between 1 and 2, again with greater oscillations in the US and Canada than in the other three graphs. As already noted, the low temperature component $T10_{std}$ exhibits essentially a mirror image trend to that of $T90_{std}$, but over negative values. That is, both contribute significantly to their respective composite indices increasing trends.

The findings are quite different for the remaining three components; i.e. the maximum 5-day precipitation (P_{std}), the drought (D_{std}) and wind power (W_{std}). In the Iberian Peninsula and in France the 5-year seasonal averages of these three variables exhibit a stationary behaviour, with small oscillations around their 0-mean. These do not contribute as significantly to increase of the PACI in Portugal, the SACI in Spain or the FACI in France. In brief, we can conclude that the increases in these indices are essentially due to the sea level, plus the high and low temperature components.

By contrast, North America experienced a significant increase in the maximum five-day precipitations (P_{std}) after the reference period. Its increasing trend shows some periodicity. With regards to droughts, the land areas of the US and Canada are very large, each region having different dry periods. Overall, the drought component (D_{std}) does not show a clear trend, but has remained slightly smaller after the reference period. Thus the trends in the precipitation (P_{std}) and drought (D_{std}) components both point to wetter weather in the US and Canada, compared to France or the Iberian Peninsula.

Even if the contribution of each component of the Actuaries Climate Index™ differs for the Iberian Actuarial Climate Index and the French Actuarial Climate Index, due to the distinct geography of each country, their composite indices show a similar increasing trend. Moreover, the index values are themselves similar, ranging from -0.5 to 1.5. Particularly in recent years, all 3 composite indices have reached the value of 1. This indicates that climate change has led to a similar increase, as a multiple of the standard deviation, both in the frequency and severity of extreme weather events, in France, Portugal, Spain or the US and Canada, as compared to the 1961-1990 reference period. In summary, the occurrence of extreme climate events is becoming increasingly common, overall, in all these regions. For a more detailed analysis and high-resolution maps of FACI per region, season and climate variable, the interested reader is referred to the Appendix.

1.2.5. Insurance applications

The sections above discuss the construction of actuarial climate indices. Before looking in more detail at the link between climate change and mortality, and to complete this first chapter, we give here a short survey of insurance applications of actuarial climate indices. More precisely at how these indices can help quantify the impact of climate change on the balance sheets of insurance companies and, therefore, its impact on the sustainability of the insurance business.

For example, Kim et al. (2016) uses regression to link the occurrence of heat waves to deaths from heat disorders in Korea. Similarly, using US data, Miljkovic et al. (2018) shows that weather

events related to climate change significantly contribute to property damages, which in turn impact on mortality rates. On the same theme, Crisóstomo Mazaira (2022) finds strong correlations between excess mortality and the 95-percentile of temperature highs, for most regions of Spain. This builds on the early work of Díaz et al. (2015) that looked at the relation between extreme temperatures and mortality in Madrid. More advanced modeling, such as extreme value theory, helps Li and Tang (2022) analyze joint extremes in temperature and mortality, using a bivariate peaks–over–threshold (POT) approach, to unveil the strongest type of dependence for US data.

One technique used commonly by actuaries to predict future mortality improvements is the so–called Lee–Carter model, (see Lee and Carter, 1992). In a series of papers, the method has been extended to include explanatory terms, including one based on a heat index (see Seklecka et al., 2017, 2019). These successfully link the physical climate risk, through the index, to the mortality risk predictions. Chapter 2 gives more details on the relation between heat, humidity and excess mortality, while Chapter 3 focuses on the relation between heat waves and human mortality in France. For additional literature on the impact of climate change on health and life insurance (see Bhattacharya-Craven et al., 2024, and Chapter 3, plus the references therein).

Finally, for references on the application of climate indices to non–life insurance see, for example, Garrido et al. (2023) that details the design and pricing of a parametric insurance product based on the French actuarial climate index (FACI), or the recent survey paper Zhou et al. (2024) that list several other studies linking, climate risk, indices and insurance losses, both in life and non-life.

2

Heat waves and mortality

2.1. Heat and health

Heat has long been known to impact health, and most people have already experienced at least mild symptoms of heat stress. While the first symptoms of heat stress may be light, prolonged exposure to heat can have severe effects on health and even lead to death. Older people are particularly vulnerable to heat, because of a reduced capability of sweating (Dufour and Candas, 2007), a larger prevalence of pathologyies that increase with heat stress and potentially reduced mobility among other factors (Åström et al., 2011).

While adverse impacts of heat on health have been known for a long time, robust data for quantifying these impacts has only become available over the course of the 20^{th} century. An important reason is that both reliable meteorological observations and health impacts are necessary to establish a robust relationship between heat and health impacts. While meteorological data is nowadays readily available, collecting adequate data on health impacts remains a complex task (Adélaïde et al., 2022). Many types of pathology can be caused by heat (Song et al., 2017) and therefore the required data collection needs to cover many different sources. Furthermore, the availability and quality of relevant data depends on the responsible health authorities' ability to categorize and store adequately information about pathologies.

The complexity can be reduced by focusing solely on the impact of heat on mortality, as the result (death) is well defined and as information about deaths is more widely available. It is also the most serious impact to address, and this is also why we focus on the impact of heat on mortality here.

Deaths during a heat wave can occur for many reasons (Song et al., 2017), and not all recorded deaths are related to heat during such events. But the total number of daily deaths is generally larger during heat waves than during the same time of the year without such an event. This concept is known as excess mortality, and it has widely been used as an indicator of heat related deaths. For instance, during the summer heat wave of 2003 in Western Europe, 14,802 excess deaths were recorded in France, 2,045 in England and Wales and 3,134 in Italy (Kovats et al., 2004). Heat waves with excess mortality have unfortunately been recorded in many places around the world such as in Western Russia (Barriopedro et al., 2011), Houston, Texas, USA (Zhang et al., 2015), Adelaide, Australia (Faunt et al., 1995), Ahmedabad, India (Azhar et al., 2014) or Rio de Janeiro, Brazil (Geirinhas et al., 2019).

Moreover, increases in mortality are most apparent during heat waves, but research has shown that mortality increases systematically above a certain optimal temperature (Gasparrini et al., 2015a). These findings are particularly worrisome in the light of global warming, as it is virtually certain that heat stress and heat waves will increase according to the last IPCC report (Seneviratne et al., 2021). This raises the question of how global warming will affect future mortality and what actions are appropriate to reduce heat-related deaths.

2.2. Building a model to predict excess mortality from heat waves

Even though available data shows clear evidence of the link between heat and increased mortality, modelling mortality based on heat data is yet another challenge. Different aspects of heat and heat waves may each have distinct impacts on mortality (Pascal et al., 2006), and modelling the combined impact is a serious challenge. For example, it is not only temperature that affects heat stress, but also humidity, radiation (sunlight and thermal radiation from surrounding structures) and wind (Di Napoli et al., 2019). The time of exposure, the intensity of the heat wave and the presence of relief periods in between, all can have an impact on heat-related deaths as well (Gasparrini and Armstrong, 2011), as do the infrastructure to protect from heat (well isolated buildings, presence of air conditioning), the health-services infrastructure and the awareness of the appropriate behavior during heat waves (Bouchama et al., 2007).

An adequate strategy to tackle this challenge starts by separating the exposure to environmental factors (temperature, humidity, etc.) from factors of vulnerability of the population. The reasoning for this is that we can tackle the two aspects independently. As mentioned previously, different environmental factors contribute to the perception of heat: temperature, humidity, radiation and wind. When assessing the impact on health of a specific situation, all these factors need to be taken into account, but when considering links between heat waves and mortality in a more aggregate sense, studies have shown that it is often sufficient to consider the effects of temperature and humidity, or even the effect of temperature alone (Pascal et al., 2006; Gasparrini et al., 2015a; Song et al., 2017). This simplifies the analysis greatly as temperature tends to be spatially more homogeneous than sunlight or wind, and thus require a less dense set of measurements.

In this work we use the NOAA Heat Index as a measure of heat (Rothfusz and Headquarters, 1990). This index takes into account the effects of temperature and water vapor (humidity). It was specifically designed as an indicator for heat impact, has been widely used in research and for issuing heat advisories (Hawkins et al., 2017), and even in the last IPCC report (Gutiérrez et al., 2021). Here we use the equivalent in degrees Celsius as unit for the Heat Index, that we denote as °C for simplicity.

2.2.1. Observations of heat waves and mortality

Equipped with a suitable index for heat, we start building a model to predict excess deaths from heat by plotting heat index data against deaths, in a region of interest. In our case a region can be any geographical area of land of interest here. Figure 2.1 shows daily data of heat and deaths in France during the summer months (June-August) as a function of the average heat index in France. We note that the number of deaths tends to be larger when the heat index is larger as well. There is some spread in deaths for a given heat index, due to variations in deaths from other causes than heat and possibly from a few hypotheses, but this is normal and expected; overall, the figure suggests that the data used was appropriate to illustrate the heat impact on deaths.

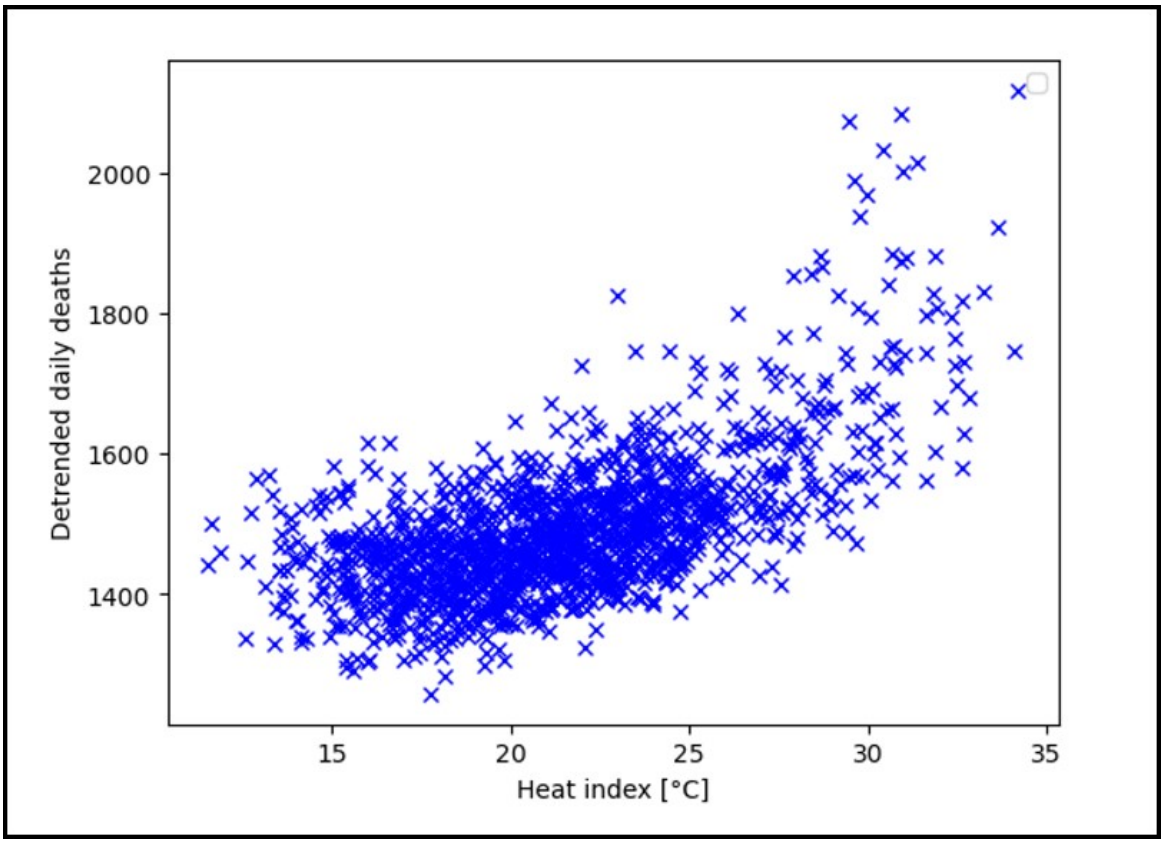

Figure 2.1. Detrended number of daily deaths vs the average Heat Index in France for every day of the summer months from 1970 to 1990. The heat index is calculated from ERA5 data and the detrended number of daily deaths data from the french National Institute of Statistics (INSEE).

Before proceeding further with building a simple model of heat-death prediction, it is worth looking at two interesting implications of Figure 2.1. First, in order to calculate the heat index over France, ERA5 reanalysis data (Hersbach et al., 2020) with a spatial resolution of 12km x 12km was used, just as in Chapter 1. This dataset naturally has biases compared to local observations, because of the resolution and for other technical reasons. But this is not important here, because days with a higher heat index in observations will also tend to have higher heat index values in ERA5 data, and therefore the relationship of larger numbers of deaths

with larger values of the heat index is conserved. Second, as heat is rarely very localized, exploitable results can generally be obtained even for larger regions, if desired, such as for France in this case. Of course, if regions become too large (examples: USA or Russia) or span different climate zones (example: Chile), the statistical information may eventually be lost. As a rule of thumb, if it is unlikely that unusually cold weather persists in a large part of a studied region during an occurrence of a heat wave in another large part of the region, then we can say that the choice of the region is suitable to study heat related impacts.

Figure 2.1 shows the tendency of increasing mortality with increasing Heat Index. However, the number of data points renders it difficult to discern the precise shape of a potential deterministic relationship. Therefore, we take averages of deaths over intervals of 1°C of Heat Index and plot the resulting values as a function of deaths (Figure 2.2).

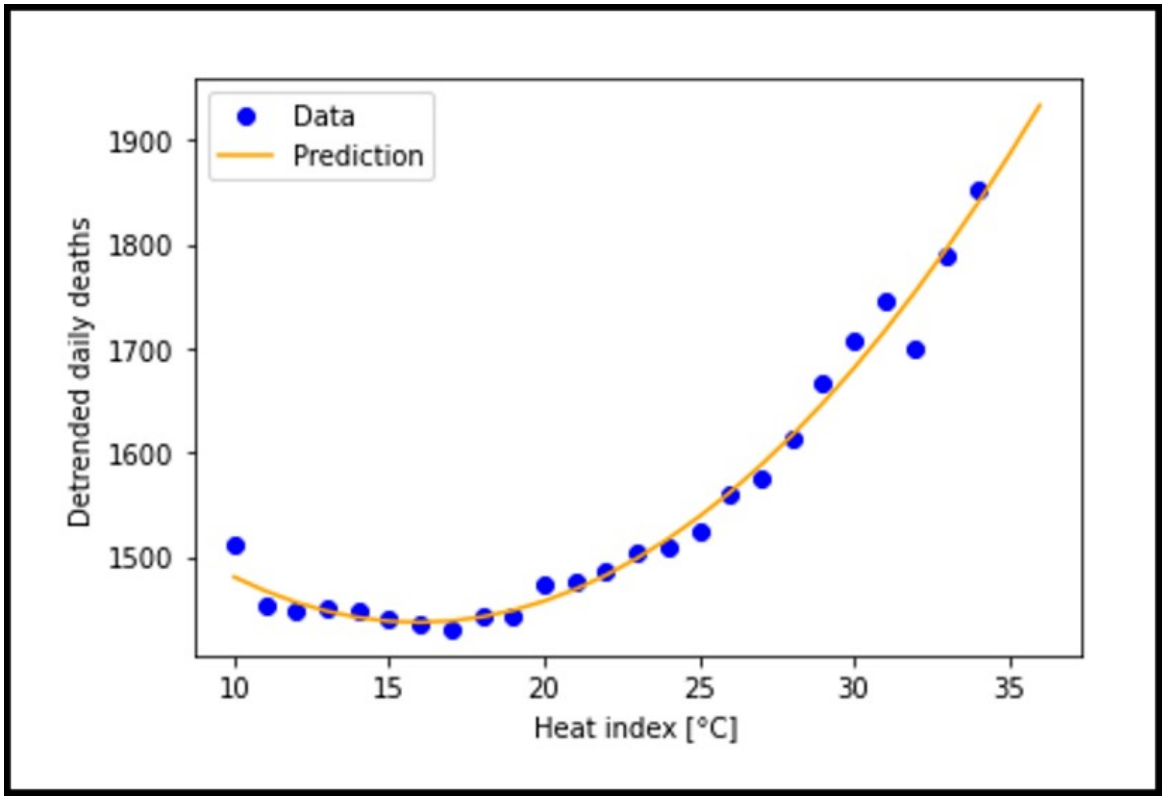

Figure 2.2. Average detrended number of daily deaths vs average Heat Index (1°C intervals) in France for every day of the summer months from 1970 to 2003. The heat index was calculated from ERA5 data and the detrended number of daily deaths from INSEE. Fitted 2^{nd} order polynomial (orange curve).

The figure reveals two things. First, in this deterministic approach, the function is convex in nature implying that the rate of increase of deaths increases with an increasing Heat Index. Second, the resulting relationship between Heat Index and deaths is reasonably smooth implying that the available data is sufficient to represent an underlying deterministic relationship.

2.2.2. Model design and testing

The simple convex relationship between deaths and heat index found in the deterministic approach can be approximated satisfactorily with a second order polynomial (Figure 2.2). Similarly, a second order polynomial can also be used in conjunction with a generalized linear model to obtain a reasonable fit for the stochastic representation of the data (Figure 2.3).

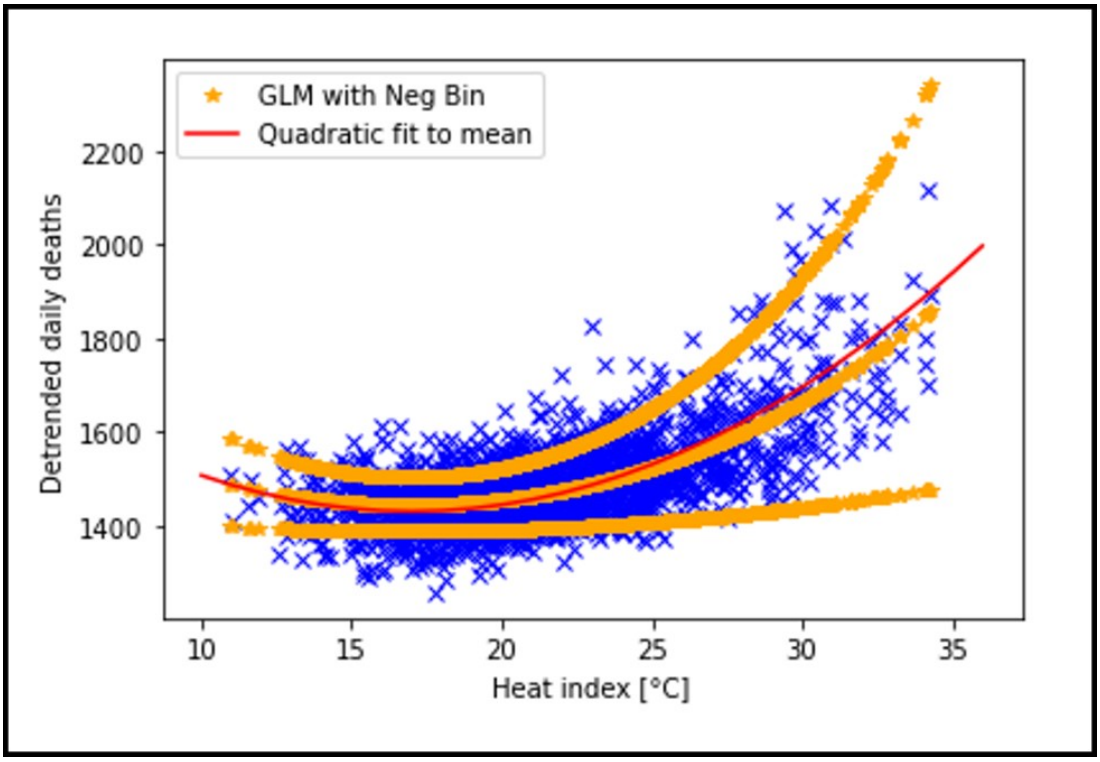

Figure 2.3. Deterministic 2^{nd} order polynomial fit (red line) and stochastic generalized linear model (GLM) fit; negative binomial distribution with log–link function (yellow). The orange curves show the best estimate (central curve) and the upper and lower bounds of the confidence interval. In blue the detrended number of daily deaths in France vs the average Heat Index in France, every day during the summer months from 1970 to 1990. Heat index from ERA5 data and detrended number of daily deaths data from INSEE.

Having found a seemingly adequate fit for the data, we can now proceed to test the model's capacity to predict deaths from the heat index. For this purpose, we divide the dataset into different parts. For France, we obtained daily data of the number of national deaths from 1968 until 2022 from the Institut National de la Statistique et des Etudes Economiques (INSEE). To divide the datasets into different parts, we need to take three effects into account. First, in order to avoid the effects of changing demographics we subtracted the overall trend. Second, to avoid the effect of the COVID19 pandemic, we omitted the years from 2020 to 2022. Third, after the deadly heat wave of 2003, an adaptation plan was implemented in France to reduce the impacts of heat waves (Pascal et al., 2006), which likely changed the relationship between deaths and the heat index (Fouillet et al., 2008). Therefore, we divide the dataset into three time periods: 1970-1990, 1991-2003 and 2005-2017. We will mostly focus on the first two

time periods and keep the 2005 to 2017 time period for discussion.

We train our models (determine the free model parameters) on the 1970-1990 period and test the results on the 1991-2003 period. The test is not aimed at predicting the deaths correctly for every day, but on predicting the overall number of deaths over the summer season. The results of the test show that the prediction of the summer deaths over the training period exhibits errors (16%-17% relative to the spread) but captures years with small and large numbers of summer deaths satisfactorily (Figure 2.4). The models also capture the years with a small and large number of deaths satisfactorily during the test period. But in every year except 2003, the predicted number of deaths is larger than the observed number.

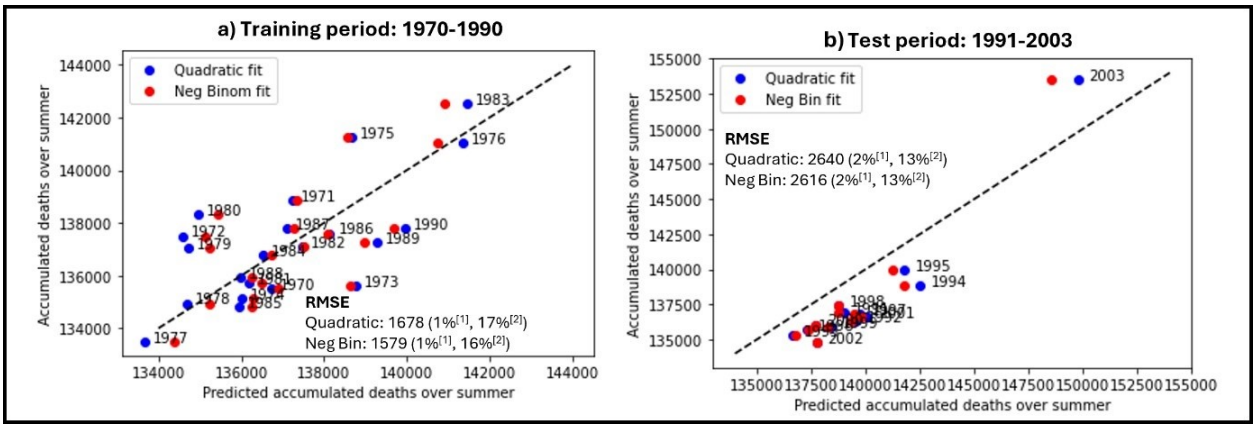

Figure 2.4. Prediction of summer deaths (June-August) in France for different years, deterministic (blue) and stochastic (red) approaches. Perfect prediction (dashed line); marks below indicate model overestimation of the number of deaths and marks above indicate underestimation. Training-period results on the left (Panel a) and test-period results on the right (Panel b). Net RMSE values, from left to right: RMSE[1] relative to the mean value of accumulated summer deaths over the respective time period, and RMSE[2] relative to the spread of accumulated summertime deaths over the respective time period.

To understand why the models overestimate the predicted number of deaths during the test period, except for 2003, it is useful to visualize the number of deaths as a function of the Heat Index in the two time periods with the deterministic approach (Figure 2.5). For given values of the heat index above 25°C, the expected mortality was higher in the 1970-1990 than in the 1991-2003 period (Figure 2.5). This means that the vulnerability of the population to heat has decreased between the two time periods. Hence, the model assumed too high a vulnerability for the period from 1991-2003 and thus predicted too many deaths.

We mentioned earlier that the vulnerability of the population to heat needed to be modelled and our models do this by adjusting how the number of deaths increases with heat (the quadratic parameter in our models). Hence, if the population is more vulnerable to heat, the number of deaths increases faster with the Heat Index as is the case in the 1970-1990 period when compared to the 1991-2003 period (Figure 2.5).

The results also highlight an important aspect of modelling vulnerability. The choice of the reference period for which the vulnerability is determined is crucial, as vulnerability can and has evolved over time. Therefore, studies performed at different times, even when performed over the same region, can suggest different heat-related deaths. This also means that uncertainties in the future evolution of the vulnerability must be considered when projecting future heat deaths.

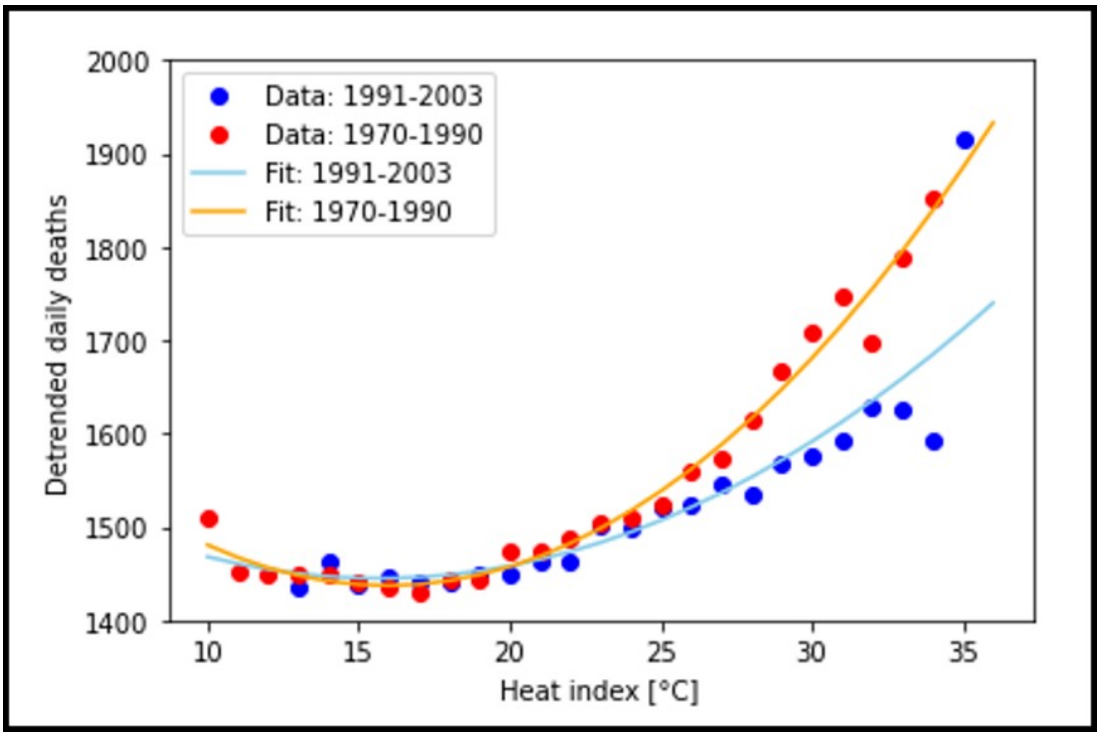

Figure 2.5. Average detrended number of daily deaths vs average Heat Index (1°C intervals) in France, every day of the summer months from 1970 to 1990 (red) and from 1991 to 2003 (blue). Data dots and fitted 2^{nd} order polynomial (solid lines).

Given that our models generally overestimate the number of summer deaths, why is the number of deaths underestimated in 2003? It can be noted in Figure 2.5 that the average number of deaths for the highest reported Heat Index (HI) during the 1991-2003 period is significantly larger than all values of HI. This may in part be because of the small number of days with such high values of HI, but it can also be indicative of a sharp increase in mortality when a critical value of HI is exceeded.

To highlight this, we explore the relationship between the Heat Index and the number of deaths in the South Region of Brazil (Região Sul do Brasil), between 1998 and 2017 (Figure 2.6). This time period is divided into two (1998-2007 and 2008-2017). The number of deaths was calculated from data obtained from the Instituto Brasileiro de Geografia e Estatística (IBGE). During the first time period, the number of deaths increases with the Heat Index (Figure 2.6).
We find a similar relationship between the two variables in the latter time period as well, but there is another, new phenomenon: above about 45°C the number of deaths sharply increases

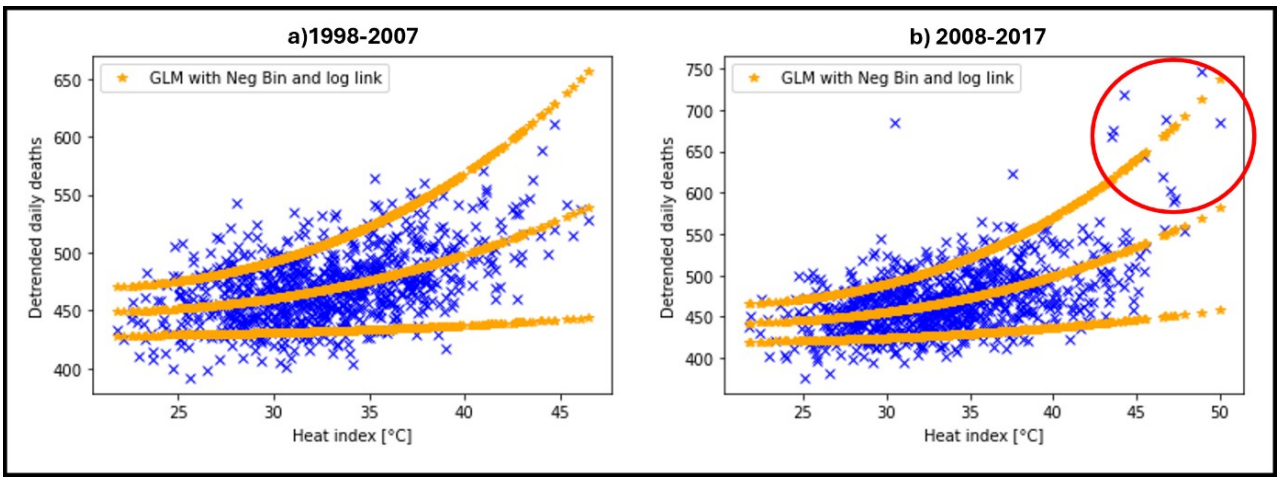

Figure 2.6. Stochastic generalized linear model fit with negative binomial distribution and log–link function, (orange). The central orange curves show the best estimate and the upper and lower bounds of the confidence interval. In blue the detrended number of daily deaths in the south region of Brazil. Detrended daily deaths vs the average Heat Index in the same region, every day during the summer months from 1998 to 2007 (panel a) and 2008-2017 (panel b). Heat index from ERA5 data and detrended number of daily deaths data from IBGE (brazilian National Institute of Statistics).

(Figure 2.6). The largest values of the Heat Index in the latter time period exceed all values observed during the first time period, suggesting that this is indeed a new type of phenomenon. Therefore, a possible interpretation is that the region entered a regime of temperatures to which it was not adapted, leading to a sharp increase in deaths. This interpretation would be similar to the one for the large number of deaths recorded during the 2003 heat wave in France and other parts of western Europe. But the daily values of Heat Index in France recorded during the 2003 heat waves did not even reach 40°C, on average, and would thus not have posed substantial problems in the South Region of Brazil.

These results highlight two important aspects. First, the impact of heat on mortality strongly depends on the location. Second, above certain location-specific critical values of heat indicators, the number of deaths may increase sharply. These aspects have already been discussed in the scientific literature before (e.g. Gasparrini et al., 2015a), but it is important to consider their implications when wishing to model future projections of heat related mortality. The presence of unknown threshold values of heat that could lead to a sharp increase in mortality is particularly worrisome, because of its implications for humans and because it is impossible to capture with a data driven model. Figure 2.5 can help us illustrate the magnitude of the excess deaths that can occur in these cases: The outlier value with a high number of deaths for a Heat Index of about 31°C for the period from 2008 to 2017 was caused by a fire that killed over 240 people (the "Kiss nightclub fire"), and this value is comparable to the number of daily excess-deaths for large values of heat index. But even in the absence of such extreme cases, it is important to remember that the number of daily deaths increases substantially with heat. Therefore, the presented modelling approach still accounts for most heat-related deaths in many cases, be-

cause extreme heat cases are comparably rare. Hence, the presented modelling approach is adequate to model the future statistical increase in mortality from global warming.

2.3. Future heat projection

In the past sections we have seen a number of factors that are important when modelling heat-induced mortality as well as two simple models designed to translate values of the Heat Index to mortality. To project the future number of daily deaths, projections of the vulnerability of the population and of the exposure to heat must also be taken into account. In this subsection, we focus on projections of heat and thus the climate, while projections of vulnerability will be discussed in future works.

State-of-the-art climate projections are performed with so-called Earth-system models (Flato, 2011). They consist of a general circulation model of the atmosphere coupled to a general circulation model of the ocean and to sea-ice and land surfaces. These general circulation models are built on physical principles. They model the equations of motions and other relevant physical processes, such as phase changes or radiation. As the governing equations, that typically are differential equations, do not have analytic solutions, they need to be solved with so-called numerical methods. For this purpose, the Earth system is represented on a grid, with each grid cell having one value of relevant variables such as temperature (Figure 2.7).

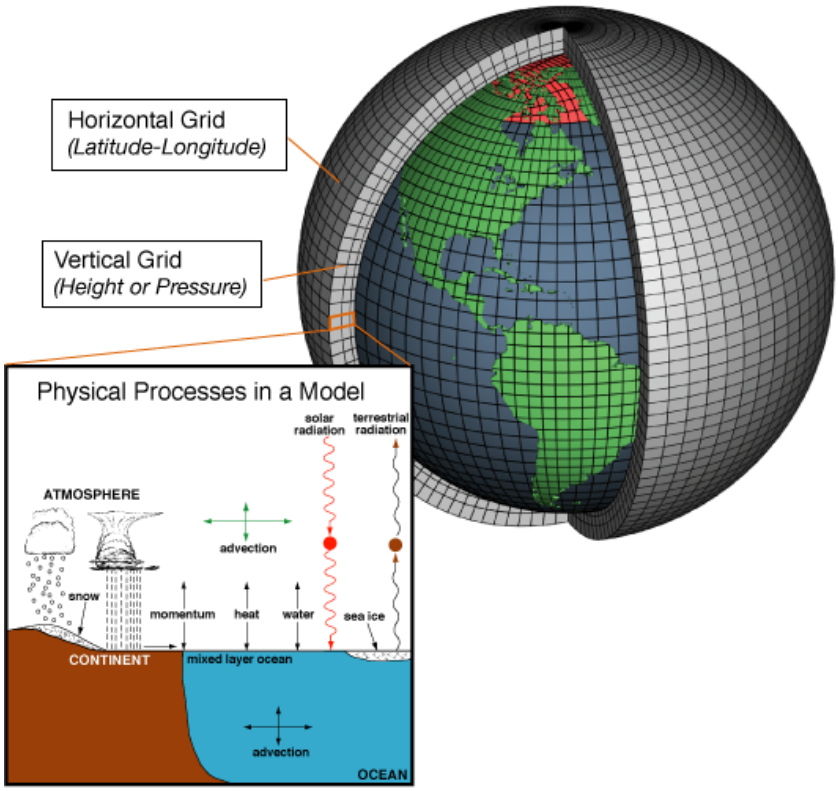

Figure 2.7. Schematic representation of an atmospheric component in a climate model with grid and examples of physical processes.
Source: celebrating200years.noaa.gov.

Computers are then used to solve the resulting equations by stepping forward in time from an initial state. Relevant processes that occur at finer spatial scales than the grid of the model, are represented with sub-models called parameterizations. Examples of processes that are often treated in this manner are radiating processes, phase changes such as condensation, and turbulent exchanges between the surface and the atmosphere. Generally, the finer the resolution of the grid of a model is, the fewer of the relevant processes need to be modelled with sub-models. But finer grids also imply more grid cells, and thus require much more computing power. Therefore, the processes that are represented with sub-models tend to be the same in most climate models. However, the sub-models themselves differ between the models and are a major source of inter-model differences.

Climate simulations are performed by feeding the model an initial state as well as boundary conditions such as insolation, topography, bathymetry, aspects of atmospheric compositions and the evolution of insolation, and letting the climate model move forward in time. Unlike weather forecasts, climate simulations do not have the objective of predicting the correct future weather patterns at the correct time and location. Instead, they only need to represent statistical properties of the Earth system correctly, such as the average temperature in Lyon, the correct frequency of storms in Brittany or the year-to-year variability of precipitation in Nice. Therefore, even though climate simulations represent a realistic evolution of weather patterns to represent the climate, the weather patterns do not need to occur simultaneously with real world events. For example, realistic climate simulations need to represent a realistic number of extreme heat waves over a given period of time, but it is not expected that they place an extreme heat wave over Western Europe in 2003. This is because the climate is defined as the statistical properties of the Earth system (under steady climate conditions).

The description and knowledge of climate is very useful, since weather patterns cannot be predicted far in the future because of the chaotic nature of the atmosphere. But a statistical description is possible for sufficiently steady boundary conditions and appropriate timescales. This is because the energetic and dynamic constraints on the Earth-system prevent major long-term changes for steady boundary conditions. Conversely, changes in the boundary conditions such as changes in CO_2 concentrations force the Earth-system to respond to these new constraints and thus induce climate change.

Typical timescales for climate analysis are 20 to 30 years. In principle, the longer the timescales the more robust the statistics, but it is often more practical to use these intermediate timescales of 20 to 30. These timescales limit the amount of data required for the analysis while still allowing for a sufficient number of occurrences of many main climate events, such as annual cycles or ENSOs.

The ongoing climate change is virtually certain to be caused by increasing concentrations of greenhouse gases caused by anthropogenic emissions that constitute a change in boundary conditions (Masson-Delmotte et al., 2021). Greenhouse gases reduce the emission of thermal radiation from Earth's surface and lower atmosphere to space, leading to an accumulation of energy at the surface and thus to surface warming. Therefore, in order to obtain adequate climate projections of future warming and climate change, assumptions about the future scenario of greenhouse gas emissions are necessary. The most commonly used climate change

scenarios are the Representative Concentration Pathways (RCP, Meinshausen et al., 2011) and the Shared Socioeconomic Pathways (SSP, Meinshausen et al., 2019). Both, model a narrative of future economic, social, political and technological developments that lead to different future trajectories of greenhouse-gas emissions. These future emission trajectories are then fed to climate models for projections of future warming. The largest source of state-of-the-art climate projections, that are climate simulations of the future, is the Coupled Model Intercomparison Project (CMIP). It regroups climate simulations of the future from most climate modelling centres in the world following a stringent methodological approach based on scenarios. For the latest phase, CMIP6 (Eyring et al., 2016), the SSP scenarios were used and for its predecessor, CMIP5 (Taylor et al., 2012), the RCP scenarios were used. A large amount of climate-simulation data generated within the CMIP framework is freely and publicly available (a registration may be necessary depending on the exact data framework) and this is the data we use.

Climate simulations provide a large range of possible climate variables including all variables required to characterize heat: Temperature, humidity, radiation (sunlight and thermal radiation from surrounding structures) and wind. For the Heat Index, we only require temperature and humidity, both of which are widely available on the CMIP repositories. With the help of climate projections, we can thus easily calculate the future Heat Index in different emission scenarios and for different climate models.

Before turning to the projections of future mortality based on projections of future heat, it is worth briefly addressing uncertainties in future climate projections.

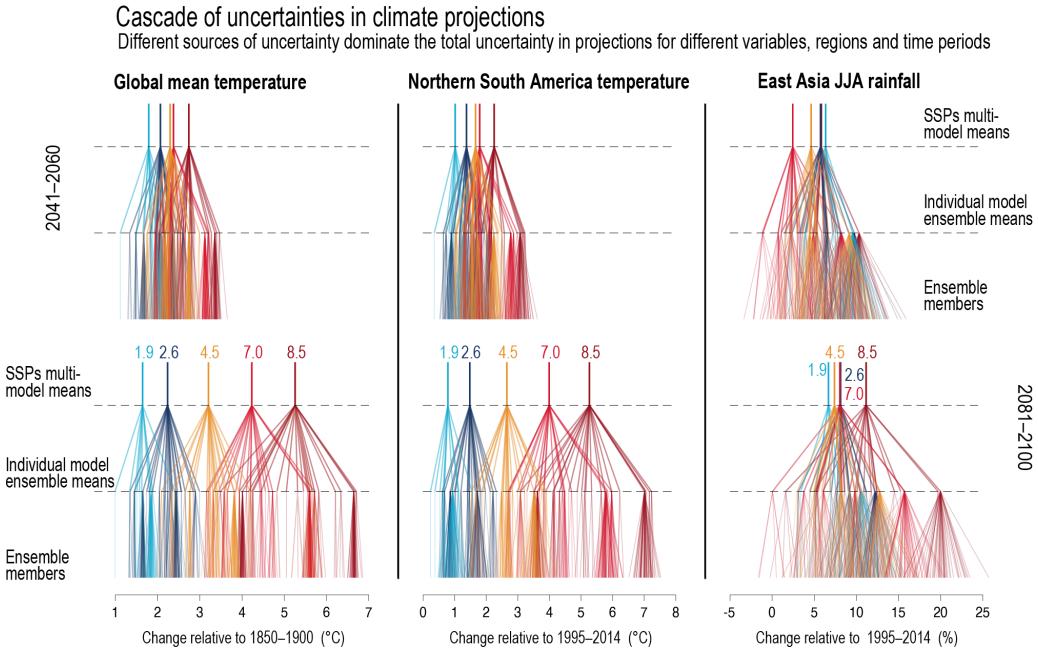

Figure 2.8. Cascade of uncertainty in CMIP6 climate projections. The first separation of lines comes from differences in emission scenarios, the second from differences between models, and the last from differences between initial states.

Source: Chen et al. (2021).

These uncertainties are an inherent part of climate projections and always need to be considered in the scientific discourse of the future climate. The uncertainties have three main sources: Uncertainties in future greenhouse-gas concentrations, uncertainty stemming from climate models, and uncertainties stemming from differences in the initial state of climate simulations (Figure 2.8).

Uncertainties from future greenhouse-gas concentrations are taken into consideration with the scenario approach (RCP, SSP) that leads to a range of different greenhouse-gas and thus climate-change trajectories.

Finally, uncertainties from differences between climate models and from differences in the initial state of the climate simulations are addressed by analyzing so-called ensembles of simulations. Instead of just using the results of one climate simulation per greenhouse-gas emission scenario, multiple simulations (so called ensembles) with different models and different initial states are used. This creates a range of possible future results that can then be interpreted as additional uncertainty. It also allows to tackle another problem of studying climate change: The climate is typically characterized over 20 to 30 years, but during climate change the climate is not steady over such extended periods of time. Using multiple simulations allows us to multiply the number of years of simulation in a given time-period and even with only 5 simulations, we can already obtain twenty years of simulation for any 4-year period.

The next chapter delves more on the relation between heat waves and mortality in France.

3

An actuarial case study: the impact of heat waves on mortality

Climate change impacts are wide-ranging and affect various aspects of the environment, society, and the economy. In recent years, the frequency and intensity of heat waves and cold snaps, and their impact on human mortality, have made climate change a hot topic for the world's major powers. As already explained in the previous chapter, this can lead to heat-related illnesses and deaths, particularly among vulnerable populations. According to recent reports by the World Health Organization (WHO), research shows that 3.6 billion people already live in areas highly susceptible to climate change, and between 2030 and 2050, climate change is expected to cause approximately 250,000 additional deaths per year, from under-nutrition, malaria, diarrhea and heat stress alone. The real question is whether human beings will be able to adapt to climate change in the future, or whether the impact will continue to grow.

In this chapter, the relationship between heat waves and human mortality in France is studied. We first aim to integrate scenario of strong excess mortality due to unusually hot temperatures (like what happened in France in 2003, see Figure 3.1).

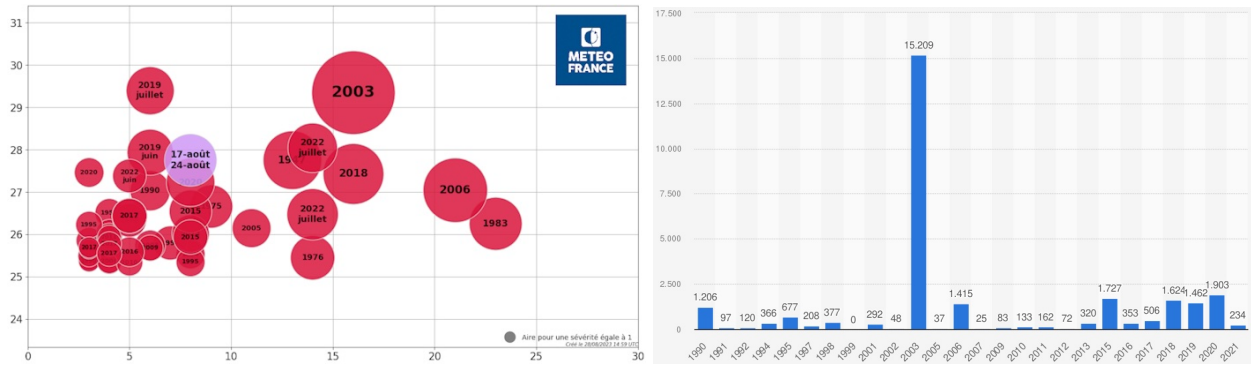

(a) Heat waves bubbles: temperature in °C in y-axis, duration in x-axis.

(b) Yearly excess of mortality (number of deaths), with peak in 2003.

Figure 3.1. Excess mortality due to a heat wave (France, 2003).

Secondly, we would like to capture the impact of global warming over mortality rates. To this

aim, we develop a stochastic model integrating this relationship in an attempt to predict the impact of heat waves on mortality.

3.1. Longevity models, a brief literature review

Longevity models are statistical tools used to predict death rates in a given population. They can be used in a variety of fields, including insurance, finance, public health and demography, to assess risk and plan public policies. These models take into account various factors, such as age, gender, health conditions and historical trends, to estimate the probability of death at different periods of life.

Early life-table constructions represent the foundational stage of mortality modeling, dating back to the 17th and 18th centuries. John Graunt, an English statistician, is often credited with producing one of the earliest life-tables in his work "Natural and Political Observations Made upon the Bills of Mortality" (Graunt, 1662). Using data from London's parish registers, Graunt presented age-specific mortality rates and life expectancy estimates, laying the groundwork for demographic analysis.

Halley (1693), best known for calculating the orbit of Halley's comet, further advanced mortality analysis by constructing life-tables based on the Breslau data, a set of mortality records from the city of Breslau (now Wroclaw, Poland). Halley's work contributed to the development of actuarial science and provided insights into mortality patterns. These early life-table constructions were pioneering efforts in quantifying mortality patterns and estimating life expectancy, based on empirical data. This laid the groundwork for the development of more sophisticated mortality models in subsequent centuries.

This first wave of works led to what are now traditional mortality models. These refer to mathematical frameworks used to describe and forecast mortality patterns, based on historical data. Here are the three key traditional approaches:

1. The **Gompertz model** (proposed by Gompertz, 1825): it describes an exponential increase of mortality rates with age, and is widely used for describing adult mortality patterns. This model is characterized by its simplicity and effectiveness in capturing age-specific mortality trends.
2. The **Makeham model**: introduced by Makeham (1825), it extends the Gompertz model by adding a constant term to account for extrinsic factors such as accidents and diseases unrelated to aging. This model is often used in conjunction with the Gompertz one to provide a more comprehensive description of mortality patterns.
3. The **Heligman-Pollard model**: developed by Heligman and Pollard (1980), it is a two-parameter mortality model that provides a flexible and accurate fit to age-specific mortality rates. This model has been widely used in mortality forecasting and actuarial applications.

These traditional mortality models provide a framework for understanding and analyzing mortality patterns based on age-specific mortality rates.

Then, the next wave of mortality models began in the early 1990s with forecasting mortality models, also known as longevity models. These models are essential tools for projecting future mortality rates and life expectancy, providing valuable insights for actuarial, financial, and public health applications. The most popular stochastic longevity model, the Lee-Carter (LC) approach, was firstly proposed by Lee and Carter (1992). This model offers a straightforward yet effective approach to decompose age-specific mortality rates into two main components: age effects and periods effects. It assumes that the logarithm of the age-specific mortality rates are explained by a linear combination of an age–specific parameter α_x and the product of an age–specific parameter β_x and a time-specific component κ_t, which is coherent with the trends observed in Figure 3.2 (mortality rates decrease over time due to medical improvements or other factors, whatever the age).

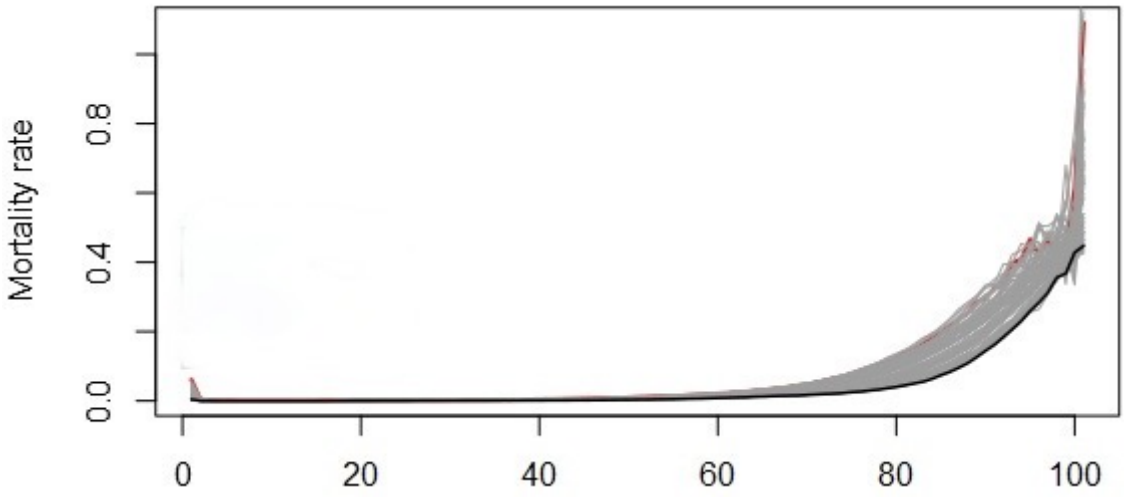

Figure 3.2. Evolution of the exponential relationship between mortality and age: improvement of mortality rates over time.

The LC model can be expressed as:

$$\ln(m_{x,t}) = \alpha_x + \beta_x \kappa_t + \varepsilon_{x,t}$$

where

- $m_{x,t} = \frac{D_{x,t}}{E_{x,t}}$ represents the central mortality rate for age x at time t. $D_{x,t}$ represents the number of people aged x who died in year t, and $E_{x,t}$ the exposure to death for age x in year t,
- α_x is the age-specific intercept term, capturing the baseline level of mortality at each age,
- β_x represents the age-specific slope term, indicating how mortality rates changes with age,
- κ_t is the time-specific index term, capturing the overall trend in mortality rates over time,
- $\varepsilon_{x,t}$ is the error term for random fluctuations (usually defined as independent and identically distributed random variable following a normal distribution).

In the work by Lee and Carter (1992), the model parameters $(\alpha_x, \beta_x, \kappa_t)$ are estimated using historical mortality data through a singular value decomposition (SVD), and the time compo-

nent κ_t is fitted using an autoregressive component or a random walk (with drift).

Over the years, the LC model has been extended and modified to address various challenges and limitations. Extensions include adding age-specific enhancement (Renshaw and Haberman, 2003) incorporating cohort effects (Renshaw and Haberman, 2006), introducing stochastic components to account for uncertainty and refining the modeling framework to improve accuracy and robustness (Cairns et al., 2006; Currie, 2006). For more details and understanding of the early literature on these models, refer to Cairns et al. (2008, 2011). After these stochastic models came the model by Plat (2009):

$$\ln(m_{x,t}) = \alpha_x + \kappa_t^{(1)} + (\bar{x} - x)\kappa_t^{(2)} + (\bar{x} - x)^+\kappa_t^{(3)} + \gamma_{t-x} + \varepsilon_{x,t}$$

where $(\bar{x} - x)^+ = max(\bar{x} - x, 0)$ and the factor $\kappa_t^{(1)}$ represents changes in the level of mortality for all ages. The term with coefficient $\kappa_t^{(2)}$ allows changes in mortality to vary between ages, to reflect the historical observation that improvement rates can differ for different age classes, and $\kappa_t^{(3)}$ is added to capture the observed difference in mortality rate dynamics at younger ages (up to 40/50) in historical data. Finally, γ_{t-x} is capturing the cohort effect as in Currie (2006) and Cairns et al. (2007). This model combines the advantages of the Lee-Carter model and its various extensions, while eliminating their drawbacks.

Later, O'Hare and Li (2012) found that the linear age coefficient of the $\kappa_t^{(3)}$ factor used to capture the observed difference in mortality rate dynamics was insufficient and that an additional quadratic term had to be added. This resulted in

$$\ln(m_{x,t}) = \alpha_x + \kappa_t^{(1)} + (\bar{x} - x)\kappa_t^{(2)} + \left[(\bar{x} - x)^+ + [(\bar{x} - x)^+]^2\right]\kappa_t^{(3)} + \gamma_{t-x} + \varepsilon_{x,t}.$$

In their paper, the model is adapted to the data of the different countries considered, and retains the advantages of the various previous stochastic models.

Note that apart from the Singular Value Decomposition (SVD) method used in Lee-Carter's paper, several other statistical approaches based on probabilistic assumptions have been developed to estimate the parameters of these models. For example, in Brouhns et al. (2002), the authors assume that the number of deaths follows a Poisson distribution (see also Currie (2016), where an approach based on Generalized Linear Models (GLMs) is developed in detail for the Lee-Carter model and its extensions).

None of these models incorporated an exogenous factor related to global warming to try to explain and predict mortality trends in the future. Seklecka et al. (2017) therefore propose a model that incorporates one coefficient related to temperature effects as a proxy for climate change. To explain the evolution of mortality rates as a function of temperature, this model is defined as

$$\begin{aligned}\ln(m_{x,t}) = \alpha_x + \kappa_t^{(1)} + (\bar{x} - x)\kappa_t^{(2)} + (\bar{x} - x)^+\kappa_t^{(3)} \\ + [(a - x)^+ + ct_x(x - a)^+]^2\kappa_t^{(4)} + \gamma_{t-x} + \varepsilon_{x,t}\end{aligned}$$

where ct_x stands for the Pearson correlation coefficient between temperatures and mortality rates, a represents the age range at which this coefficient starts to become stronger and

more stable, and time-dependent factor $\kappa_t^{(4)}$ designed to capture some of the nonlinear and temperature effects. However, although this approach incorporates one term related to temperature, it suffers from crucial issues. In particular, the magnitude of heat waves cannot be taken into account, and their estimated Pearson coefficient is negative (since the effect of the improvement of mortality over time beats the effect of increased temperatures at some times). In reality, one desirable property of the modelling would be to allow for possible increases in mortality rates when temperatures increase.

3.2. Relationship between temperature and mortality

We used open source datasets in order to challenge the well-known relationship existing between temperature and mortality rates. We first describe these data.

3.2.1. Database for mortality

Here we use two databases for mortality: the *Human Mortality Database*[1] (HMD) and the *Short-term Mortality Fluctuations*[2] database (STMF).

The HMD provides detailed information on mortality in several countries. In our study, we consider data on observed deaths in France, each year from 1980 to 2019, and for every age from 20 to 85+. A limitation of this database is that data are only available on an annual basis, yet weekly or even daily death counts are the most objective and comparable means of assessing the extent of short-term mortality increases across countries and over time. In response to the COVID-19 pandemic, the HMD team decided to establish a new data resource: the STMF dataset. Thanks to this database, we now have weekly death data for the French population, by sex and by age group: 0-14, 15-64, 65-74, 75-84 and 85+. This information dates from the year 2000 to the most recent completed week of the current year. We will see that this data will be useful to study the correlation between temperature and mortality. In our study, the HMD mortality database is split in two subsets: 1980-2011 as the training data, and 2012-2019 as the test period.

3.2.2. Data for temperature

Heat waves correspond to abnormally high temperatures, observed for several consecutive days. However, there is no universal definition of the phenomenon: the temperature levels and duration of the episode used to characterize a heat wave vary from one region of the world to another, and from one area to another (climatological characterization, research activity, meteorological vigilance). In France, a heat wave is defined by precise statistical criteria, which depend on the national heat index. The national heat index is defined as the daily temperature averaged over 30 French weather stations (Nice, Marseille, Caen, Cognac, Bastia, Dijon, Besançon, Montélimar, Brest, Nîmes, Toulouse, Bordeaux, Rennes, Châteauroux, Nantes, Orléans, Agen, Reims, Nancy, Nevers, Lille, Clermont-Ferrand, Pau, Perpignan, Strasbourg,

[1] www.mortality.org
[2] https://www.mortality.org/Data/STMF

Lyon, Le Mans, Bourg- Saint-Maurice, Paris, Poitiers). According to Météo-France, a heat wave is defined as a phenomenon in which the daily value of the national heat indicator reaches or exceeds 25.3°C and remains at or above 23.4°C for at least three days. Moreover, a heat wave is a phenomenon in which an episode of high temperatures is observed both day and night, with specific thresholds defined for each French department. In view of this, we worked with two different databases.

The first database comes from the Goddard Institute for Space Studies[3] (GISS), and the second from the Météo-France website[4]. GISS is an American research laboratory specializing in the study of Earth's atmosphere and exoplanets. As such, it is one of the main players in the study of global warming. Through the GISS platform, we have access to average temperature measurements on a monthly basis, and over an observation depth ranging from 1950 to the present day, depending on the meteorological station selected. The problems encountered when extracting data from this platform lie in the presence of missing data for certain time ranges and for certain weather stations. It should also be noted that of the 30 stations defining the thermal indicator, only 14 are available on this platform. Based on these constraints, we calculate the thermal indicator using temperature measurements taken at weather stations in the following cities: Bordeaux, Brest, Dijon, Lyon, Marseille, Montélimar, Nancy, Nantes, Nice, Perpignan, Reims, Rennes, Strasbourg and Toulouse.

The second database concerns observational data from international surface observation messages (SYNOP) circulating on the World Meteorological Organization (WMO) Global Telecommunications System (GTS). The atmospheric parameters measured include temperature, humidity, wind direction and strength, atmospheric pressure and precipitation height, while observed parameters include sensible weather, cloud description and visibility. All these parameters are measured or observed from the Earth's surface. Depending on instrumentation and local conditions, other parameters may also be available (snow depth, ground conditions, etc.). These data are collected at 3-hourly intervals from over 60 stations in mainland France and overseas, and are available from January 1996 to the present day.

3.2.3. Mortality rate as a function of temperature

Temperature is known to have a U-shaped relationship with mortality. Extreme temperatures, such as heat waves or cold snaps, increase the risk of death, particularly among vulnerable populations such as the elderly, children and people with chronic health problems. A representative study by Fu et al. (2018) of mortality attributable to hot and cold ambient temperatures in India found that most of the relevant health problems due to temperature occurred above the age of 30 years old (yo).

Mortality from all medical causes between the ages of 30yo to 69yo showed excessive risks at moderately cold and hot temperatures. The lowest mortality risk was at 30°C and increased sharply at warmer temperatures, with an average excess risk of around 9% for each degree of temperature increase from 35°C to 40°C. Similarly, the risk of medical mortality increases

[3] https://data.giss.nasa.gov/gistemp/station_data_v4_globe/
[4] https://donneespubliques.meteofrance.fr/?fond=produit&id_produit=90&id_rubrique=32

with decreasing temperatures, with an average excess risk of around 3% for each degree of temperature decrease from $30°$C to $16°$C, at which point the risk curves and decreases.

Mortality risks were similar for all ages and for those aged 70 and over, but with significant and higher risks at warmer temperatures for those aged 70 and over. Similar studies have been carried out for the Chinese population (Renjie et al., 2018) and for other populations (Gasparrini et al., 2015b), with similar conclusions. The differences mainly lie in the thresholds from which excess mortality is observed, keeping in mind that each population has its own intrinsic ability to adapt to extremely hot or cold temperatures (recall that this was discussed in Chapter 2).

Hereafter, to assess the correlation between mortality and heat waves, we focus on summer periods (June to August) and define a set of points $(x_i, y_i)_k$ where x_i represents the number of deaths recorded, y_i the maximum temperature recorded, in the i-th summer week from the first year of study considered, and k represents the age range in the STMF database. We then perform a Pearson correlation test (Pearson, 1985) to select the age at which heat waves have an impact on mortality. This way, we establish a link between mortality peaks and temperature peaks.

In order to decide on some threshold at which warm temperatures are supposed to increase death risk, we should carry out this test for each age. Due to the lack of granularity in the data, we limit ourselves to studying age groups. The results of the correlation test are shown in Table 3.1. The final choice for the threshold related to age is 65yo, which is also in line with the literature on this topic.

	Males		**Females**	
Age range	Pearson statistics	p-value	Pearson statistics	p-value
0 to 14 years old	0.087849	0.243595	0.023190	0.758646
15 to 64 years old	-0.019469	0.796446	0.091434	0.224810
65 to 74 years old	0.225189	0.002510	0.297935	5.3666e-05
75 to 84 years old	0.150618	0.044771	0.180854	0.015699
85+	0.149829	0.045915	0.246246	0.000922

Table 3.1. *Pearson test results for age threshold selection. Strong positive correlation between mortality excess and hot temperature appears from 65yo, both for females and males.*

Note also that the correlations obtained here are almost all positive, which is consistent with the fact that a temperature spike must necessarily result in an increase in mortality and not the other way round. This must therefore be included in the modelling, unlike the SPO model developed by Seklecka et al. (2019) in which the correlation appears negative.

3.3. A new modelling approach integrating heat wave intensity

3.3.1. The model

Based on all these preliminary studies, the new model we propose is expressed as follows:

$$\begin{aligned}\ln(m_{x,t}) &= \alpha_x + \kappa_t^{(1)} + (\bar{x}-x)\kappa_t^{(2)} + (\bar{x}-x)^+\kappa_t^{(3)} + \left[(x_1-x)^+ + c(x-x_2)^+\right]^2\kappa_t^{(4)} \\ &\quad + [(x-a_c)^+][I_t-\bar{I}_t]^+\kappa_t^{(5)} + \gamma_{t-x} + \varepsilon_{x,t}. \end{aligned} \quad \textbf{[3.1]}$$

Firstly, the model construction was based on the integration of a heat wave indicator, equal to 1 if the average summer temperature exceeds the threshold defined by Météo-France, and 0 otherwise. Investigations using this approach led to overlearning. Another limit was that there were few observed heat waves in the historical data, implying a $k_t^{(5)}$ factor with insufficient points to calibrate and make forecasts using standard ARIMA models. An alternative was to lower the Météo-France threshold, but the risk is to loose the notion of heat wave we are trying to capture. All these analyses led to consider a deviation from the average summer temperature to be able to quantify the impact of heat waves, as well as to take into account the magnitude of the heat wave. Digging deeper into the term $[(a-x)^+ + ct_x(x-a)^+]^2$ by Seklecka et al. (2017), we realized that the latter can be modified to take into account only non-linearity in mortality data. In this spirit, we can separate the temperature effect from the nonlinear effects.

The model [3.1] thus preserves the same characteristics as previous models, the only difference being that a new term is added to control the impact of temperature. The parameters c, x_1 and x_2 are considered hyperparameters, chosen by cross-validation, after estimation of the other model parameters. In the second added term, a_c represents the age at which humans become vulnerable to high temperatures. According to the above correlation analysis, we set $a_c = 65$. Finally, I_t represents the mean temperature over the summer period in year t (from 1^{st} of June to the end of August), $\bar{I}_t$ stands for the average of I_t for all t values in the learning period, and the difference $(I_t - \bar{I}_t)^+$ quantifies the magnitude of the impact of temperature on mortality.

3.3.2. Estimation

Estimation of model parameters

The first parameter α_x of the model is not plotted here for conciseness, but is in line with the global aspect of the mortality curve against ages, see Figure 3.2 above. Then, Figure 3.3 provides illustrations of the various time series embedded in our model, as well as the fitted cohort effect.

The calibrated time series as well as other fitted effects are in line with previous publications on this topic, even though our modelling integrates also the effect of heat waves on mortality. At this point, it is not straightforward to interpret this effect over time, which also depends on the ability of the population to adapt to changing climate conditions.

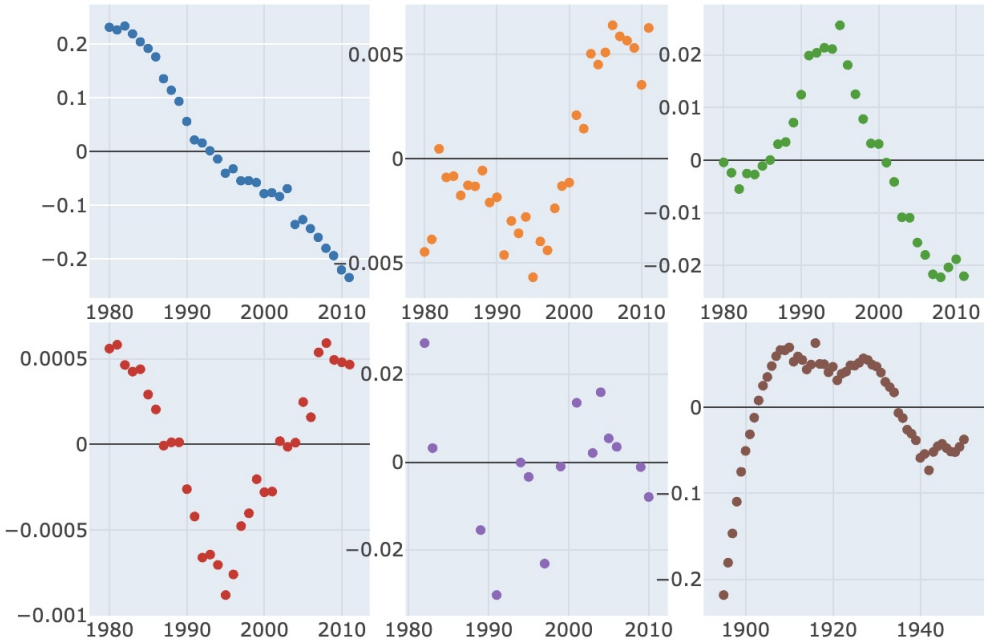

Figure 3.3. Estimated factor values based on data for men in France, aged 20 to 85, between 1980 and 2011. From top left to bottom right: $\kappa_t^{(1)}$, $\kappa_t^{(2)}$, $\kappa_t^{(3)}$, $\kappa_t^{(4)}$, $\kappa_t^{(5)}$, γ_{t-x}.

Selection of model hyperparameters

To assess the model goodness of fit, compare it to other existing models on the basis of the Mean Absolute Percent Error (MAPE) and Bayesian Information Criterion (BIC) criteria. The MAPE formula is intuitive:

$$MAPE = \frac{1}{XT} \sum_{x,t} \frac{|\hat{m}_{x,t} - m_{x,t}|}{m_{x,t}},$$

where $X = 66$ represents the dimension of the age range considered (20yo to 85yo), and $T = 32$ the number of years of the period of study (1980-2011 for the learning period). Using the definition in Cairns et al. (2006), the BIC criterion follows

$$BIC = L(\psi) - \frac{p}{2} \ln(n),$$

where $L(\psi)$ is the log-likelihood of the estimated parameter ψ in the chosen probabilistic framework, n is the number of observations, and p is the number of parameters being estimated. When used on some test sample, MAPE evaluates the ability of the model to extend into the future what happened in the past. The BIC criterion enables to consider a trade-off between the model goodness of fit and its complexity, keeping in mind that the best statistical models are parameterized sufficiently to account for main effects, but have limited dimension to avoid overfitting. This is the so-called parsimonious principle: the more complex the model, the larger the loss of predictive power.

To choose optimal hyperparameters c, x_1 and x_2, we split the training set (1980-2011) into two parts (1980-2005, and 2006-2011) and look for the parameters c, x_1 and x_2 that simultaneously optimize MAPE on these two subsets (once other parameters calibrated on period

1980-2005). Choose $x_1 \in [45, 52]$, $x_2 \in [52, 60]$ and, since it is known a priori that non-linearity is more pronounced at younger ages, then take $c \in [0, 1]$. For illustrative purposes, we set $x_1 = 50$ yo and $x_2 = 60$ yo, and present the MAPE curve and choice of c (see Figure 3.4).

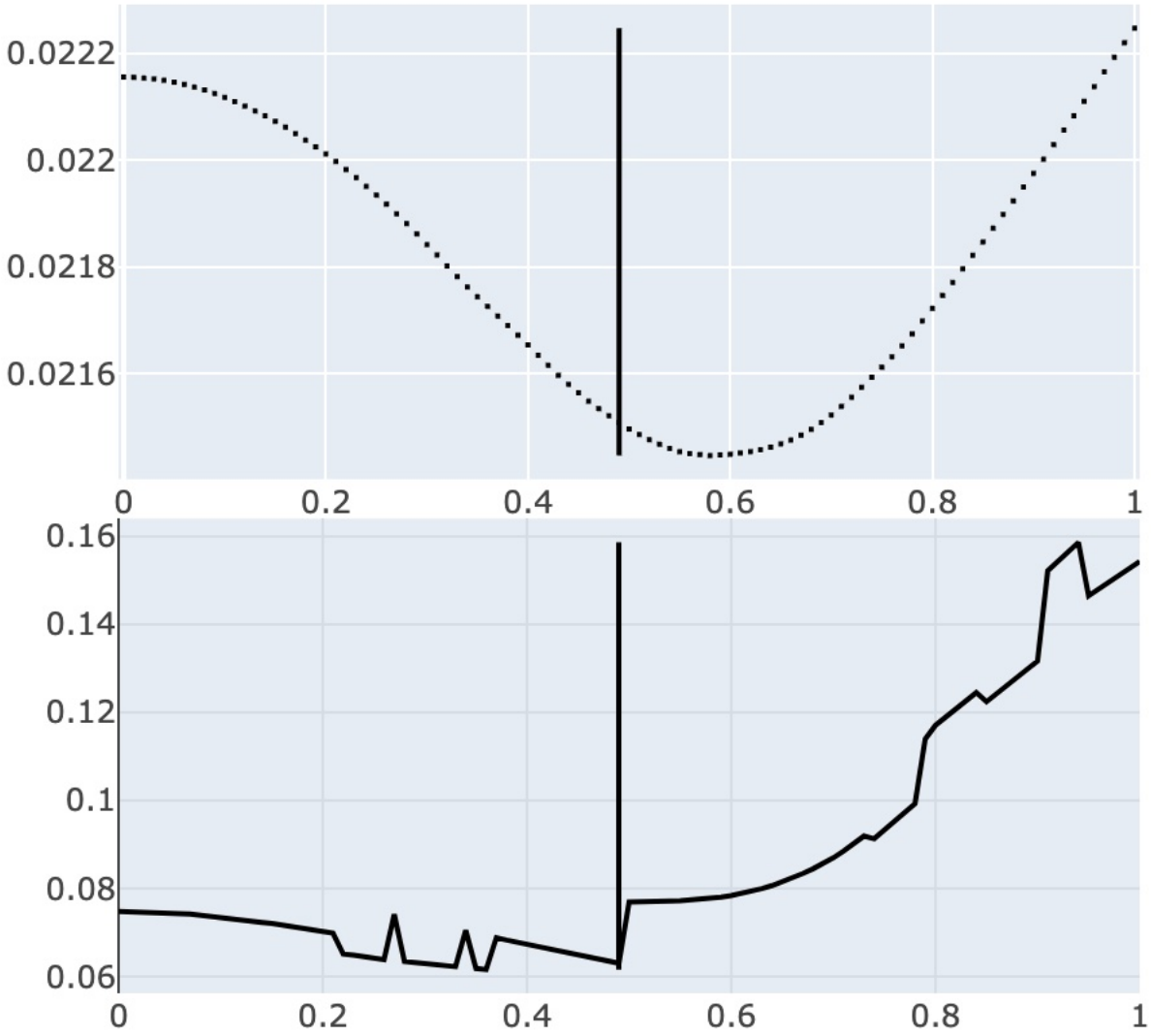

Figure 3.4. MAPE plot. Top panel for years 1980-2005, bottom panel for years 2006-2011, for $x_1 = 50$ yo and x_2 =60 yo (c varying from 0 to 1). The best choice of c being 0.49 here.

The final choice made after testing all the grid values for these hyperparameters in the case of men and women is presented in Table 3.2.

	c	x_1	x_2	MAPE (1980-2005)	MAPE (2006-2011)
Males	0.54	45	60	2.16%	5.50%
Females	0	45	60	3.09%	11.71%

Table 3.2. *Choice of best hyperparameters for both genders.*

Coming back to the selection criteria used, the results of this comparison are shown in Table 3.3.

Models	MAPE males	MAPE females
Lee and Carter	4.87%	4.32%
Plat	3.15%	3.65%
O'Hare and Li	2.81%	3.61%
Seklecka et al.	2.63%	3.30%
Proposed model	**2.52%**	**3.25%**
	BIC males	BIC females
Lee and Carter	-16735.85	-12619.43
Plat	-13468.45	-12266.24
O'Hare and Li	-12958.99	-12331.3
Seklecka et al.	-12842.01	-12189.61
Proposed model	**-12738.59**	**-12176.78**

Table 3.3. *Goodness-of-fit of benchmark models compared to ours, on the learning set (1980-2011). Here, BIC must be maximized and MAPE must be minimized.*

3.4. Forecasting mortality rates with the proposed model

Forecasting consists in generating future values for the time series $k_t^{(1)}$, $k_t^{(2)}$, $k_t^{(3)}$, $k_t^{(4)}$, $k_t^{(5)}$ and γ_{t-x} model components. Given that the data are available up to 2020, we consider the period from 2012 to 2019 as a test period for evaluating the performance of our model (the year 2020 being ruled out due to the COVID-19 pandemic). This evaluation is carried out by comparison on the basis of the MAPE criterion, with the Lee and Carter (1992) model (the classical benchmark in stochastic mortality modelling) and with the Seklecka et al. (2017) model (the sole extension of the Lee and Carter model integrating the temperature effect). The results are reported in Table 3.4. Our model [**3.1**] is generally better adapted to the test data, both for females and males. The predictive power has thus been improved, in addition to the fact that heat waves now would give rise to excess-of-mortality for the older population.

Models	MAPE males	MAPE females
Lee and Carter	8.33%	10%
Seklecka et al.	10.95%	7.99%
Proposed model	**8.01**%	**7.84%**

Table 3.4. *Forecasting performance in terms of MAPE over the test sample (2012-2019). MAPE must be minimised.*

Since the aim here is to incorporate the impacts of heat waves into mortality models, it remains to be checked whether our mortality rate estimates and forecasts meet our expectations. Figure 3.5 shows a comparison in 2003 of actual mortality rates and those estimated by our model and the SPO model (developed by Seklecka et al. (2019)), for ages 75, 80 and 84 yo.

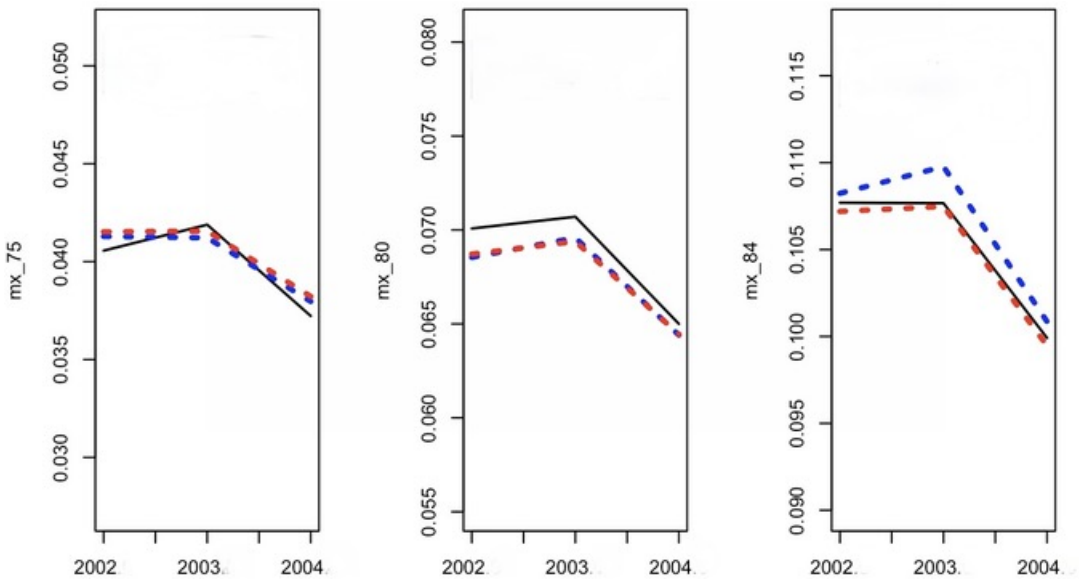

Figure 3.5. Observed and estimated mortality rates in 2003 in France at 75, 80 and 84 yo (from left to right). Observations (**-** line), estimations using [**3.1**] (**-** dashed line) and Seklecka et al. (2019) (**-** dashed line).

The predictions are pretty closed, except for oldest people where our model tends to overestimate the actual observed mortality rate. Furthermore, Figure 3.6 shows a comparison between actual mortality rates and the projections obtained over the back-testing period (2012 to 2019) for men aged 75 and 80 yo using our model and that of Seklecka et al. (2019). As can be seen, our model in [**3.1**] responds better to the 2015 heat peak and is closer to the general trend in mortality rates over this test period.

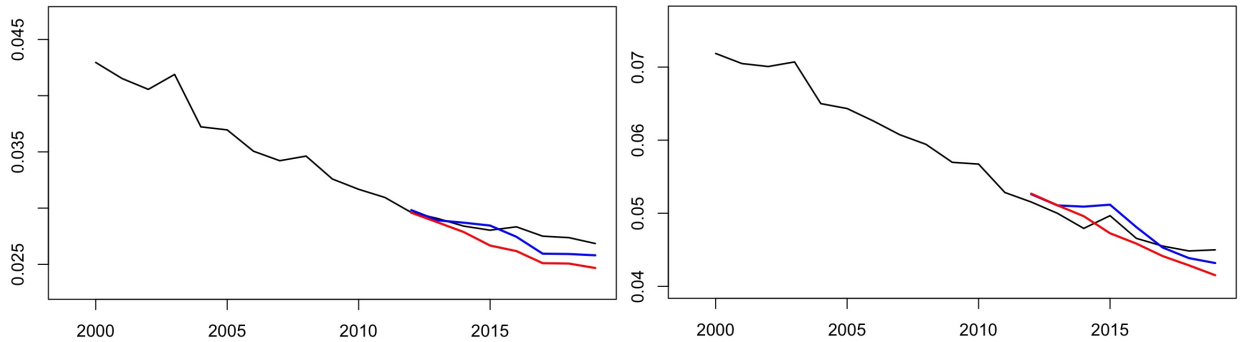

(a) 75 yo. (b) 80 yo.

Figure 3.6. Projected male mortality rates between 2012 and 2019 (**–**: using [**3.1**], **–**: using SPO model, **–**: observed rates).

To give future projections, it is necessary to consider various climate scenarios that allow to integrate uncertainty in mortality predictions. The proposed new model in [**3.1**] uses the mean summer temperature per year, which means that forecasting to future years requires forecast-

ing the future temperatures. As this task is not core in our work, we use various temperature projections from Météo-France; their website DRIAS Climate Futures[5] provides regionalised projections for France of various climatic factors (temperature, wind, humidity, etc.) based on the different RCP scenarios of the 5^{th} Assessment Report of the Intergovernmental Panel on Climate Change (IPCC). In this work, temperature data projected according to the RCP2.6, RCP4.5 and RCP8.5 scenarios were needed, for all regions in France.

For illustration, we focus on scenario RCP2.6, which is the most optimistic scenario. To improve the robustness of our model projections, we build confidence intervals by simulation for different projections, using the second simulation method proposed by Renshaw and Haberman (2008). In our case, given that the parameter $\kappa_t^{(5)}$ does not have the same dimension as the other time series $(\kappa_t^{(1)}, ..., \kappa_t^{(4)})$, we simulated 5,000 multivariate random walk scenarios based on estimates of the vector $(\kappa_t^{(1)}, \kappa_t^{(2)}, \kappa_t^{(3)}, \kappa_t^{(4)})$, and 5,000 future scenarios based on the ARIMA estimates obtained for the parameter $\kappa_t^{(5)}$. With the scenarios obtained, we went back to the mortality rates to produce confidence intervals, available in Figures 3.7 and 3.8.

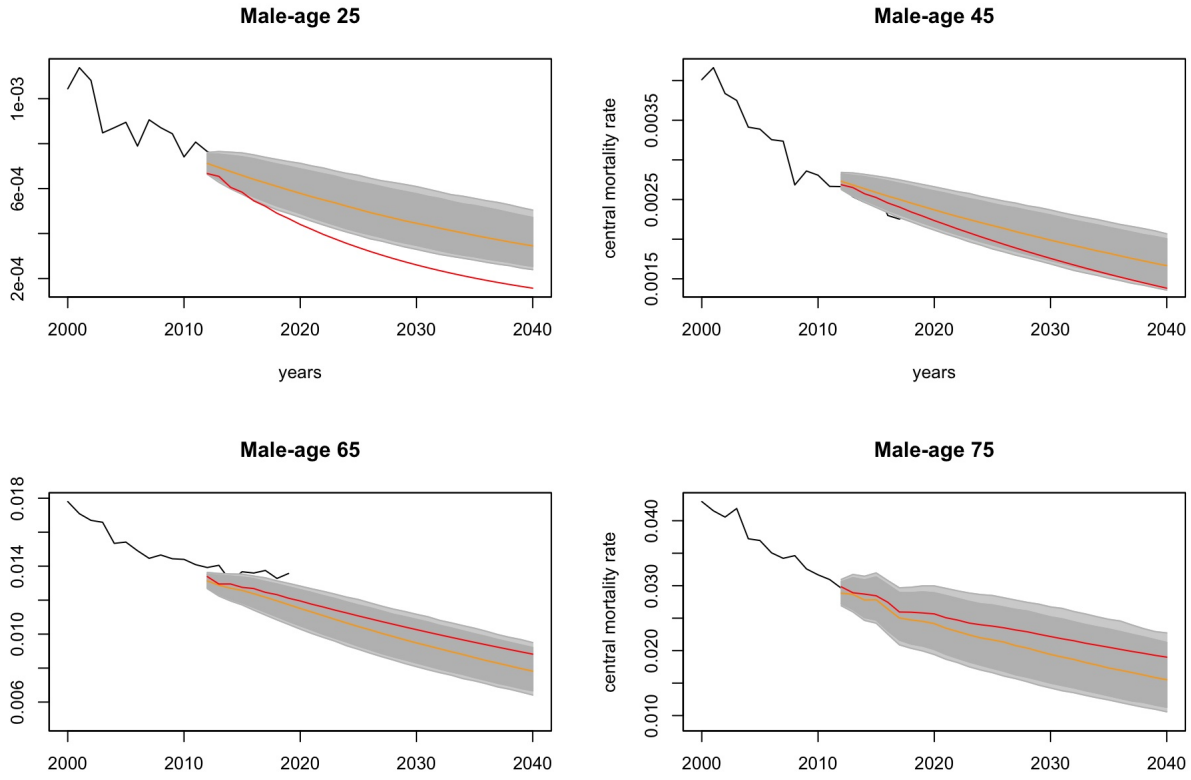

Figure 3.7. Projected male rates to 2040, with 90% and 95% confidence bands in RCP2.6 scenario
(-: observed rates, -: model prediction, -: central trajectory of simulationss).

[5] https://www.drias-climat.fr/

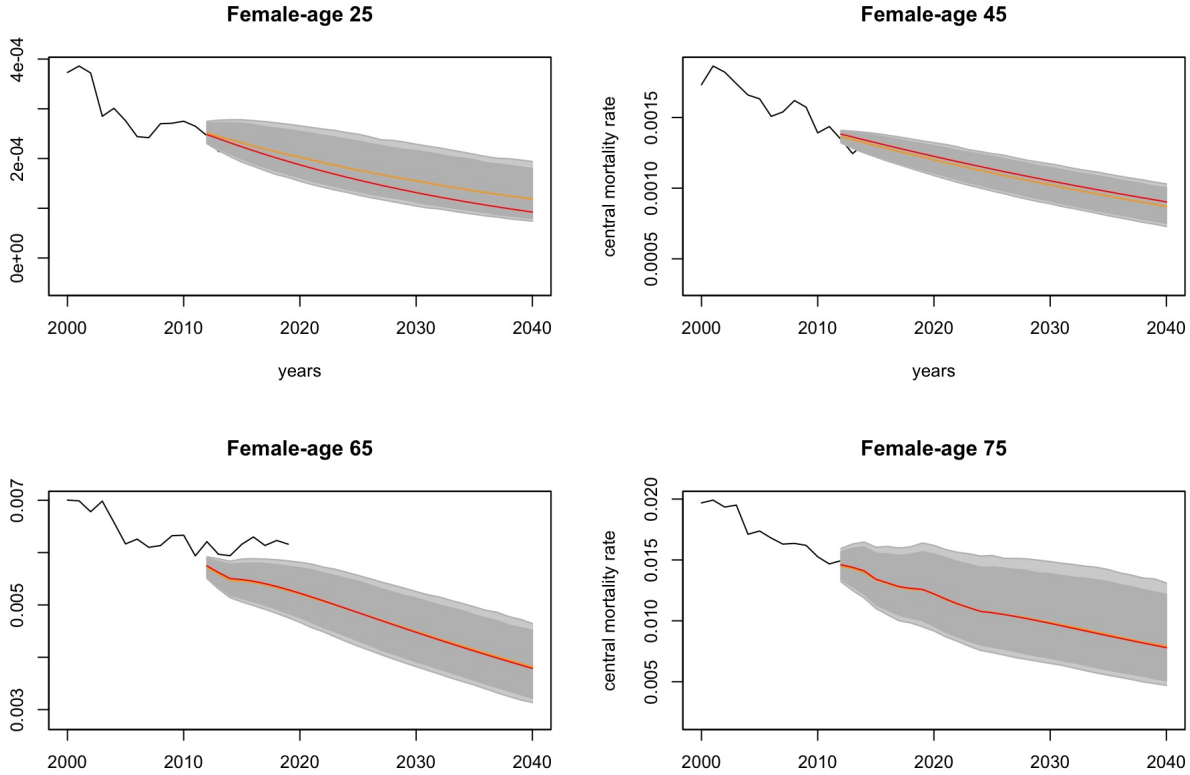

Figure 3.8. Projected female rates to 2040, with 90% and 95% confidence bands in RCP2.6 scenario
(-: observed rates, -: model predictio, -: central trajectory of simulations).

First, the impact of the scenario RCP2.6 is clearly not negligible. Indeed, the upper bound of confidence intervals corresponds to the worst case scenario for temperature projections (sharp increase of the mean temperature in the future). On the other hand, the lower bound relates to the best case scenario. Second, notice that the oldest people get, the more uncertainty about future mortality rates. This means that the variability of predicted mortality rates increases with age, which is not surprising. Third, the slopes of these curves suggest that mortality rates will continue to decrease at the same improvement rate for young people (whatever the gender), but this improvement in mortality seems to be more balanced for older people since they are the population most likely to be impacted by heat waves. The same graphs can be made for other RCP scenarios, leading to the same conclusions but with even more pronounced impacts.

Finally, this analysis enables to confirm the importance for insurers and public policies to integrate global warming in their future demographic projections. Doing so, they can anticipate to some extent the worsening induced by climate change and more specifically heat waves. However, longevity models aim to provide only the global picture. In practice this means that these models give results in expectation, but are not adapted to predict what would happen in exceptional circumstances. They are thus more useful in a global risk management perspective than in the case of a crisis (e.g. pandemic), which should be kept in mind when focusing on extreme scenario analyses and Solvency Capital Requirements. More globally, statistical models remain effective as long as there is no major change in the future as compared to the

past. On the topic of climate change, it is not obvious that future trends are well represented by current trends. It is therefore crucial to use these models as quantitative tools only; they are not designed to account for large sudden changes.

Conclusion

As experts in quantifying and managing risks, actuaries can and have contributed solutions to the challenges generated by climate change. The professional actuarial societies in North America and Australia have led the way, defining in 2018 actuarial climate indices that capture and summarize climate anomalies in their countries and respective regions. These indices have been proven useful in several ways; first to measure and quantify climate risk, then to raise awareness and educate actuaries on climate change issues, and lastly to help measure the impact of climate change on the insurance industry.

This book provides an introduction to the pioneering work of these first "climate actuaries". It then reviews more recent work completed by the DIALog Research Chair team that defined an actuarial climate index for France (FACI), and compares its evolution to that of the indices calculated in other countries, such as Canada, the US, Australia, Portugal and Spain. Applications of FACI to different insurance sectors are proposed, including the definition and pricing of a parametric insurance product based on the French index. Throughout the chapters, the focus is on the impact of climate risk on the insurance industry, and more particularly in health and life insurance.

Prolonged exposure to heat has been shown to adversely impact health and increase mortality, especially among older adults. This impact has been particularly worrisome during heat waves in the 21st century, such as the 2003 European heat wave, where significant spikes in mortality occurred during extreme heat events. Despite the well documented links between heat and excess mortality, predicting mortality from heat remains a challenge, due to factors such as limited availability of mortality data, the vulnerability dependence on location and age, and the different environmental factors contributing to heat impact.

Using data from France, we show nonetheless that it is possible to build data driven models to predict the number of summer-time deaths as a function of a heat index. Both statistical and deterministic approaches suggest that a simple convex relationship exists between the heat index (combining temperature and humidity) and the number of deaths. However, some caveats remain. First, we show in particular that the quality of the prediction can quickly deteriorate if the vulnerability of the population to heat changes over time. Therefore, the selected reference period for estimating model parameters is key, and assumptions about the future evolution of this vulnerability to heat are essential. Second, a predicting model that works in one region does not necessarily work in other regions as the vulnerability to heat may differ. Third, the results suggest that location-dependent threshold values for heat exist, above which the number of deaths increases at a much-accelerated rate. Our results also suggest that this occurs when unprecedented levels of heat are attained at a particular location.

In order to obtain projections of future heat-induced mortality, simulations of the future evolution of heat, and more generally of climate, are necessary. These simulations are performed with Earth-system models that represent different future climate evolution paths, based on scenarios that consider different socio-economic developments. These models are built on well-established physical principles and represent all the necessary variables to calculate heat indicators such as temperature and humidity. Despite inherent uncertainties in these models, ensemble simulations provide a range of possible outcomes, ensuring robust projections of future heat, thus allowing to model its impact on mortality.

Once climate projections have been made, longevity models need to be designed to integrate climate change in mortality projections. The model presented here is grounded on recent extensions of the Lee-Carter model, but this approach still underestimates the excess mortality due to unexpected large events. It underscores the importance of using a scenario-based approach when investigating the future impact of heat on mortality for solvency purposes.

Bibliography

AACI. Design documentation: Australian Actuaries Climate Index, 2018. URL https://www.actuaries.asn.au/microsites/climate-index/about/development-and-design.

ACI. Actuaries Climate Index™ development and design. (for Version 1.1, April 2019, see https://actuariesclimateindex.org/wp-content/uploads/2019/05/ACI.DevDes.2.20.pdf), 2018.

ACI. Actuaries Climate Index™ sample calculations, 2019. URL https://actuariesclimateindex.org/wp-content/uploads/2019/05/SampleCalcEng.5.19.pdf.

L. Adélaïde, O. Chanel, and M. Pascal. Health effects from heat waves in France: an economic evaluation. *The European Journal of Health Economics*, pages 1–13, 2022.

D. O. Åström, B. Forsberg, and J. Rocklöv. Heat wave impact on morbidity and mortality in the elderly population: A review of recent studies. *Maturitas*, 69:99–105, 2011.

G. S. Azhar, D. Mavalankar, A. Nori-Sarma, A. Rajiva, P. Dutta, A. Jaiswal, P. Sheffield, K. Knowlton, and J. J. Hess. Heat-related mortality in India: excess all-cause mortality associated with the 2010 Ahmedabad heat wave. *PLOS ONE*, 9(3):e91831, 2014.

D. Barriopedro, E. M. Fischer, J. Luterbacher, R. M. Trigo, and R. García-Herrera. The hot summer of 2010: redrawing the temperature record map of Europe. *Science*, 332(6026):220–224, 2011.

A. Bhattacharya-Craven, M. Golnaraghi, M. Thomson, and T. Caplan. Climate change: What does the future hold for health and life insurance?, 2024. URL https://www.genevaassociation.org/sites/default/files/2024-02/cch-report_web-270224.pdf.

A. Bouchama, M. Dehbi, G. Mohamed, F. Matthies, M. Shoukri, and B. Menne. Prognostic factors in heat wave–related deaths: a meta-analysis. *Archives of Internal Medicine*, 167(20): 2170–2176, 2007.

N. Brouhns, M. Denuit, and J. K. Vermunt. A Poisson log-bilinear regression approach to the construction of projected lifetables. *Insurance: Mathematics and Economics*, 31:373–393, 2002. URL https://doi.org/10.1016/S0167-6687(02)00185-3.

A. Cairns, D. Blake, K. Dowd, G. Coughlan, D. Epstein, A. Ong, and I. Balevich. A quantitative comparison of stochastic mortality models using data from England & Wales and the United States. *Working paper, Heriot-Watt University and Pensions Institute Discussion*, Paper PI-0701, 2007.

A. J. Cairns, D. Blake, and K. Dowd. A two-factor model for stochastic mortality with parameter uncertainty: Theory and calibration. *Journal of Risk and Insurance*, 73(4):687––718, 2006. URL http://www.ma.hw.ac.uk/~andrewc/papers/jri2006e.pdf.

A. J. Cairns, D. Blake, and K. Dowd. Modelling and management of mortality risk: A review. *Scandinavian Actuarial Journal*, 2008:79––113, 2008. URL https://doi.org/10.1080/03461230802173608.

A. J. Cairns, D. Blake, K. Dowd, G. D. Coughlan, D. Epstein, and M. Khalaf-Allah. Mortality density forecasts: An analysis of six stochastic mortality models. *Insurance: Mathematics and Economics*, 48:355––367, 2011. URL https://doi.org/10.1016/j.insmatheco.2010.12.005.

California. California insurance market rattled by withdrawal of major companies, 2023. URL https://apnews.com/article/california-wildfire-insurance-e31bef0ed7eeddcde096a5b8f2c1768f.

A. Charpentier. Insurability of climate risks. *The Geneva Papers on Risk and Insurance-Issues and Practice*, 33:91–109, 2008.

D. Chen, M. Rojas, B. Samset, K. Cobb, A. Diongue Niang, P. Edwards, S. Emori, S. Faria, E. Hawkins, P. Hope, P. Huybrechts, M. Meinshausen, S. Mustafa, G.-K. Plattner, and A.-M. Tréguier. Framing, context, and methods. *Climate Change 2021: The Physical Science Basis. Contribution of Working Group I to the Sixth Assessment Report of the Intergovernmental Panel on Climate Change*, Chapter 1, 2021.

Copernicus Climate Change Service (C3S), Climate Data Store (CDS). ERA5-land hourly data from 1950 to present, 2022. URL https://cds.climate.copernicus.eu/cdsapp#!/dataset/reanalysis-era5-land?tab=overview.

C. Courbage and M. Golnaraghi. Extreme events, climate risks and insurance. *The Geneva Papers on Risk and Insurance-Issues and Practice*, 47(1):1–4, 2022.

C. Crisóstomo Mazaira. Modelo actuarial de la medida del impacto del cambio climático en los riesgos de mortalidad y longevidad. Master's thesis, University Carlos III of Madrid, Spain, 2022. URL https://e-archivo.uc3m.es/handle/10016/36527.

I. D. Currie. Smoothing and forecasting mortality rates with P-splines. *Talk given at the Institute of Actuaries*, June 2006. URL https://www.actuaries.org.uk/system/files/documents/pdf/currie.pdf.

I. D. Currie. On fitting generalized linear and non-linear models of mortality. *Scandinavian Actuarial Journal*, 2016:356–383, 2016. URL https://doi.org/10.1080/03461238.2014.928230.

C. Curry. Extension of the actuaries climate index to the UK and Europe. a feasibility study, 2015. URL https://www.actuaries.org.uk/system/files/field/document/UK_ACI_scoping_FINAL.pdf.

C. Di Napoli, F. Pappenberger, and H. L. Cloke. Verification of heat stress thresholds for a health-based heat-wave definition. *Journal of Applied Meteorology and Climatology*, 58(6):1177–1194, 2019.

M. G. Donat, L. V. Alexander, H. Yang, I. Durre, R. Vose, and J. Caesar. Global land-based datasets for monitoring climatic extremes. *Bulletin of the American Meteorological Society*, 94(7):997–1006, 2013.

A. Dufour and V. Candas. Ageing and thermal responses during passive heat exposure: sweating and sensory aspects. *European Journal of Applied Physiology*, 100:19–26, 2007.

L. A. Dundon, K. S. Nelson, J. Camp, M. Abkowitz, and A. Jones. Using climate and weather data to support regional vulnerability screening assessments of transportation infrastructure. *Risks*, 4(3):28, 2016.

J. Díaz, R. Carmona, I. Mirón, C. Ortiz, and C. Linares. Comparison of the effects of extreme temperatures on daily mortality in Madrid (Spain), by age group: The need for a cold wave prevention plan. *Environmental Research*, 143:186–191, 2015.

V. Eyring, S. Bony, G. A. Meehl, C. A. Senior, B. Stevens, R. J. Stouffer, and K. E. Taylor. Overview of the coupled model intercomparison project phase 6 (CMIP6) experimental design and organization. *Geoscientific Model Development*, 9(5):1937–1958, 2016.

J. Faunt, T. Wilkinson, P. Aplin, P. Henschke, M. Webb, and R. Penhall. The effete in the heat: heat-related hospital presentations during a ten day heat wave. *Australian and New Zealand Journal of Medicine*, 25(2):117–121, 1995.

G. M. Flato. Earth system models: an overview. *Wiley Interdisciplinary Reviews: Climate Change*, 2(6):783–800, 2011.

A. Fouillet, G. Rey, V. Wagner, K. Laaidi, P. Empereur-Bissonnet, A. Le Tertre, P. Frayssinet, P. Bessemoulin, F. Laurent, P. De Crouy-Chanel, et al. Has the impact of heat waves on mortality changed in France since the European heat wave of summer 2003? A study of the 2006 heat wave. *International Journal of Epidemiology*, 37(2):309–317, 2008.

S. H. Fu, A. Gasparrini, P. S. Rodriguez, and J. Prabhat. Mortality attributable to hot and cold ambient temperatures in India: A nationally representative case-crossover study. *PLOS Medecine*, Juillet 2018. URL https://doi.org/10.1371/journal.pmed.1002619.

J. Garrido, X. Milhaud, and A. Olympio. On the definition of a French actuarial climate index, 2023. URL https://hal.science/hal-04491982. preprint.

A. Gasparrini and B. Armstrong. The impact of heat waves on mortality. *Epidemiology*, 22(1): 68–73, 2011.

A. Gasparrini, Y. Guo, M. Hashizume, E. Lavigne, A. Zanobetti, J. Schwartz, A. Tobias, S. Tong, J. Rocklöv, B. Forsberg, et al. Mortality risk attributable to high and low ambient temperature: a multicountry observational study. *The lancet*, 386(9991):369–375, 2015a.

A. Gasparrini, Y. Guo, M. Hashizume, E. Lavigne, A. Zanobetti, P. J. Schwartz, A. Tobias, S. Tong, J. Rocklöv, B. Forsberg, M. Leone, M. D. Sario, M. L. Bell, Y.-L. L. Guo, C.-F. Wu, H. Kan, S.-M. Yi, M. de Sousa Zanotti Stagliorio Coelho, P. H. N. Saldiva, Y. Honda, H. Kim, and B. Armstrong. Mortality risk attributable to high and low ambient temperature: a multicountry observational study. *The Lancet*, 386:369–375, 2015b. URL https://doi.org/10.1016/S0140-6736(14)62114-0.

J. L. Geirinhas, R. M. Trigo, R. Libonati, L. C. Castro, P. M. Sousa, C. A. Coelho, L. F. Peres, and F. Mônica de Avelar. Characterizing the atmospheric conditions during the 2010 heatwave in Rio de Janeiro marked by excessive mortality rates. *Science of The Total Environment*, 650: 796–808, 2019.

M. Golnaraghi. Climate change risk assessment for the insurance industry. *The Geneva Association, Switzerland*, 2021.

B. Gompertz. On the nature of the function expressive of the law of human mortality, and on a new mode of determining the value of life contingencies. *Philosophical Transactions of the Royal Society of London*, 115:513––585, 1825.

J. Graunt. *Natural and political observations made upon the bills of mortality*. London, 1662.

A. Gupta and S. Venkataraman. Insurance and climate change. *Current Opinion in Environmental Sustainability*, 67:101412, 2024.

J. Gutiérrez, R. Ranasinghe, A. Ruane, R. Vautard, N. Arnell, E. Coppola, et al. Climatic impact-driver and extreme indices. *Climate Change 2021: The Physical Science Basis. Contribution of Working Group I to the Sixth Assessment Report of the Intergovernmental Panel on Climate. 2021*, Annex VI:2205–2214, 2021.

E. Halley. VI. An estimate of the degrees of the mortality of mankind; drawn from curious tables of the births and funerals at the city of Breslaw; with an attempt to ascertain the price of annuities upon lives. *Royal Society*, 17, January 1693.

M. D. Hawkins, V. Brown, and J. Ferrell. Assessment of NOAA national weather service methods to warn for extreme heat events. *Weather, Climate, and Society*, 9(1):5–13, 2017.

L. Heligman and J. Pollard. The age pattern of mortality. *Journal of the Institute of Actuaries*, 107:49–80, January 1980.

H. Hersbach, B. Bell, P. Berrisford, S. Hirahara, A. Horányi, J. Muñoz-Sabater, J. Nicolas, C. Peubey, R. Radu, D. Schepers, et al. The ERA5 global reanalysis. *Quarterly Journal of the Royal Meteorological Society*, 146(730):1999–2049, 2020.

IAE. El ICA español. In *Sostenibilidad y cambio climático. Índice Climático Actuarial*, June 2023. URL https://formacion.actuarios.org/courses/webinar-sostenibilidad-y-cambio-climatico-indice-climatico-actuarial/.

IPCC. Climate change 2023. AR6 synthesis report. https://www.ipcc.ch/report/ar6/syr/, 2023.

D.-W. Kim, J.-H. Deo, R.C.and Chung, and J.-S. Lee. Projection of heat wave mortality related to climate change in Korea. *Natural Hazards*, 80:623––637, 2016.

S. Kovats, T. Wolf, and B. Menne. Heatwave of August 2003 in Europe: provisional estimates of the impact on mortality. *Weekly Releases (1997–2007)*, 8(11):2409, 2004.

R. D. Lee and L. R. Carter. Modeling and forecasting U.S. mortality. *Journal of the American Statistical Association*, 87(419):659–671, 1992.

H. Li and Q. Tang. Joint extremes in temperature and mortality: A bivariate pot approach. *North American Actuarial Journal*, 26(1):43–63, 2022.

W. M. Makeham. On the law of mortality and the construction of annuity tables. *Journal of the Institute of Actuaries*, 8(6):301–310, January 1825.

V. Masson-Delmotte, P. Zhai, A. Pirani, S. L. Connors, C. Péan, S. Berger, N. Caud, Y. Chen, L. Goldfarb, M. Gomis, et al. Climate change 2021: the physical science basis. *Contribution of Working Group I to the Sixth Assessment Report of the Intergovernmental Panel on Climate Change*, 2(1):2391, 2021.

M. Meinshausen, S. J. Smith, K. Calvin, J. S. Daniel, M. L. Kainuma, J.-F. Lamarque, K. Matsumoto, S. A. Montzka, S. C. Raper, K. Riahi, et al. The RCP greenhouse gas concentrations and their extensions from 1765 to 2300. *Climatic Change*, 109:213–241, 2011.

M. Meinshausen, Z. Nicholls, J. Lewis, M. J. Gidden, E. Vogel, M. Freund, U. Beyerle, C. Gessner, A. Nauels, N. Bauer, et al. The SSP greenhouse gas concentrations and their extensions to 2500. *Geoscientific Model Development Discussions*, 2019:1–77, 2019.

M. J. Menne, I. Durre, B. Korzeniewski, S. McNeill, K. Thomas, X. Yin, S. Anthony, R. Ray, R. S. Vose, B. E.Gleason, and T. G. Houston. Global Historical Climatology Network - Daily, 2012.

T. Miljkovic, D. Miljkovic, and K. Maurer. Examining the impact on mortality arising from climate change: important findings for the insurance industry. *European Actuarial Journal*, 8: 363–381, 2018.

Munich Re. Record thunderstorm losses and deadly earthquakes: the natural disasters of 2023, 2024. URL https://www.munichre.com/en/company/media-relations/media-information-and-corporate-news/media-information/2024/natural-disaster-figures-2023.html.

J. Muñoz-Sabater, E. Dutra, A. Agustí-Panareda, C. Albergel, G. Arduini, G. Balsamo, S. Boussetta, M. Choulga, S. Harrigan, H. Hersbach, et al. ERA5-land: A state-of-the-art global reanalysis dataset for land applications. *Earth System Science Data*, 13(9):4349–4383, 2021.

E. Nevruz, R. Y. Atici, and K. Yildirak. Actuaries Climate Index: An Application for Turkey. *İstatistik Araştırma Dergisi*, 12(2):14–25, 2022.

C. O'Hare and Y. Li. Explaining young mortality. *Insurance: Mathematics and Economics*, 50: 12–25, 2012. URL https://doi.org/10.1016/j.insmatheco.2011.09.005.

Q. Pan, L. Porth, and H. Li. Assessing the effectiveness of the actuaries climate index for estimating the impact of extreme weather on crop yield and insurance applications. *Sustainability*, 14(11):6916, 2022.

M. Pascal, K. Laaidi, M. Ledrans, E. Baffert, C. Caserio-Schönemann, A. Le Tertre, J. Manach, S. Medina, J. Rudant, and P. Empereur-Bissonnet. France's heat health watch warning system. *International Journal of Biometeorology*, 50:144–153, 2006.

K. Pearson. VII. Note on regression and inheritance in the case of two parents. *The Royal Society of London*, 58:240–242, 1985. URL https://doi.org/10.1098/rspl.1895.0041.

T. Peterson, C. Folland, G. Gruza, W. Hogg, A. Mokssit, and N. Plummer. Report on the activities of the working group on climate change detection and related rapporteurs, 2001. URL https://core.ac.uk/download/pdf/9700748.pdf.

L. Pineau-Guillou, P. Lazure, and G. Wöppelmann. Large-scale changes of the semidiurnal tide along North Atlantic coasts from 1846 to 2018. *Ocean Science*, 17(1):17–34, 2021. doi: 10.5194/os-17-17-2021. URL https://os.copernicus.org/articles/17/17/2021/.

R. Plat. On stochastic mortality modelling. *Insurance: Mathematics and Economics*, 45: 393––404, 2009. URL https://doi.org/10.1016/j.insmatheco.2009.08.006.

L. Pryor. The impacts of climate change on health. *A paper presented to the Institute & th Faculty of Actuaries in London on July 6*, 2017.

PSMSL. Tide gauge data, 2023. URL http://www.psmsl.org/data/obtaining/.

S. Rao and X. Li. China's experiences in Climate Risk Insurance and suggestions for its future development. *Annual Report on Actions to Address Climate Change (2019) Climate Risk Prevention*, pages 157–171, 2023.

C. Renjie, Y. Peng, W. Lijun, L. Cong, N. Yue, W. Weidong, J. Yixuan, L. Yunning, L. Jiangmei, Q. Jinlei, Y. Jinling, K. Haidong, and Z. Maigeng. Association between ambient temperature and mortality risk and burden: time series study in 272 main Chinese cities. *BMJ*, 2018. URL https://doi.org/10.1136/bmj.k4306.

A. E. Renshaw and S. Haberman. Lee-Carter mortality forecasting with age-specific enhancement. *Insurance: Mathematics and Economics*, 33:255––272, October 2003.

A. E. Renshaw and S. Haberman. A cohort-based extension to the Lee-Carter model for mortality reduction factors. *Insurance: Mathematics and Economics*, 38:556–570, June 2006.

A. E. Renshaw and S. Haberman. On simulation-based approaches to risk measurement in mortality with specific reference to Poisson Lee–Carter modelling. *Insurance: Mathematics and Economics*, 42(2):797–816, 2008.

L. P. Rothfusz and N. S. R. Headquarters. The heat index equation (or, more than you ever wanted to know about heat index). *Fort Worth, Texas: National Oceanic and Atmospheric Administration, National Weather Service, Office of Meteorology*, 9023:640, 1990.

R. Savitz and M. Dan Gavriletea. Climate change and insurance. *Transformations in Business & Economics*, 18(1), 2019.

M. Seklecka, A. A. Pantelous, and C. O'Hare. Mortality effects of temperature changes in the United Kingdom. *Journal of Forecasting*, 36:824–841, 2017. URL https://doi.org/10.1002/for.2473.

M. Seklecka, A. A. Pantelous, and C. O'Hare. The impact of parameter uncertainty in insurance pricing and reserve with the temperature-related mortality model. *Journal of Forecasting*, 38(4):327–345, 2019.

S. I. Seneviratne, X. Zhang, M. Adnan, W. Badi, C. Dereczynski, A. Di Luca, S. Ghosh, I. Iskander, J. Kossin, S. Lewis, et al. Weather and climate extreme events in a changing climate. *Climate Change 2021: The Physical Science Basis. Contribution of Working Group I to the Sixth Assessment Report of the Intergovernmental Panel on Climate Change*, Chapter 11, 2021.

Solterra Solutions. Determining the impact of climate change on insurance risk and the global community, Phase I: Key climate indicators, Nov 2012. URL https://www.actuary.org/sites/default/files/files/ClimateChangeRpt_FINAL_12Nov_Web_0.pdf.

X. Song, S. Wang, Y. Hu, M. Yue, T. Zhang, Y. Liu, J. Tian, and K. Shang. Impact of ambient temperature on morbidity and mortality: an overview of reviews. *Science of the Total Environment*, 586:241–254, 2017.

Swiss Re. More risk: the changing nature of p&c insurance by 2040. No4/2021, 2021.

K. E. Taylor, R. J. Stouffer, and G. A. Meehl. An overview of CMIP5 and the experiment design. *Bulletin of the American Meteorological Society*, 93(4):485–498, 2012.

J. Thistlethwaite and M. O. Wood. Insurance and climate change risk management: rescaling to look beyond the horizon. *British Journal of Management*, 29(2):279–298, 2018.

K. R. Wagner. Designing insurance for climate change. *Nature Climate Change*, 12(12): 1070–1072, 2022.

G. Warren-Myers, G. Aschwanden, F. Fuerst, and A. Krause. Estimating the potential risks of sea level rise for public and private property ownership, occupation and management. *Risks*, 6 (2):37, 2018.

K. Zhang, T.-H. Chen, and C. E. Begley. Impact of the 2011 heat wave on mortality and emergency department visits in Houston, Texas. *Environmental Health*, 14:1–7, 2015.

N. Zhou, J.-L. Vilar-Zanón, J. Garrido, and A.-J. Heras Martínez. On the definition of an actuarial climate index for the Iberian Peninsula. *Anales del Instituto de Actuarios Españoles*, 29:37–59, 2023. URL https://doi.org/10.26360/2023_3.

N. Zhou, J.-L. Vilar-Zanón, J. Garrido, and A. Heras-Martınez. Measuring climate change from an actuarial perspective: a survey of insurance applications. *Preprint*, 2024. URL https://hal.science/hal-04507165.

Glossary

IPCC : intergovernmental panel on climate change

FACI : french actuarial climate index

CPI : consumer price index, "a measure of the average change over time in the prices paid by urban consumers for a market basket of consumer goods and services."[6]

NOAA : National Oceanic and Atmospheric Administration

RCP : Representative Concentration Pathway

[6] Definition from the Bureau of Labor Statistics

AFTERWORD

In 2023, losses caused by natural disasters worldwide reached 250 billion dollars[7], of which 95 billion dollars were insured. By 2040, a rise from 30 to 63% in insured catastrophe losses is expected [8].

How far can insurers go? And how can they increase their solvency capital without causing policyholder premiums to soar?

In the United States, climate change has already forced insurers to withdraw strategically from certain markets. Will it be necessary to go to such extremes in Europe, and particularly in France?

Climate change is threatening the fundamental principles of insurance, namely the insurability of risks and mutualisation. It is up to us, the insurers and investors in the marketplace, to reinvent them together.

Working together is the future of our industry. Initiatives such as the Fonds Objectif Climat, which was recently renewed and opened up to new institutional investors, and the Fédération des Garanties et Assurances Affinitaires are advancing the understanding of risks and the performance of guarantees. The sharing of knowledge and relevant indicators from the Green and White Papers published by the major French insurers is a step in the same direction.

You can count on CNP Assurances, a player committed to pushing back the boundaries of insurability, a member of France's major public finance group and a beneficiary of the support of Caisse des Dépôts, to work together to advance the science of insurance in France and throughout the world.

Véronique Weill, Chairman of the Board of Directors of CNP Assurances

[7] Munich RE (2024)
[8] Swiss RE (2021)

APPENDICES

A. High-resolution analyses per region and season

This appendix presents a high resolution analysis of the evolution of the ICAF and all its components. This will provide a better understanding of what is influencing climate change in France and the extent to which specific regions need to be focused on when designing effective practical measures at a micro level.

A.1. FACI per region/season

Figures A.1 to A.4 show the evolution of the seasonal FACI over the last 11 years, at a very high resolution (cells at 0.1° of latitude $\times$ 0.1° of longitude). First consider the evolution of winter FACI seasonal values over the years 2011-2021, and then other seasons. Indeed, for now, the sea level variable is not available at most French tidal stations for recent years (from winter of 2022), thus we graph the spring, summer and fall FACI values only for the 11 years 2011-2021. Note the evolution of colors across years, whatever the season. Indeed, the red color tends to be more present, confirming the global increasing trend observed for FACI values in previous illustrations.

Secondly, extreme climate events seem to occur more frequently during the spring, across most of France (Figure A.2). The south of France seems to be more at risk, as compared to the North-East or North-West. Warmest years can be easily detected thanks to these maps; for instance, year 2020 clearly appears to have been particularly warm (especially in spring and fall seasons), a well-known fact in France (and also in Europe).

In some locations, the index reaches values around 3. At a single component level, this would mean that the index has increased by an average of 3 standard deviations over the reference period average. For the composite FACI (combining 6 components), the interpretation is not as straightforward; here the standard deviation of the average of 6 correlated components is not 1. It would be closer to $1/\sqrt{6}$ if they were independent. Hence, a seasonal index value of 3 is significantly high, as it is a possibly large multiple of $1/\sqrt{6}$.

However, note how the evolution of FACI varies across different cells within a region. Each individual grid cell is affected by climate change in a unique manner. This means that the impact of climate change in each specific area may differ. This heterogeneity also implies that the frequency of extreme climate events varies per region. This could indicate also that the level of vulnerability and/or adaptability to extreme weather conditions can differ from one cell to another, meaning that such a granular study could be of very high added value for the design of agricultural insurance products.

To better separate the contribution of each component to the FACI, one could perform the same analysis for all its components (temperature, precipitation, drought, wind, sea level). For conciseness, we have chosen to focus on the temperature, since the latter seems to be the variable that most contributes to FACI. However, the interested reader can access the complete analysis in Appendix C of Garrido et al. (2023) that plots the progress of the temperature, precipitation, drought and wind variables over the years 2011-2022.

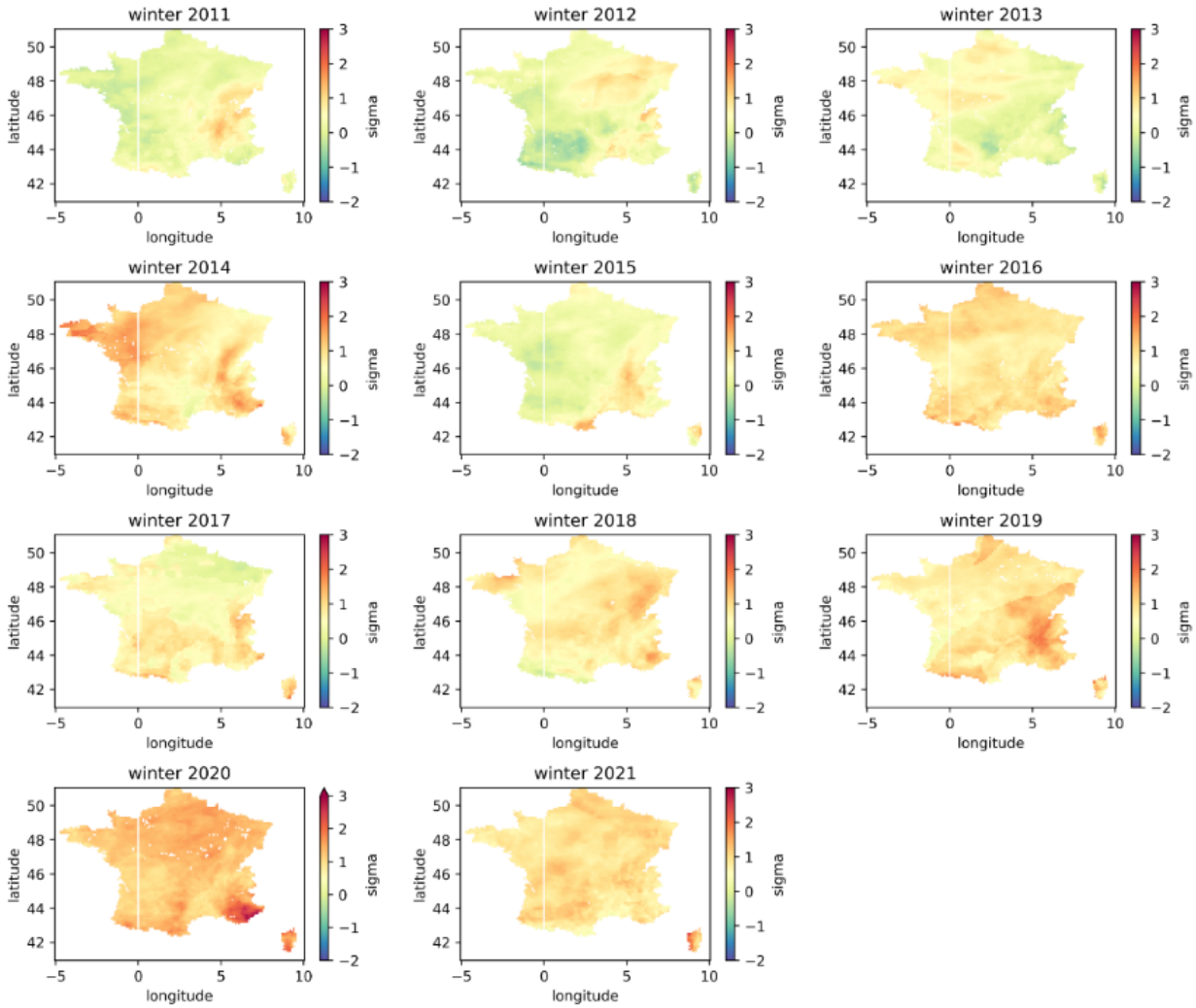

Figure A.1. Winter FACI, 2011-2021.

A.2. Seasonal temperatures per region

When focusing on temperatures, recall that we are interested in two different phenomenons. They correspond to extremes for warm as well as cold temperatures. Figures A.5 to A.12 plot the progress of the temperature over the years 2011-2022. First consider the high temperature $T90_{std}$ variable. Note how summers are producing less frequent extreme low temperatures, at the same time as more frequent high temperatures (see Figure A.7). To a certain extent, the

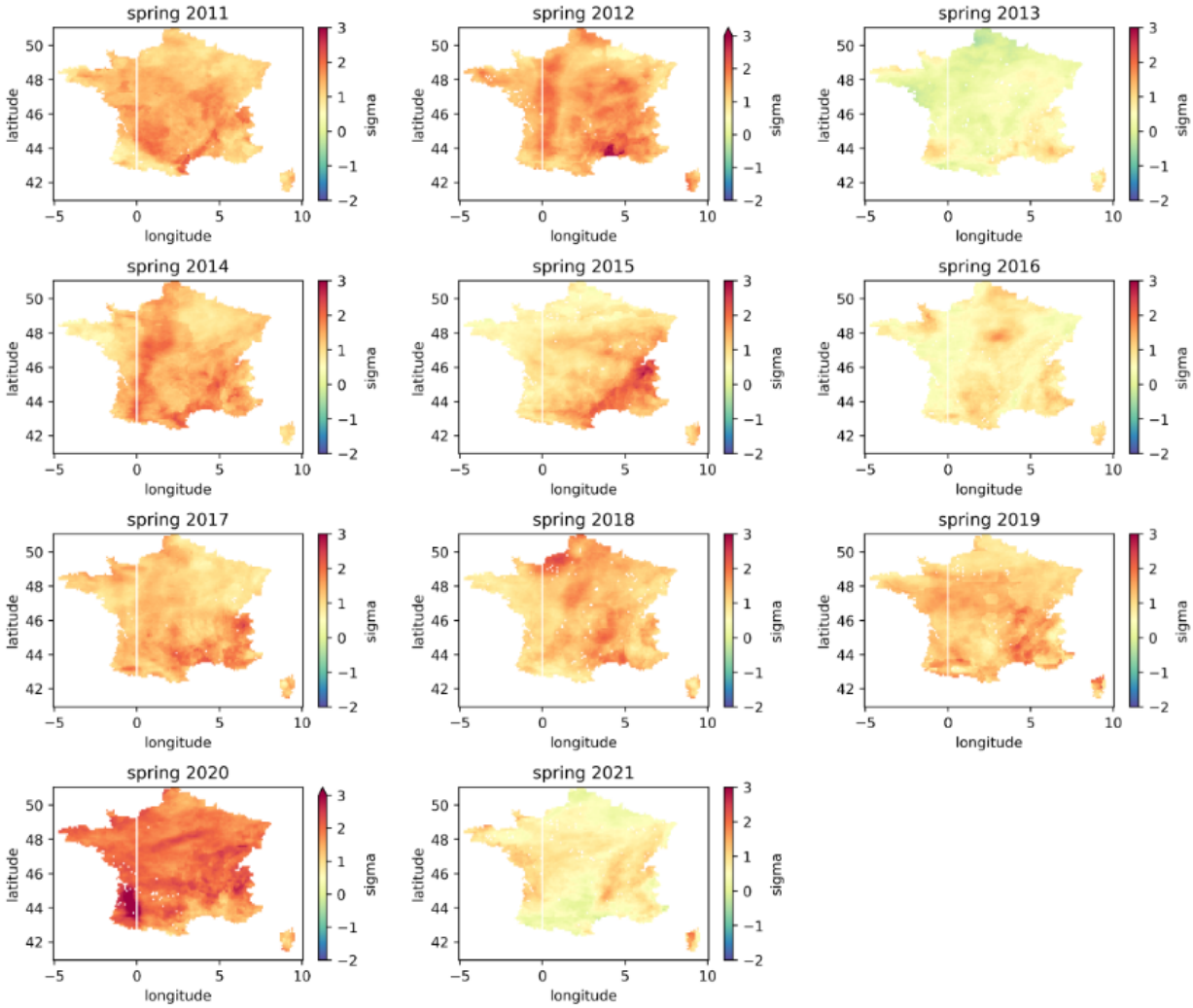

Figure A.2. Spring FACI, 2011-2021.

same can be said about winters. The case of springs and falls is not as clear-cut. Whatever the season, these maps clearly confirm the warming trend. Not surprisingly, highest FACI values were observed in Spring and Summer seasons. Significantly high FACI values were also observed in winter, although much more dispersed geographically. Thanks to these high-resolution maps, it is easy to see that the impact (in terms of FACI values) can be very different even for two close regions (take for instance Spring 2015), which makes sense considering the topography of France. However, what is striking is that some regions (like the South-East) are almost exclusively red FACI areas, meaning that these regions seem to be the most impacted by climate change (according to the selected weather variables).

Now consider the low temperatures $T10_{std}$. We plot $-T10_{std}$ instead, so that high values (in red) mean less frequent extreme lows, that is warmer days.

Looking at the coldest temperatures, the same phenomenon appears. For the winter season, there are no negative FACI values for recent years. Furthermore, there are very significant

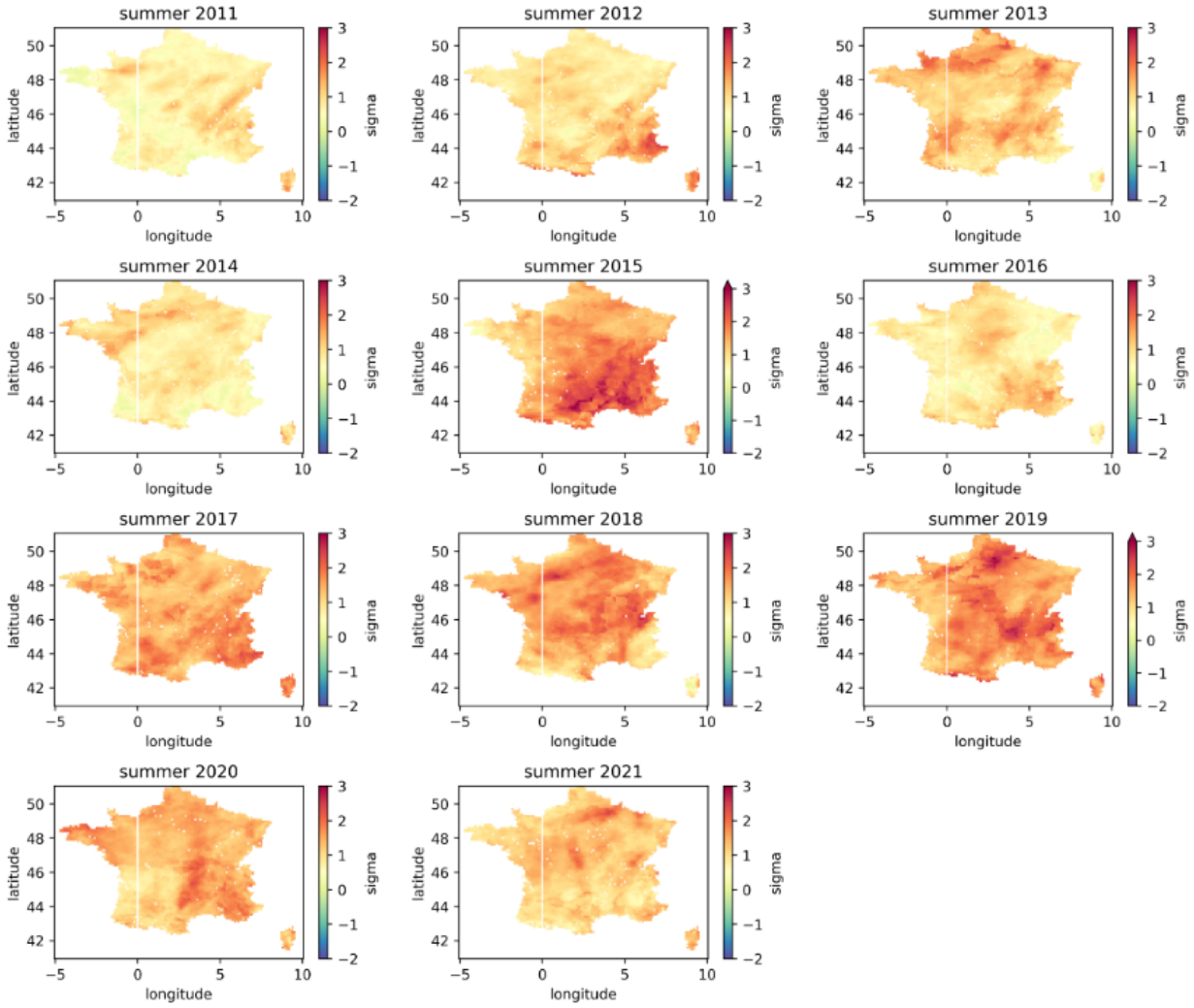

Figure A.3. Summer FACI, 2011-2021.

changes in Spring, especially in the southern part of the country. What we observe there with temperatures mostly drives the evolution of FACI through the years. However, the really exciting thing here is the possibility to get FACI values at a very granular level. This is key to be able to adapt to specific constraints and local environment, which is mandatory for effective micro-level actions.

A.3. Seasonal precipitations per region

The following plots are for the precipitations P_{std} variable.

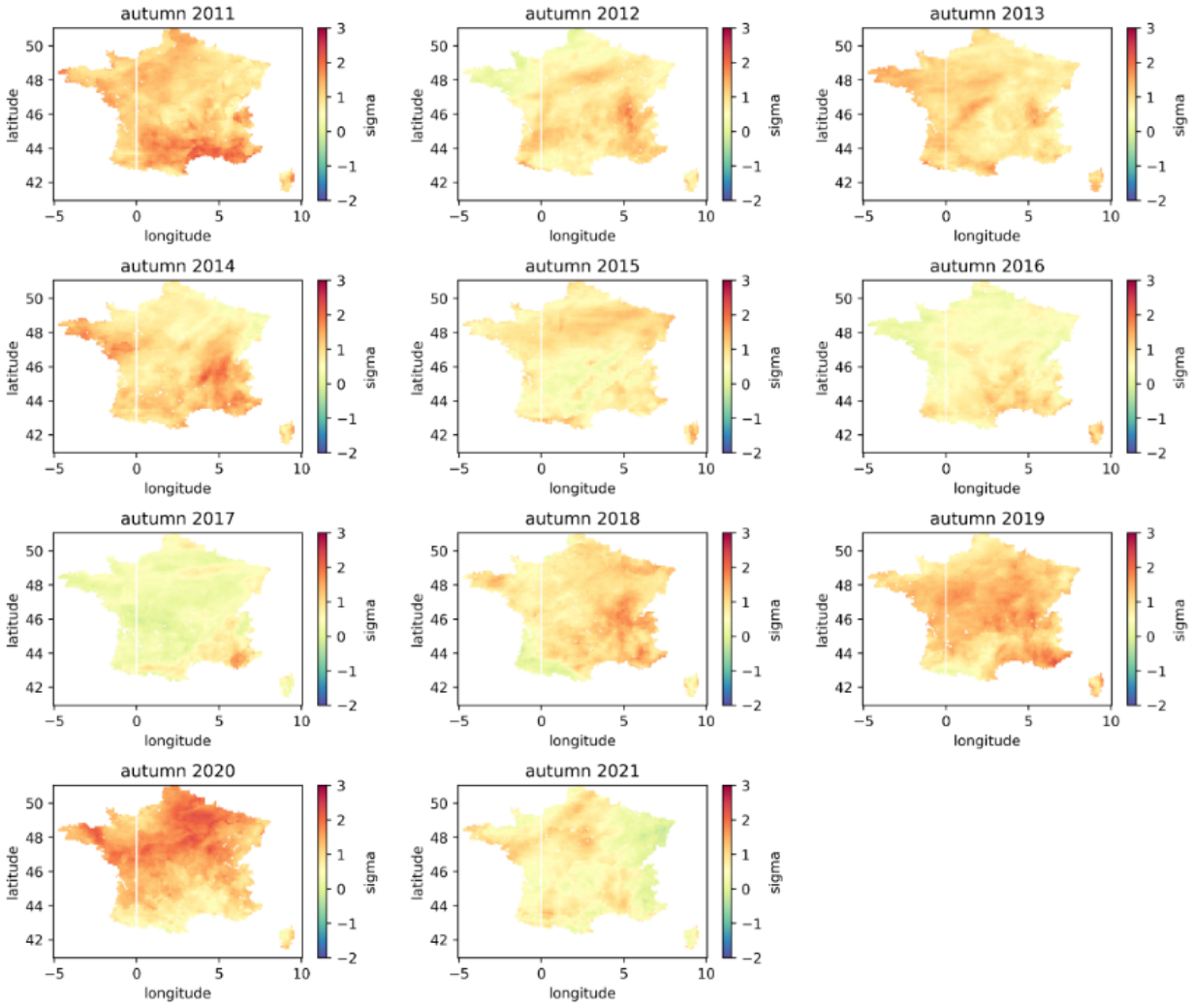

Figure A.4. Autumn FACI, 2011-2021.

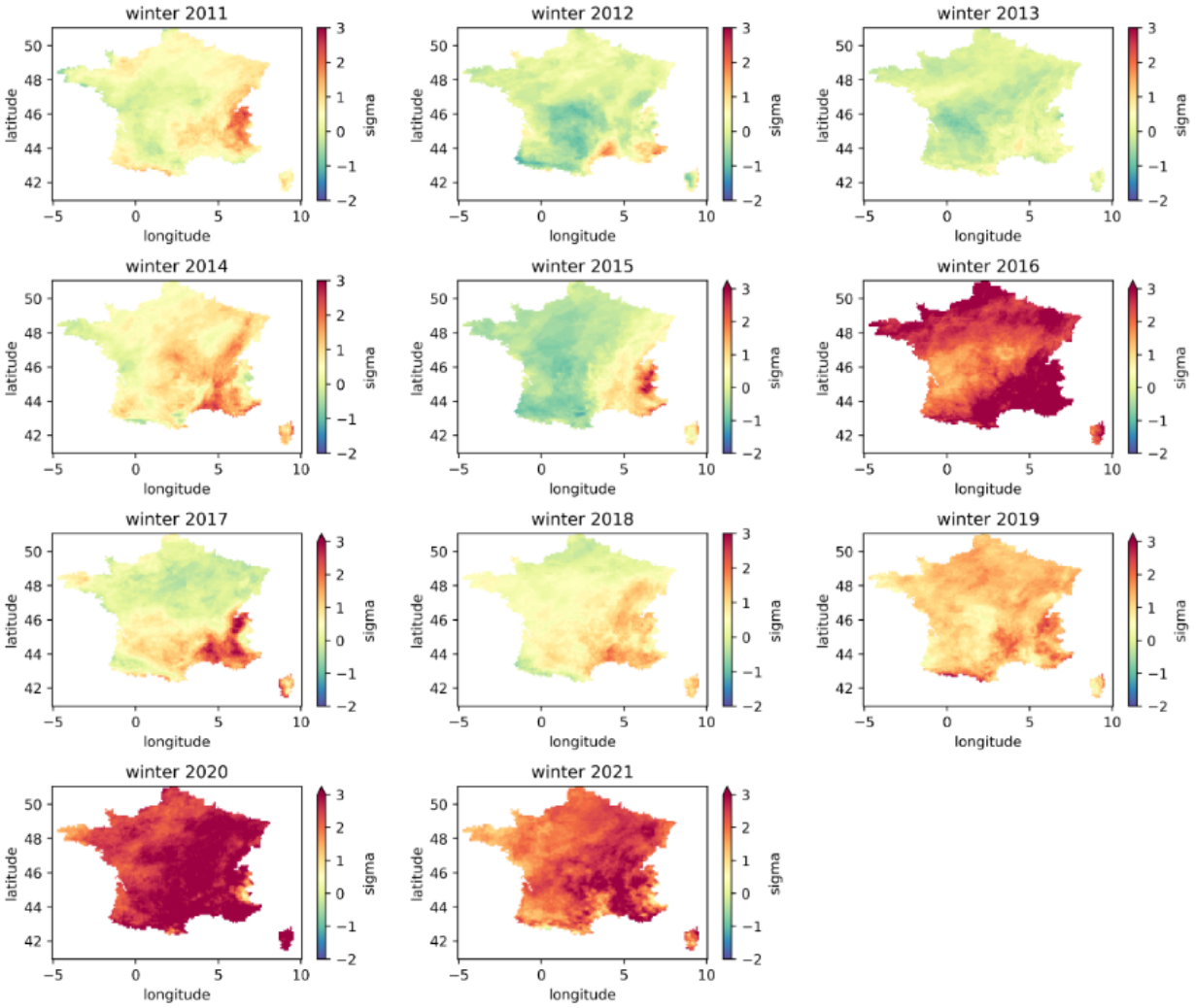

Figure A.5. Winter seasonal $T90_{std}$ values, 2011-2021.

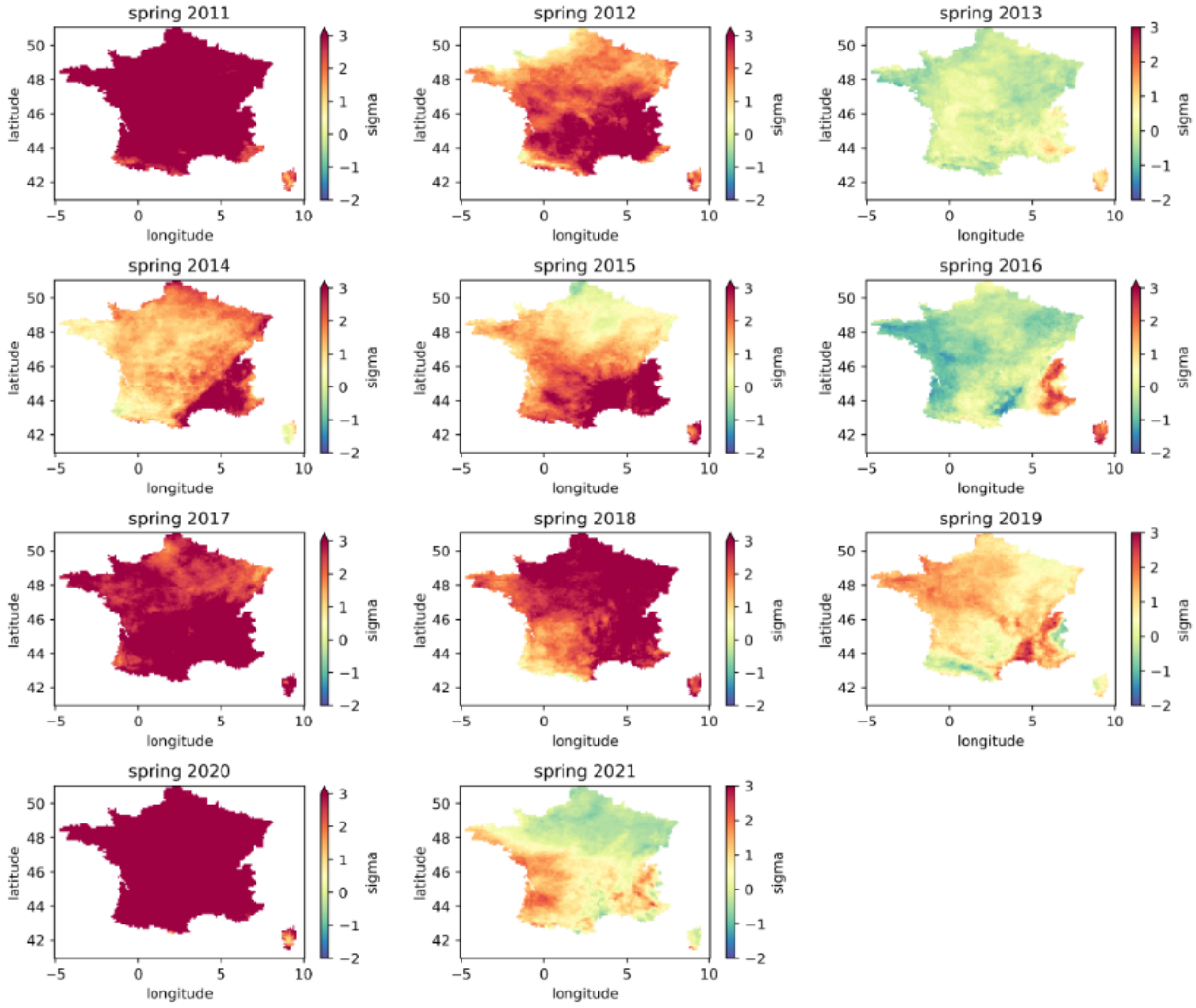

Figure A.6. Spring seasonal $T90_{std}$ values, 2011-2021.

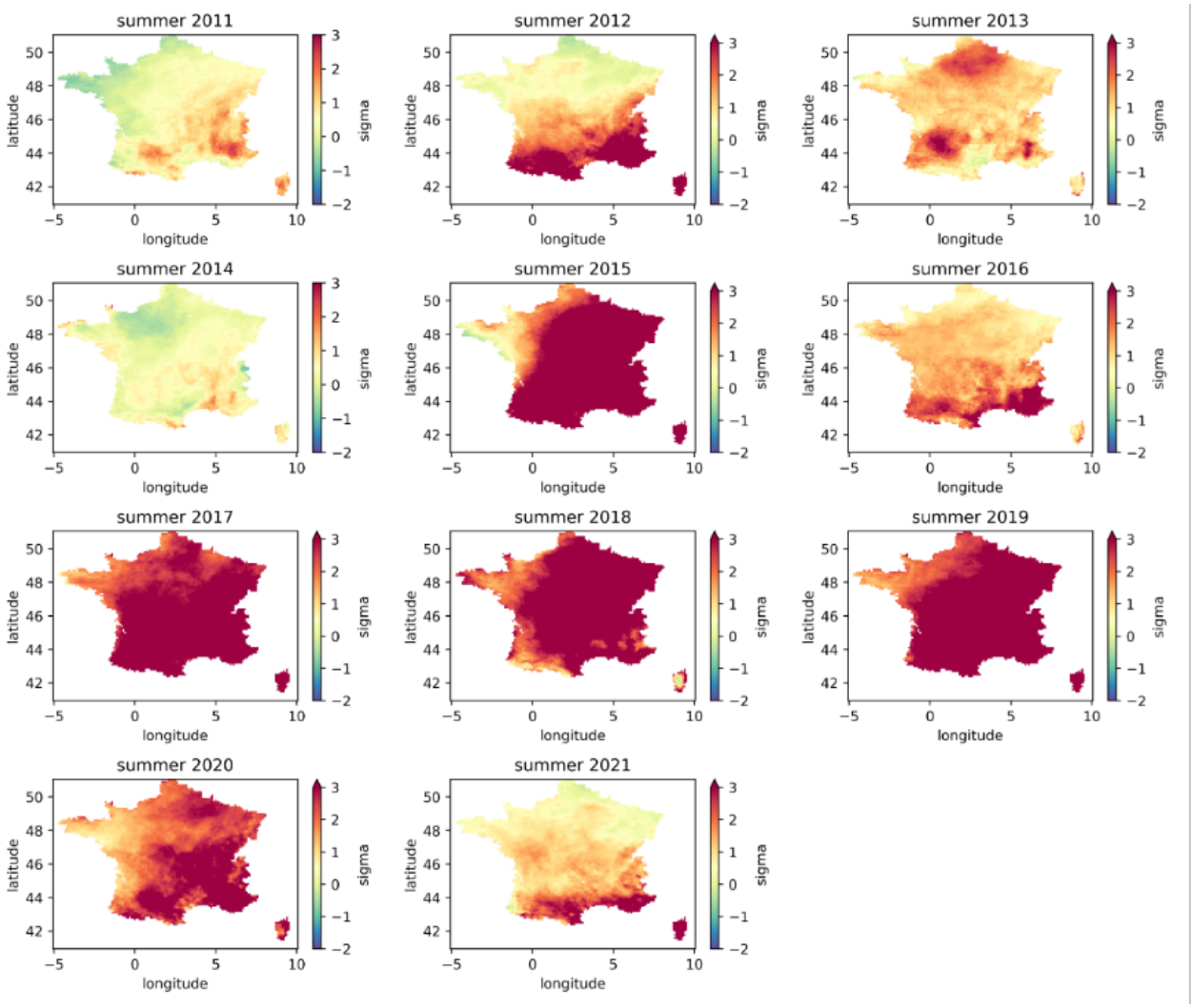

Figure A.7. Summer seasonal $T90_{std}$ values, 2011-2021.

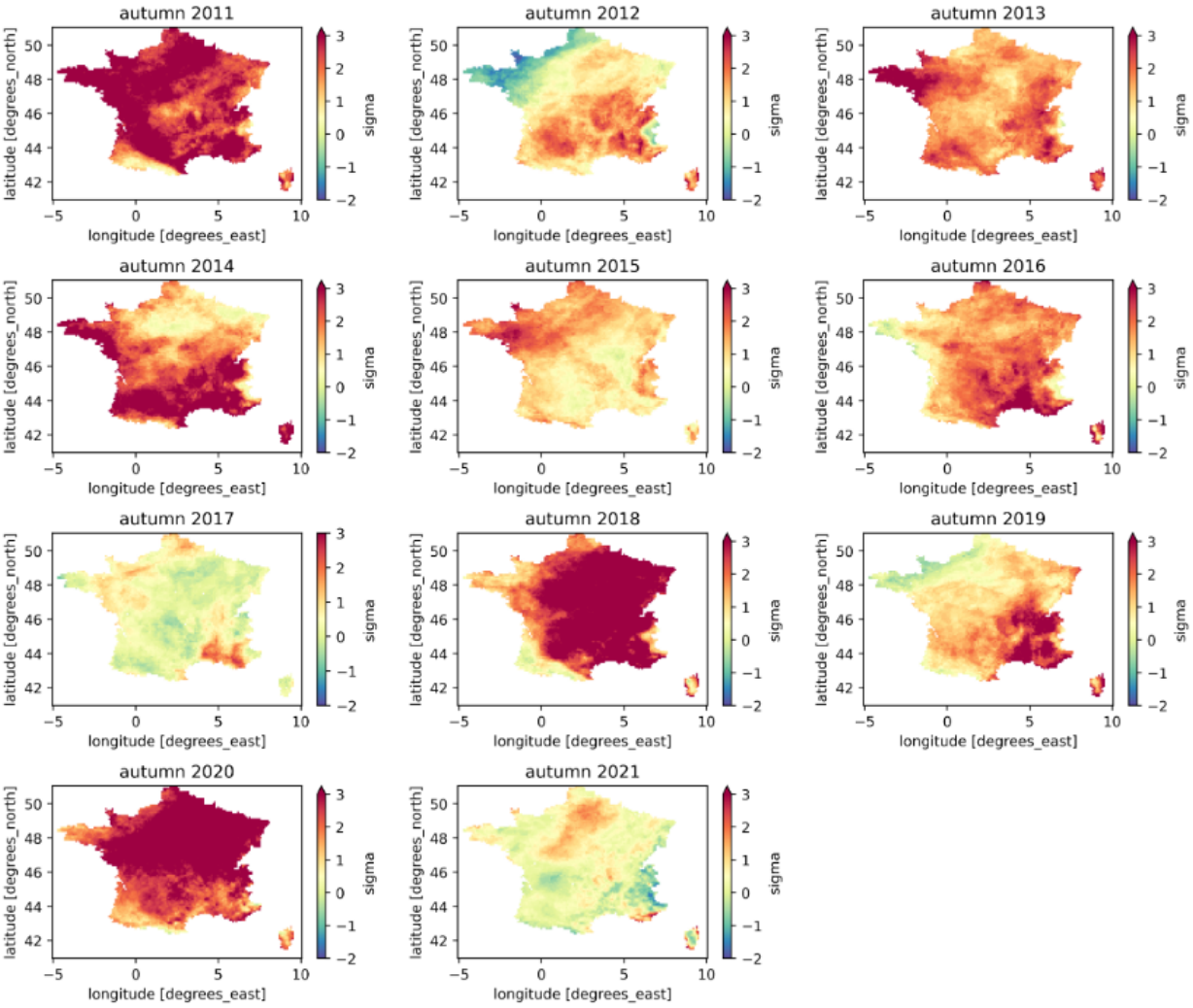

Figure A.8. Fall seasonal $T90_{std}$ values, 2011-2021.

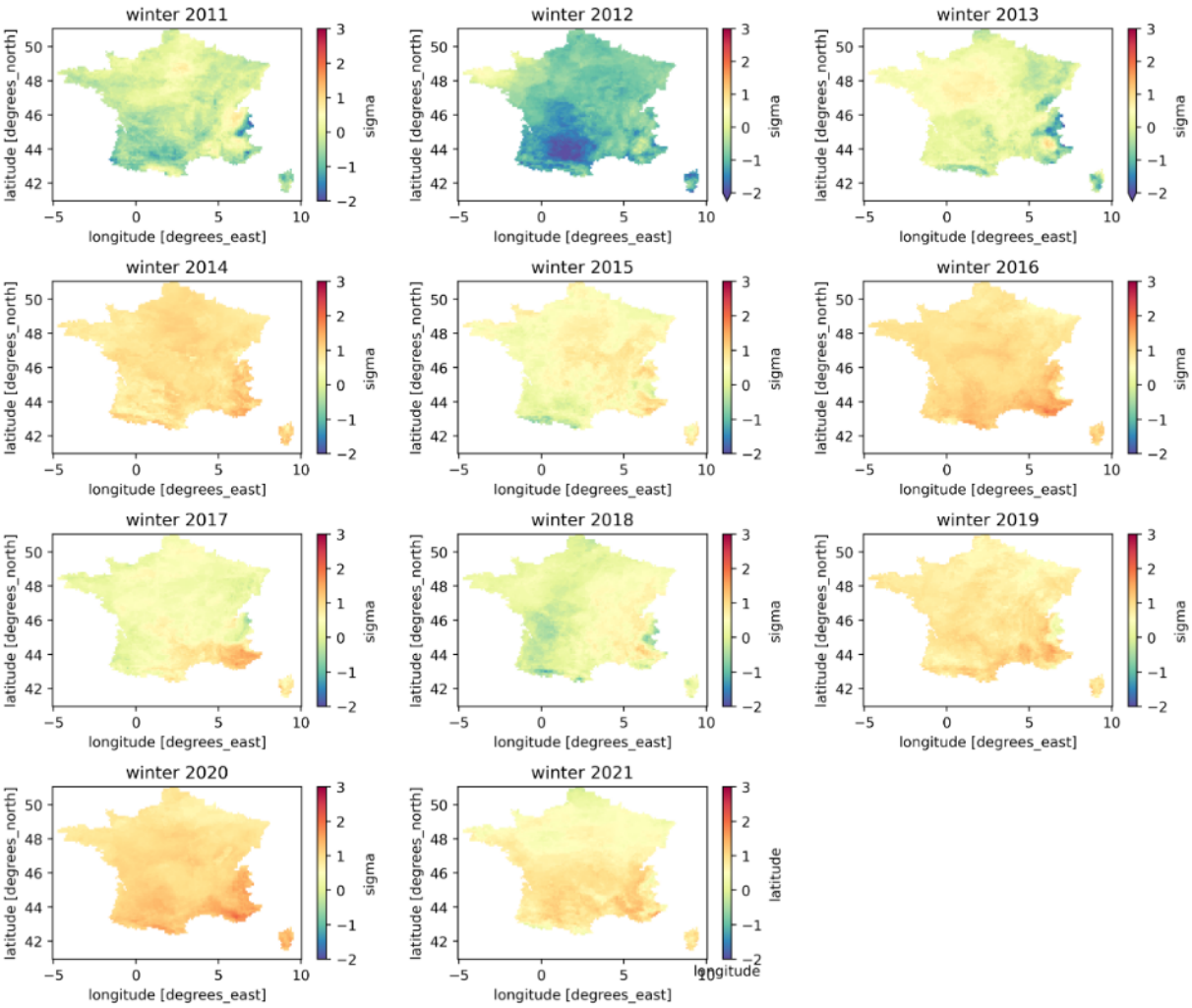

Figure A.9. Winter seasonal $-T10_{std}$ values, 2011-2021.

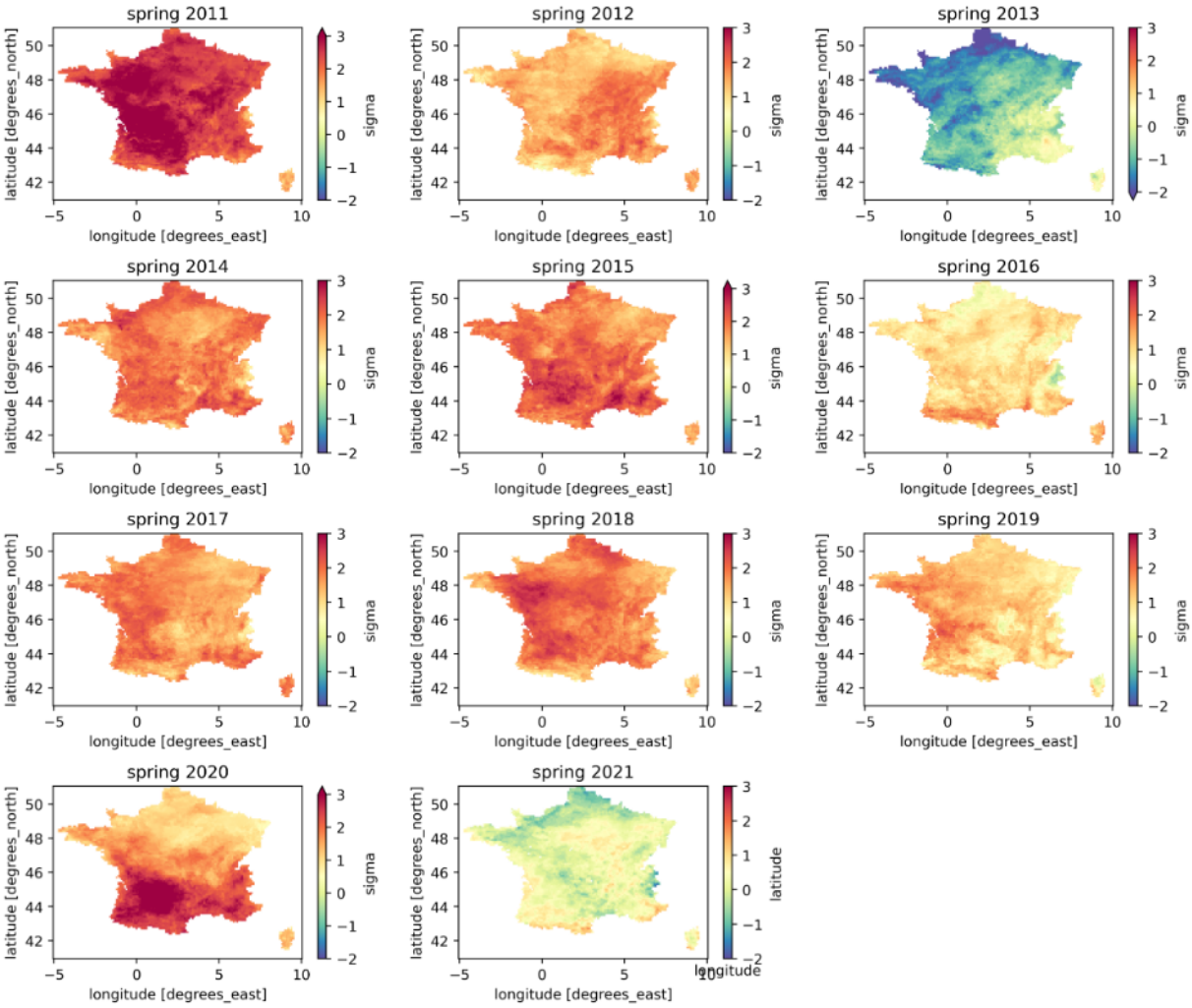

Figure A.10. Spring seasonal $-T10_{std}$ values, 2011-2021.

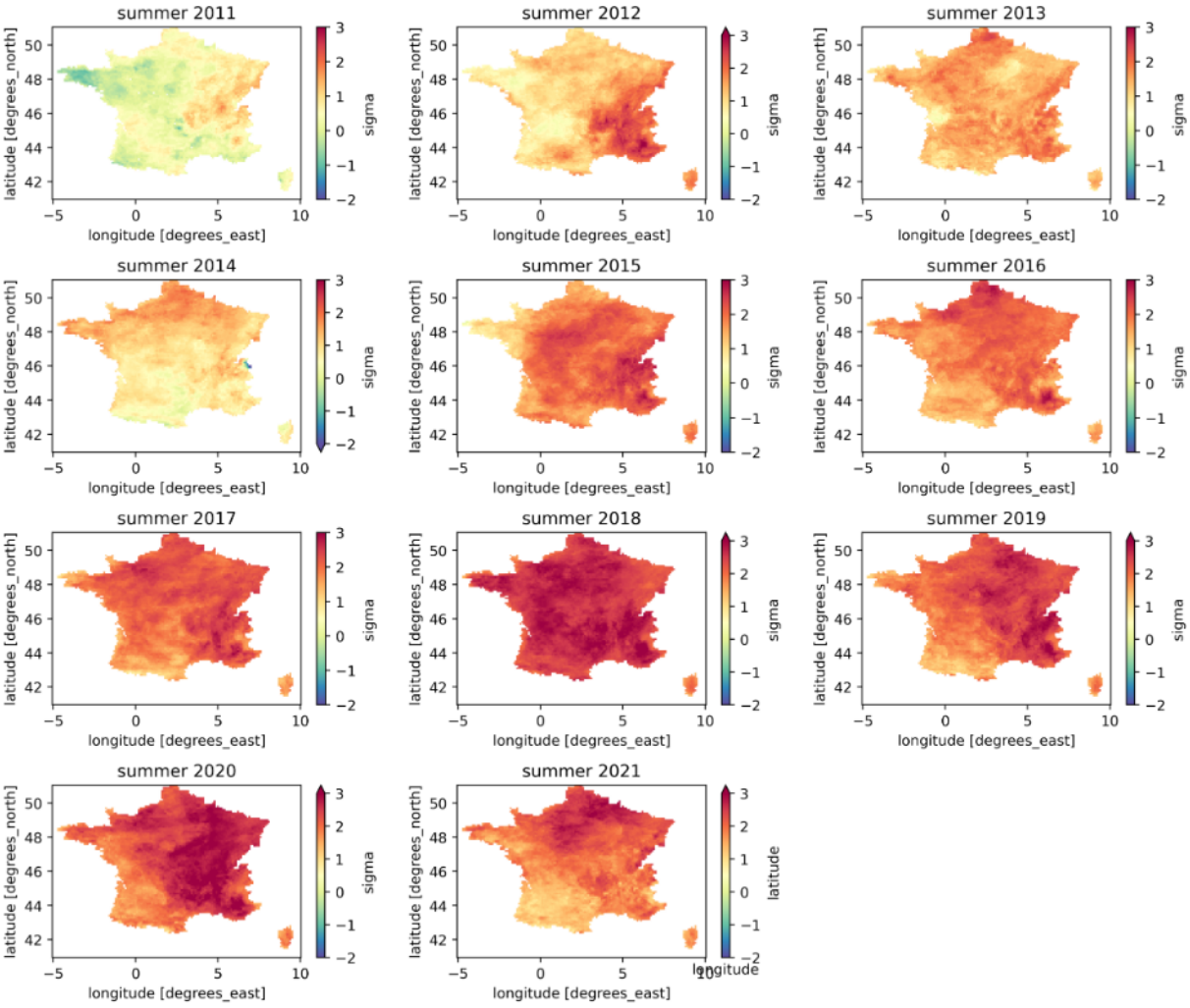

Figure A.11. Summer seasonal $-T10_{std}$ values, 2011-2021.

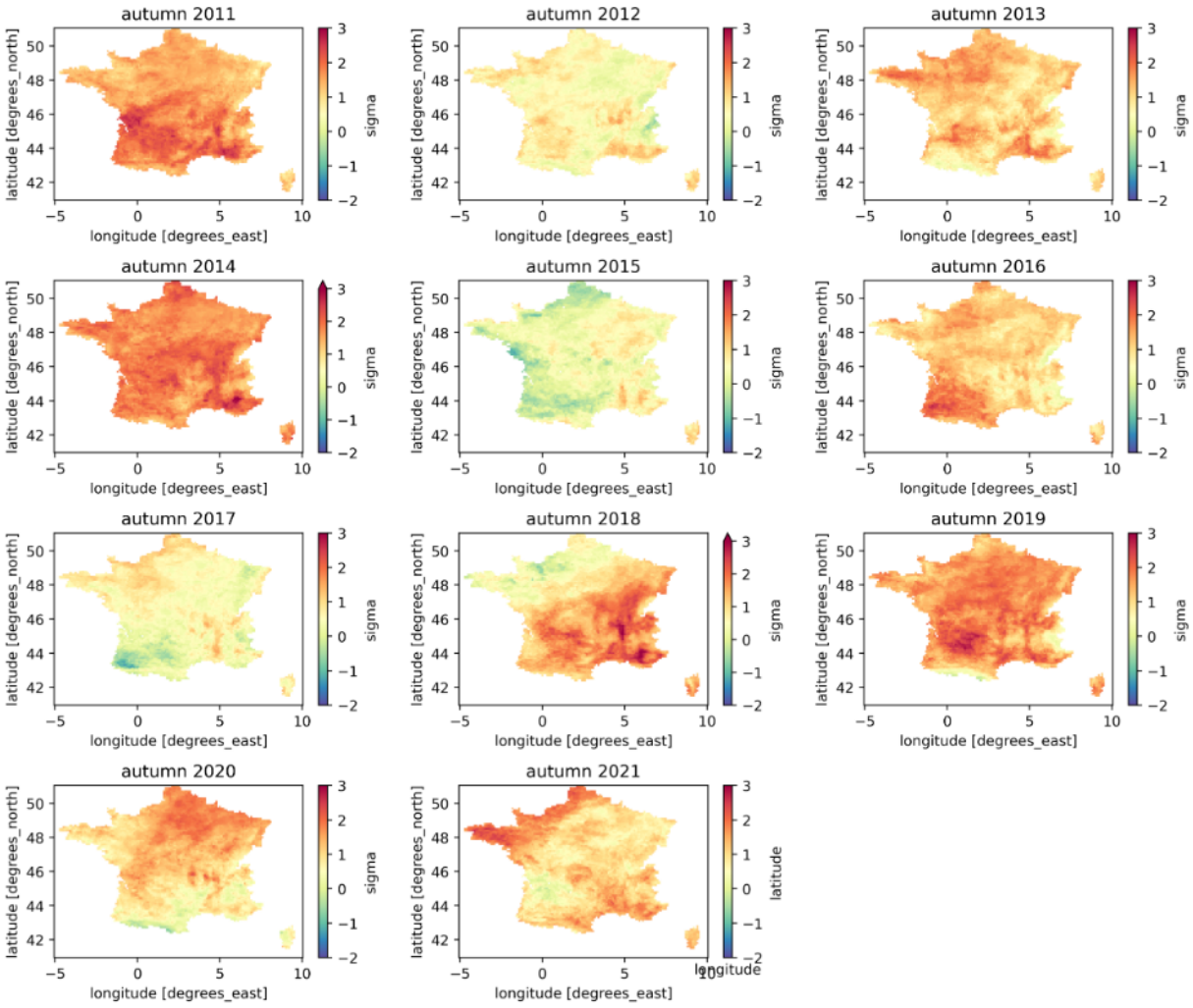

Figure A.12. Fall seasonal $-T10_{std}$ values, 2011-2021.

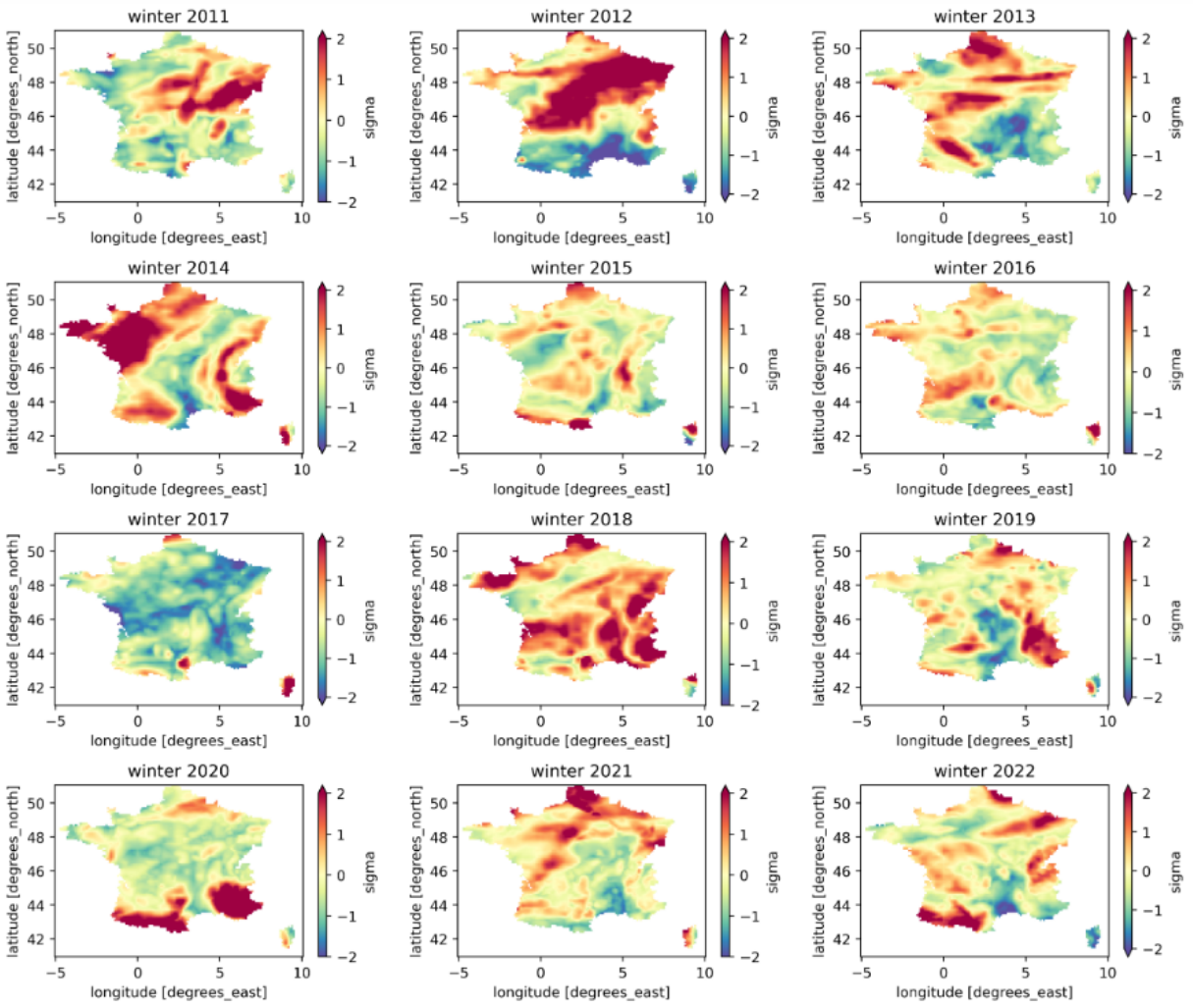

Figure A.13. Winter seasonal P_{std} values, 2011-2022

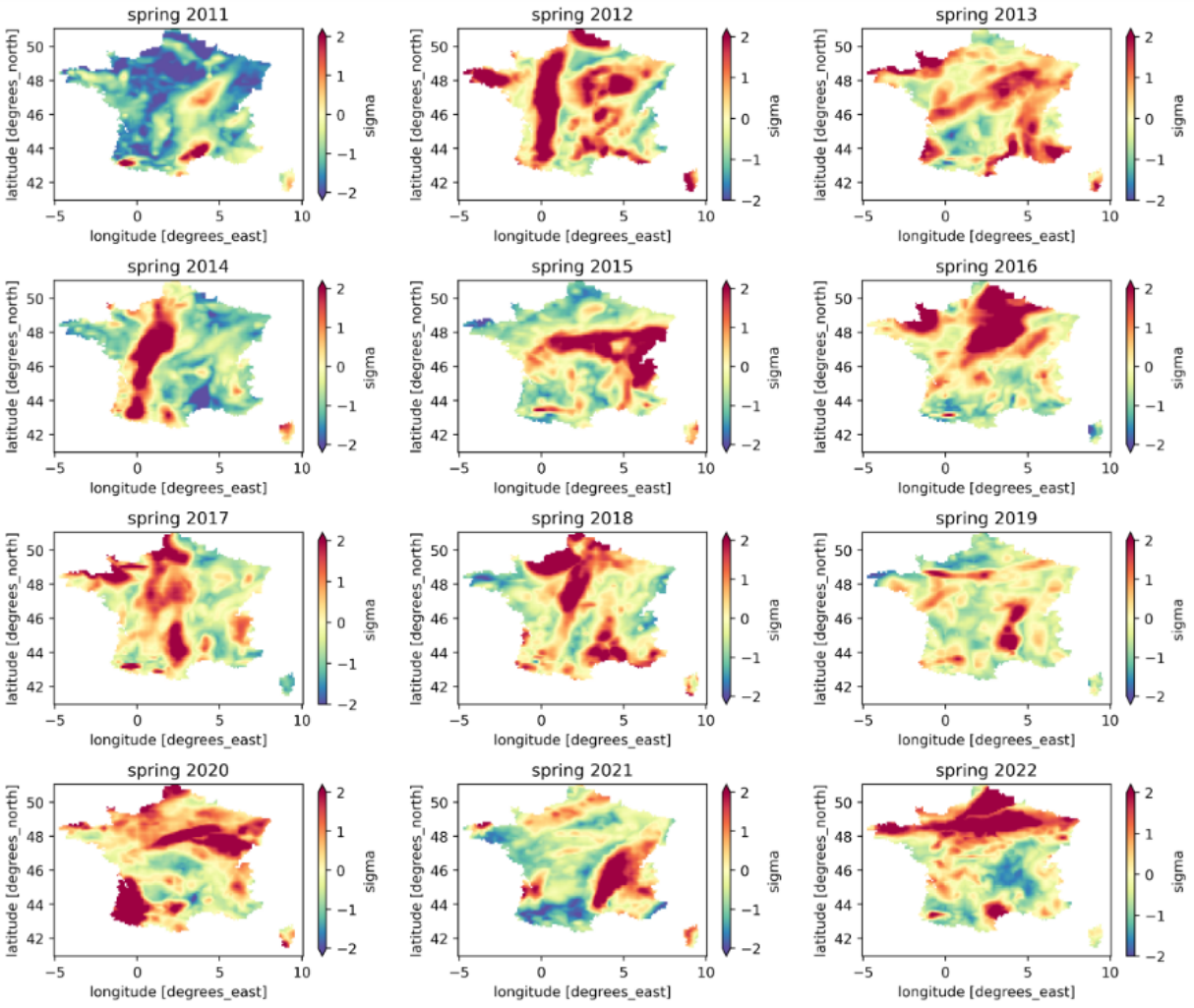

Figure A.14. Spring seasonal P_{std} values, 2011-2022

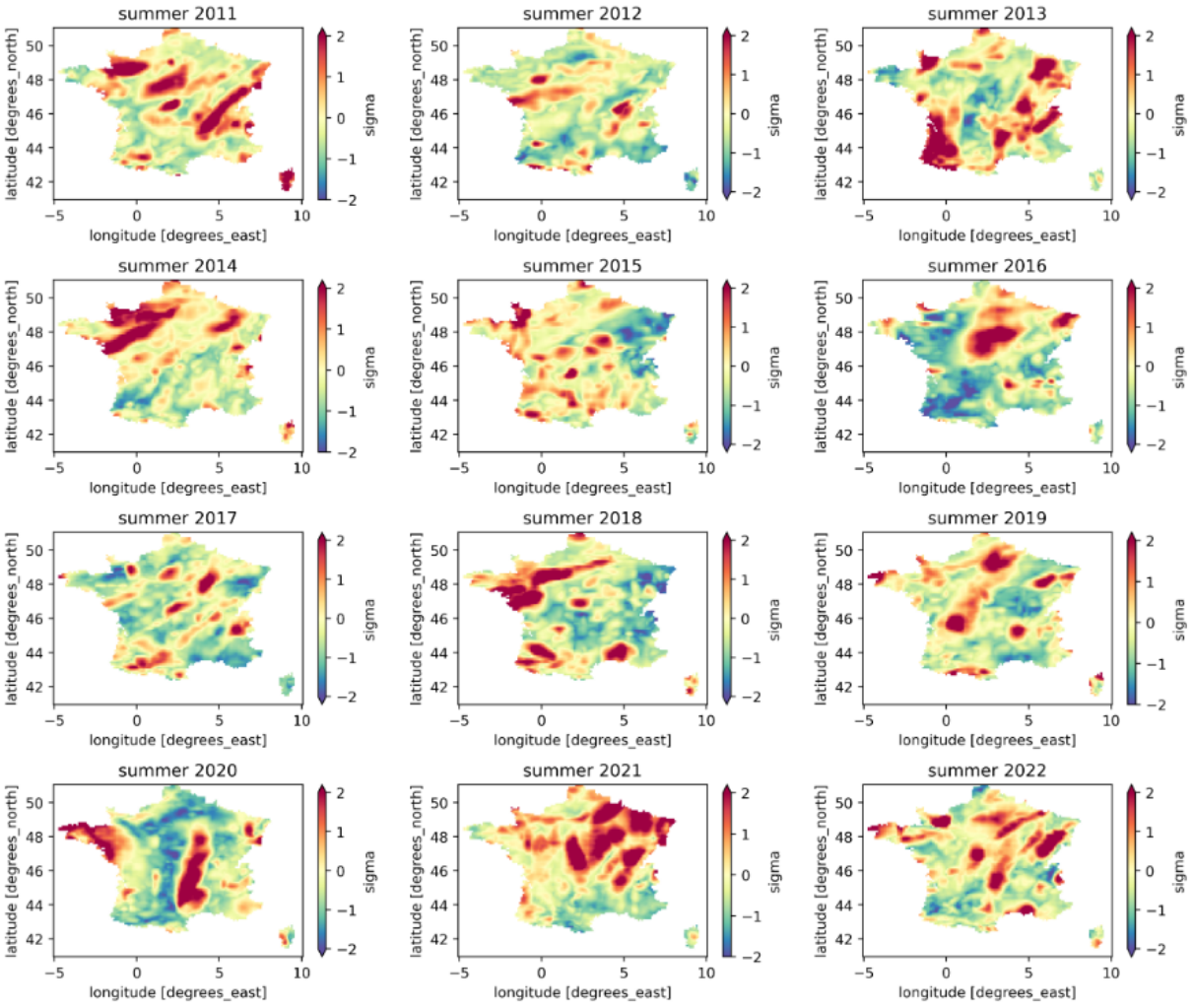

Figure A.15. Summer seasonal P_{std} values, 2011-2022

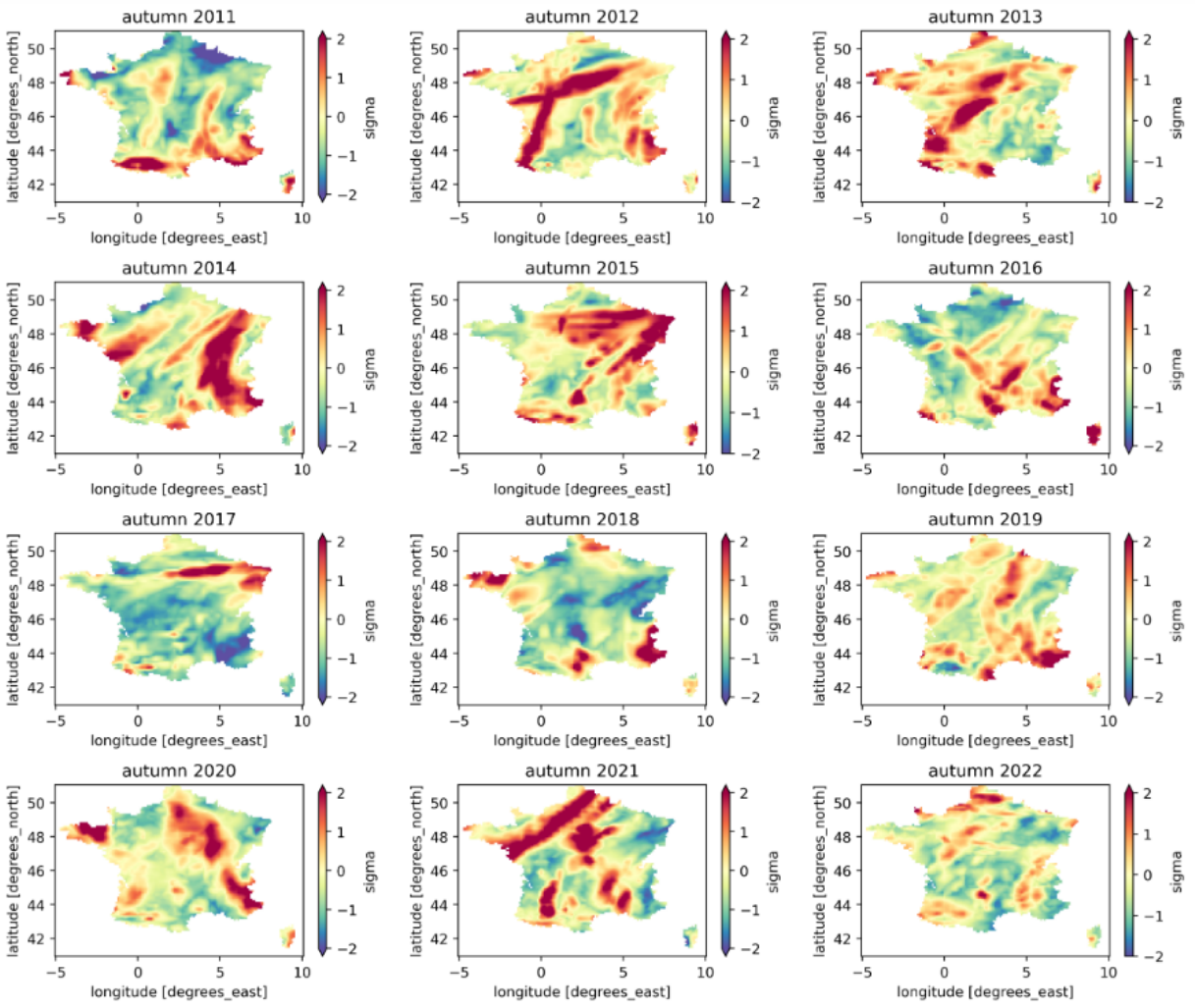

Figure A.16. Fall seasonal P_{std} values, 2011-2022

A.4. Seasonal droughts per region

Now, this section gives the drought variable D_{std} plots.

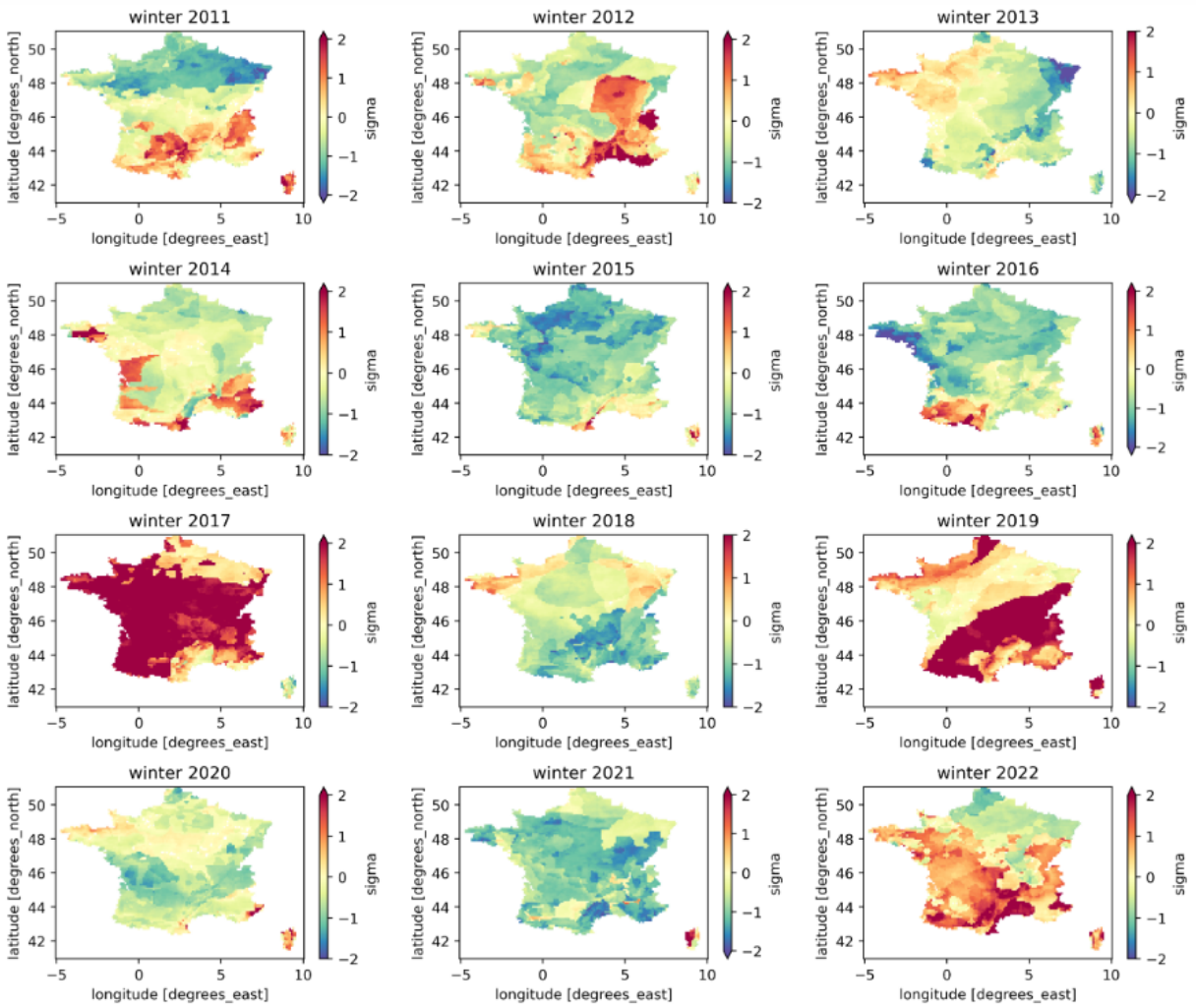

Figure A.17. Winter seasonal D_{std} values, 2011-2022

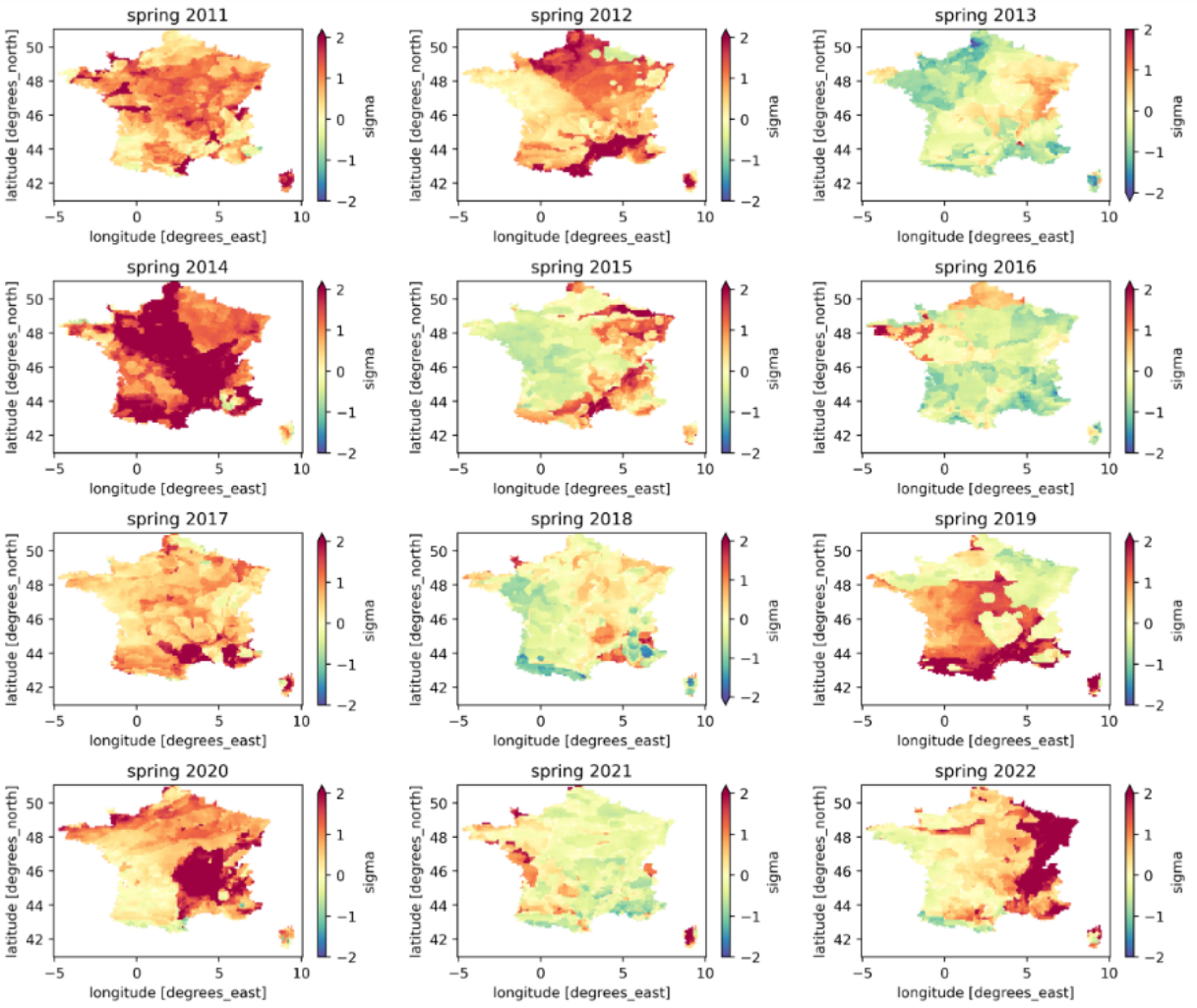

Figure A.18. Spring seasonal D_{std} values, 2011-2022

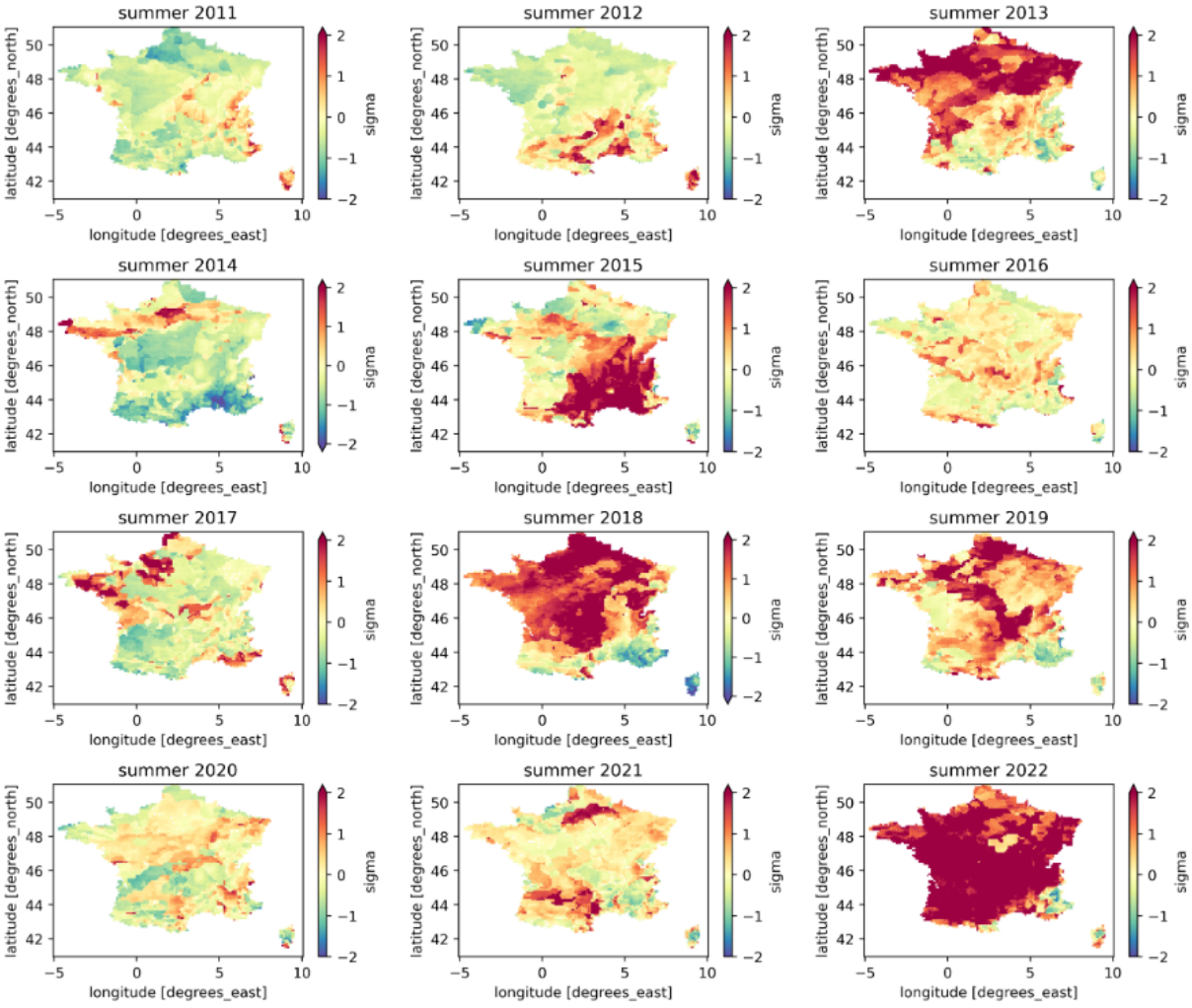

Figure A.19. Summer seasonal D_{std} values, 2011-2022

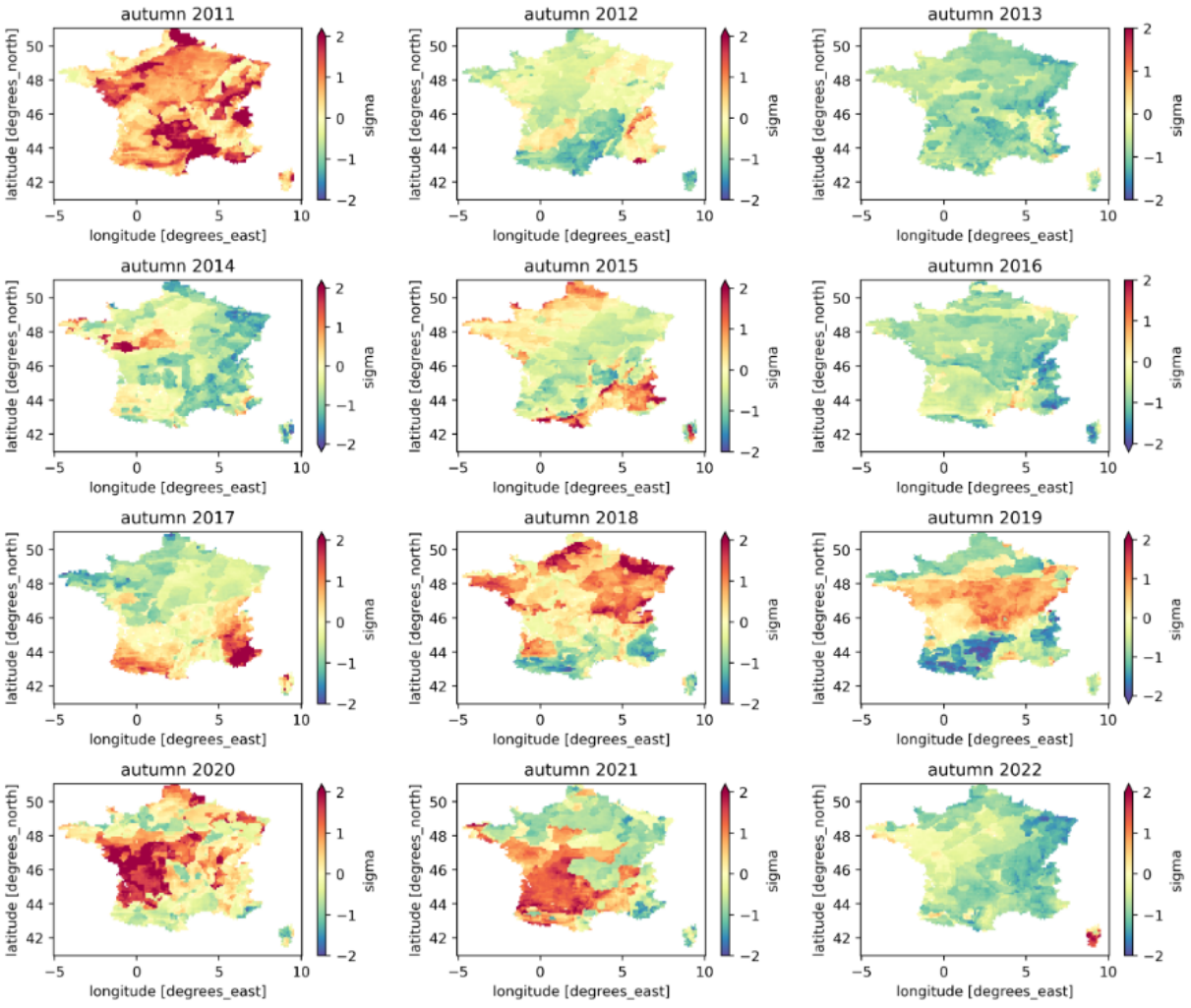

Figure A.20. Fall seasonal D_{std} values, 2011-2022

Insuring
a more
open world

CNP Assurances – Registered office: 4, promenade Cœur de Ville 92130 Issy-les-Moulineaux - Tel.: +33 (0)1 42 18 88 88 – www.cnp.fr
Société anonyme (joint-stock company) with fully paid-up share capital of €686,618,477
Registered in the Nanterre Trade and Companies Register under no. 341 737 062
Company governed by the French Insurance Code (Code des assurances)